Thèse de doctorat

Université Paris Cité

Ecole doctorale Bio Sorbonne Paris cité (ED 562)

IHU Imagine-Institut des Maladies Génétiques

Laboratoire de Génétique des maladies mitochondriales

Mitochondrial RNA metabolism defects in the development of mitochondrial diseases

Par Cérane CAFOURNET

Thèse de doctorat en Génétique

Dirigée par Dr. Metodi METODIEV, codirigée par Dr. Benedetta RUZZENENTE

Présentée et soutenue publiquement à Paris, le 7 Octobre 2022

Pr. Benoit FUNALOT, PU-PH, Université Paris Est Créteil	Rapporteur
Dr. Guy Lenaers, DR, Université d'Angers	Rapporteur
Dr. Yolanda NAVARRO CAMARA, PhD., Vall d'Hebron Research Institute	Examinatrice
Pr. Véronique PAQUIS, PU-PH, Université côte d'Azur	Examinatrice
Dr. Metodi METODIEV, CR (HDR), Université Paris Cité	Directeur de thèse
Dr. Benedetta RUZZENENTE CR (HDR), Université Paris Cité	Co-directrice de thèse

Doctoral thesis

Université Paris Cité

Doctoral school Bio Sorbonne Paris Cité (ED 562)

IHU Imagine-Institut des Maladies Génétiques

Laboratory of Genetics of mitochondrial diseases

Mitochondrial RNA metabolism defects in the development of mitochondrial diseases

By Cérane CAFOURNET

PhD thesis in Genetics

Directed by Dr. Metodi METODIEV, codirected by Dr. Benedetta RUZZENENTE

Presented and publicly defended in Paris, on 7 October 2022

Pr. Benoit FUNALOT, PU-PH Université Paris Est Créteil	Reporter
Dr. Guy LENAERS, DR., Université d'Angers	Reporter
Dr. Yolanda NAVARRO CAMARA, PhD., Vall d'Hebron Research Institute	Examiner
Pr. Véronique PAQUIS, PU-PH, Université côte d'Azur	Examiner
Dr. Metodi METODIEV, CR (HDR), Université Paris Cité	Thesis director
Dr. Benedetta RUZZENENTE, CR (HDR), Université Paris Cité	Thesis co-director

A Denise, Axelle & Victoire

Acknowledgments

I would like to express my sincere thanks to my thesis committee who promptly agreed to examine and evaluate the work done during this PhD thesis. In this respect, I would like to thank the rapporteurs of my thesis work, Pr. Benoit Funalot and Dr. Guy Lenaers, for the time and consideration they gave me, allowing me to improve this manuscript. I would also like to thank Dr. Yolanda Navarro Camara and Pr. Véronique Paquis for their role as examiners of my thesis work.

For giving me the opportunity to work on this project, but more importantly for their scientific vision, dedication to their work, I would like to thank my thesis supervisors; For her role as supervisor during my Master 2, Dr. Benedetta Ruzzenente first introduced me to the world of mitochondrial diseases and it was a good experience; for her technical, scientific advice and supervision, I am grateful; For his scientific knowledge, attention to detail, rigorous work, and supervision, I also extend many thanks to my thesis director Dr. Metodi Metodiev; You created this project, you allowed me to share it at the YR2I congress, and to improve my work and my writing. Thank you for your time and consideration.

I am very grateful to Dr. Agnès Rötig, Head of the Mitochondrial Genetics Laboratory, for accepting my application almost four years ago as a master trainee, for creating such a stimulating and dynamic environment for mitochondrial diseases research, for supporting me during the grant application process to FRM, for giving me valuable advice and confidence to defend this thesis project and throughout these last three years and nine months. Thank you for your wisdom, your kindness and giving us the freedom to work in such a welcoming atmosphere.

I also address sincere gratitude to my monitoring committee, Dr. Olga Corti and Dr. Alessandra Pierani, for the scientific input brought to my work in the 2nd and 4th year PhD, for their kindness and understanding, especially during the year 2020. Their advice and knowledge gave interesting and significant orientation to my thesis project and allowed me to return to my benchwork with more confidence.

I am thankful to all the platforms and facilities that allowed to create the unique foundation for this thesis project; to the Imagine Institute, for giving me the opportunity to work in such an incredible environment and to benefit from nine additional months; the LEAT Necker, and in particular Beata Turanska for her professionalism managing the mouse lines, the imaging and histology platforms, in particular Nicolas Goudin, Béatrice Durel, for teaching me their knowledge in confocal imaging, Sophie Berissi and Damien Conrozier for their availability and their efficiency with my fragile brain samples. I would like to thank the laboratory of Dr. Alessandra Pierani, Yoann Saillour and Dr. Frederic Causeret for allowing me to use their

vibratome and cryostat; Pr. Chris Ottolenghi for the collaboration with the mass spectrometry platform of the Saint-Antoine hospital under the supervision of Pr. Antonin Lamazière and Pr. Germain Trugnan. I would also like to thank Brigitte Nadelec for teaching me how to use the cryostat, where I certainly spent many hours, and Dr. Sofia Zanin, for her advice and expertise on histological and imaging techniques but especially for her precious help at the end of my thesis; thank you for your availability and help with the confocal SP5.

A special thanks also goes to Pr. Julie Stefann, Kalliopi, Pr. Jean-Paul Bonnefont, Dr. Clément Pontoizeau, and Pr. Manuel Schiff from the laboratory of genetics of mitochondrial diseases who listened to my work during laboratory meetings. They may never know how much it meant to sometimes hear appreciation and satisfaction regarding the work done, even if it was not complete.

What would be a team without its young members? I would like to warmly thank the people who formed the core of the mito laboratory at the beginning, Christelle and Juliette who gave me a glimpse of what the life of a PhD student was like; Floriane, who was my thesis companion for two years, and who shared with me the experimental successes as well as the numerous failures; I appreciated your hard work and your wholeheartedness; Coralie, and in particular Lucas for his sense of humour, his legendary composure, his warm support after the two months of interruption due to the health crisis; the members who were there for a short but significant period of time -Leslie, Paul, Vincent, Farah and Chloe - the master and medical students that brought their youth, their freshness and with who I shared meaningful conversations - Chloé, the sweet Irina and the "Mitomanes" Francesca, Yamina & Elisa- I wish you the best for your professional adventures.

I express my gratitude for the sunny and precious personalities I have met during these years; Alessandra for her passion, for instilling a sense of *famiglia* in this lab; Martin for closing the lab with me many nights, for his kindness and his love for cryptos; Marcelo for kindly accepting to read my introduction, for his encouraging words on days of endless despair; Ema from the "Eye team", who encouraged me to share my knowledge and expertise in newly born pups; Vanessa for her advice, her funniness, but most of all for her great sense of justice, for supporting me when the pressure was too high.

Sofia, I am delighted that you can stay longer and continue to enlighten the lab with your brilliance and your kindness; Mirella, I wish you good luck in your new adventures, in the land of gingerbread and half-timbered houses, sharing the office with you was a pleasure.

I could not end this thesis without expressing my sincere love to the core group of MitoManes -who have dubbed me the Queen of Hearts-, my teammates, whom I can humbly call my friends, my professional support system; Manon the ears and heart of this team, my office neighbour, with whom I have shared so much. I may have looked a little furtive when we first met in July 2020, still in my secluded "cave", trying to capture z-stack images with my precious LSM 700; I appreciated your positivity in the morning, your zest for life and your love for Disney movies. I promise you'll be catsitting with my little Plume but watch your toes! Nolan, always ready for a "Milanese" from Keiser's, always with a little joke to lighten the mood, and a great sense of listening; I enjoyed our crazy conversations with Manon on Friday lunches when you first joined the team; Matthieu who always makes sure that no one is in need, the scuba diving

expert, with his great sense of organisation and his great skills at preparing mojitos, I will give you a call for my next holidays for sure!; Mariam from Gryffindor house, I'm happy to have met you, we shared so many stories at the end of the afternoons, in office 417. I appreciated your will, your thoroughness, and your sense of honour, I wish you good luck in the land of maple syrup and ice hockey, you will do great things; and finally, speaking of maple syrup, Clovis, thank you for being unapologetically yourself, for your authenticity and your audacity, for your good taste, the laughter, and the tears, for having contributed to spreading the famous story of the pistachio and bean pie! For your joie de vivre and your catchy songs; I must provide chocolate bars and chouquettes for the many times I let my timer beep in your ears!

You all enabled me to get through the days with more serenity. This experience has been a big rollercoaster, I still hesitate between an Oziris or a Goudurix, but you have underlined it with your positive energy.

To the “lab next door”, the hallway buddies, Valeria, Lisa, Nancy, Camille, Iris, Sabrina, Clementine, Tobias, Simon, Ekin, Fatma, I am grateful for the great advice.

To all the people I have met during this unique life experience, from the doors of the Imagine Institute -Alexis and Roger- to Guadeloupe and beyond, who have enquired about my well-being and the progress of my work; Thank you.

To my golden friends, whom I have known from secondary to engineering school and beyond, for being such a lighthouse, a support system throughout this adventure, I send you my sincere love; Lorna, my sister for many years, I wish you success in this last year of your PhD, full of challenges; Rivka, Gwenaelle, my fairy godmothers, for looking after me, and making sure I was in good shape mentally; Louis-Phillipe , Nelly and Nayanka for making me see the good side of things; Marielle, Cédric & Ludmina, David & Sarah, Ariles & Nicolas, Monica, Anne-Laure, Mathilde, & Anthony, Lisa, Anne-Harrya, Mathias & Tanaïs, Bettina & Joselita, Nathan, Olivia, and Eva, thank you for popping into my life from time to time and giving me the possibility to breathe some fresh air.

Finally, how could I reach the top of this mountain without my pillars, the blood in my veins, my family, who have nurtured me with love, care, and support, through thick and thin, through health and coughing fits. To the joyful members of La cousinerie, to Lois, Sully and their wonderful Sarah, to the adventurers of the Reunion, to Anne, Françoise, Alexandre, Claude and Celine, to Caroline & Patrice my parents in Paris, Lywell & Pearl with their innocence, Jules and the boys, Orlane & Célian and their fearless spirit, Mamie & Papi, Maman & Papa, you made me who I am, with my strengths and weaknesses; You provided me with day and night counselling; luckily I am a night owl, therefore the six-hour time difference was never a problem, on the contrary, it was a lifeline. Without asking for anything in return, except to see me prosper, you taught me courage, tenacity in adversity, humility. You saw my worth, you gave me confidence and freedom to express myself, you reassured me along the way. I am eternally grateful. I did my best and I sincerely hope I made you proud.

Telle une rose cayenne d’Aichi, qui comme le roseau, ploie mais jamais ne fléchit, soumise aux vents violents des ouragans, je me dessine, robuste plante des Antilles.

Table of content

Acknowledgments 3
Abstract 11
Résumé 12
List of figures 13
List of tables 15
List of Abbreviations 16
Chapter I: Introduction 23
I. Mitochondria 24
1. Structure and principal functions of mitochondria 24
2. Mitochondrial DNA organisation 26
2.1 Mt DNA replication 27
2.2 MtDNA transcription 28
2.3 Transcript processing and maturation 29
2.4 Mitochondrial translation 30
3. The oxidative phosphorylation (OXPHOS) system 30
4. LRPPRC, an mRNA-stability factor involved in Leigh Syndrome 33
4.1 Structure 33
4.2 Function of LRPPRC 33
5. ELAC2, a protein with an RNase Z activity, involved in mitochondrial diseases 36
5.1 Structure of ELAC2 36
5.2 Function of ELAC2 36
II. Mitochondrial diseases 38
1. mitochondrial diseases definition 38
2. Mode of inheritance 38
3. Diagnosis of mitochondrial diseases 40
3.1 Clinical presentation 41
3.2 Biochemical analyses 42
3.3 Histological analyses 42
3.4 OXPHOS activity 42
3.5 Imaging analyses 43
3.6 Genetic diagnosis of mitochondrial diseases 43
4. Leigh syndrome 44
4.1 Clinical and biochemical characteristics of LS 44
4.2 Genetics of LS 45
4.3 LRPRPC and LS 48
4.4 Brain structures involved in LS and their development 51
4.4.1 Brainstem formation, structure, and function 52

4.4.2 *Cerebellum formation, structure, and function* 53
5. Role of mitochondria in the neurogenesis and mature neurons 56
6. Mechanism of neurodegeneration 58
7. Mitochondrial cardiomyopathies 59
8. ELAC2 and mitochondrial diseases 60
8.1 Clinical and molecular phenotypes associated with *ELAC2* variants 60
8.2 ELAC2 mutations recapitulative table 62
Objectives 65
Objective I 65
Objective II 66
Chapter II: Materials and methods 68
I. Generation of mouse model and mouse breeding 69
II. Mouse genotyping 69
III. Tissue processing for immunostaining 71
IV. Immunostaining in mouse tissues 71
V. Histochemistry 72
1. Nissl staining 72
2. Haematoxylin Eosin staining 72
3. COX/SDH staining 73
VI. Primary cell culture of ventral mesencephalon 73
VII. Immunostaining in primary cells 74
VIII. Confocal microscopy 75
IX. Image processing 75
X. Fibroblasts culture 75
XI. RNA extraction and Northern blot 76
XII. Protein extraction from mouse tissues 76
XIII. Protein extraction from human fibroblasts 77
XIV. SDS-PAGE 77
1. Semi-dry transfer 77
2. Immunodetection 78
XV. Lactate in brain tissues measurement by liquid chromatography-tandem mass spectrometry (LC-MS/MS) 78
XVI. Statistics 78
XVII. Table 6. Primary and secondary antibodies used for immunostaining and SDS-PAGE 79
Chapter III: Results 82
I. Characterisation of midbrain-and-cerebellum specific Lrpprc knock-out mice (MCKO) 83
1. Expression pattern of the EN1-driven Cre recombinase 83
2. Specificity of En1-driven Lrpprc knockout 87

3. Loss of Lrpprc in the midbrain and cerebellum causes early postnatal lethality 87
4. Delayed development of cerebellar and midbrain regions showed in absence of Lrpprc 88
5. OXPHOS deficiency in midbrain and cerebellum of MCKO mice 91
6. Lactate level in brain tissues 93
7. Loss of Lrpprc causes cerebellar disorganization and underdeveloped Purkinje cell dendrites 94
8. Dopaminergic neurons of the substantia nigra are sensitive to loss of Lrpprc 95
9. Response to mitochondrial dysfunction caused by loss of Lrpprc. 97
a. Neuroinflammatory response 97
b. Oxidative stress and UPRmt 98
c. Autophagy 100
d. Apoptosis 101
II. Loss of Lrpprc during mouse embryonic development 102
1. Cerebellar developmental delay during embryogenesis of MCKO mice 102
2. Abundance of dopaminergic neurons in substantia nigra from MCKO embryos is mildly affected at E15.5 104
3. Activated caspase 3 in midbrain of MCKO embryos suggests an increase in apoptosis 105
4. Impaired dendrite and axonal growth, in vitro, of dopaminergic neurons isolated from MCKO mice 105
III. ELAC2 and mitochondrial disease 107
1. Identification of novel homozygous and compound heterozygous pathogenic variants in the *ELAC2* gene. 107
2. Decreased abundance of ELAC2 in patient fibroblasts 109
3. Accumulation of unprocessed $tRNA^{VAL}$ precursor in patient fibroblasts 110
4. ELAC2 defects in fibroblasts of patients did not lead to defects in OXPHOS proteins 111
Chapter IV: Discussion 114
Part 1: Characterisation of a midbrain-and-cerebellum-specific *Lrpprc* knock-out mouse model 115
The midbrain-and-cerebellum-KO (MCKO) mouse model broadly recapitulates the LS phenotype observed in patients with LRPPRC mutations. 116
Loss of Lrpprc in the MCKO mouse model led to defects in neurogenesis 122
Does this model recapitulate the tissue-specificity of LRPPRC-linked disease? 123
Conclusion 123
Part 2: Identification of novels homozygous and compound heterozygous pathogenic mutations in the *ELAC2* gene in three unrelated patients 124
Case study and comparison with known mutations 124
Conclusion 125
Bibliography 127
Résumé en français 154

Abstract

Mitochondrial RNA metabolism defects in the development of mitochondrial diseases

Mitochondrial RNA metabolism is regulated by different nuclear encoded factors including LRPPRC and ELAC2. LRPPRC is a mitochondrial mRNA stability and polyadenylation factor whose variants result in a multisystemic pathology invariably including Leigh or Leigh-like disease accompanied by hepatopathy or cardiomyopathy. *ELAC2* encodes a ribonuclease essential for maturation of mitochondrial tRNAs and its variants have been linked to hypertrophic cardiomyopathy, developmental delay, and lactic acidosis. The global aim of my PhD thesis was to better understand the clinical, biochemical, and molecular consequences of mitochondrial RNA metabolism defects associated with *LRPPRC* and *ELAC2* variants.

The first aim of my PhD thesis was to understand how loss of LRPPRC affects the development and function of the midbrain and cerebellum, two structures affected in Leigh syndrome. To this aim, I generated a conditional knockout mouse model wherein Lrpprc expression was ablated in midbrain and cerebellum. Knockout mice died soon after birth and their (immuno)histochemical analysis revealed severe developmental and structural defects in the midbrain and cerebellum. Analysis of different cellular populations in these brain structures revealed that Lrpprc plays an important role for survival of dopaminergic neurons and Purkinje cells.

The second aim of my PhD thesis was to characterize newly identified *ELAC2* variants using patient fibroblasts. Immunoblot analyses revealed that the mutations led to a decreased abundance of the ELAC2 protein but did not dramatically affect the abundance of OXPHOS proteins. However, an accumulation of unprocessed mitochondrial $tRNA^{VAL}$ precursor was detected. This study expands the genetic spectrum associated with ELAC2 variants.

Keywords: Mitochondrial RNA metabolism, *LRPPRC*, Leigh syndrome, *ELAC2*, hypertrophic cardiomyopathy

Résumé

Défauts du métabolisme des ARN mitochondriaux dans le développement des maladies mitochondriales

Le métabolisme des ARN mitochondriaux est régulé par différents facteurs codés par le noyau, dont LRPPRC et ELAC2. LRPPRC est un facteur de stabilité et de polyadénylation de l'ARNm mitochondrial dont les mutations entraînent une pathologie multisystémique comprenant invariablement une maladie de Leigh ou de type Leigh accompagnée d'une hépatopathie ou d'une cardiomyopathie. *ELAC2* code pour une ribonucléase essentielle à la maturation des ARNt mitochondriaux et ses variants ont été associés à une cardiomyopathie hypertrophique, un retard de développement et une acidose lactique. L'objectif global de ma thèse était de mieux comprendre les conséquences cliniques, biochimiques et moléculaires des défauts du métabolisme de l'ARN mitochondrial associés aux mutations de *LRPPRC* et *ELAC2*.

Le premier objectif de ma thèse était de comprendre comment la perte de LRPPRC affecte le développement et la fonction du mésencéphale et du cervelet, deux structures affectées dans le syndrome de Leigh. À cette fin, j'ai généré un modèle de souris knock-out conditionnel dans lequel l'expression de LRPPRC a été supprimée dans le mésencéphale et le cervelet. Les souris knock-out sont mortes peu après la naissance et leur analyse (immuno)histochimique a révélé de graves défauts de développement et de structure dans le mésencéphale et le cervelet. L'analyse de différentes populations cellulaires dans ces structures cérébrales a révélé que Lrpprc joue un rôle important pour la survie des neurones dopaminergiques et des cellules de Purkinje.

Le deuxième objectif de ma thèse était de caractériser les variants d'*ELAC2* nouvellement identifiés en utilisant des fibroblastes de patients. Des analyses par immunoblot ont révélé que les mutations entraînaient une diminution de l'abondance de la protéine ELAC2, mais n'affectaient pas de façon significative l'abondance des protéines OXPHOS. Cependant, une accumulation du précurseur de l'ARNt-Val mitochondrial non-clivé a été détectée. Cette étude élargit le spectre génétique associé aux variants d'ELAC2.

Mots clés : métabolisme des ARNm mitochondriaux, *LRPPRC,* syndrome de Leigh, *ELAC2*, cardiomyopathie hypertrophique.

List of figures

Chapter I: Introduction

Figure 1. Mitochondrial compartmentalization (Kühlbrandt, 2015).....26

Figure 2. Map of the human mitochondrial genome (Stewart and Chinnery, 2021).....27

Figure 3. Initiation of mtDNA transcription adapted from (Hillen *et al.*, 2017).....29

Figure 4. Schematic illustration of the oxidative phosphorylation system (OXPHOS) (Kühlbrandt, 2015) 32

Figure 5. Clinical presentation of mitochondrial diseases, (Gorman et al., 2016) 41

Figure 6. Comparative schematic representation of human and mouse brain structures adapted from (Sjöstedt et al., 2020).....52

Figure 7. Dorsal and ventral overview of a human brainstem specimen from (Adil et al., 2021).....53

Figure 8. Murine and human cerebellar structure from (Apps and Hawkes, 2009) 54

Figure 9. Cerebellar cortex cellular organisation. (Consalez et al., 2021).....56

Chapter II: Materials and Methods

Figure 10. Generation of the cerebellum and midbrain knockout mouse model.....69

Chapter III: Results

Figure 11. Expression pattern of En1 promoter was detected in the midbrain and cerebellum of newly born En1-Cre/Rosa26 tdTomato mouse.....85

Figure 12. En1-driven Cre expression detected in Pcs, GCPs and DNs from newly born En1-Cre/Rosa26 tdTomato mouse.....86

Figure 13. MCKO mice did not exhibit loss of Lrpprc skin tissues.....87

Figure 14. Early postnatal lethality of MCKO mice.....88

Figure 15. Loss of Lrpprc in cerebellum and midbrain alters the development of these two brain regions as visualised by morphometric analysis and Nissl staining.....90

Figure 16. Abundance of different OXPHOS proteins in L/L and L/L, Cre mice in different brain regions at P0.....92

Figure 17. Loss of Lrpprc leads to complex IV deficiency in MCKO mice.....93

Figure 18. Loss of Lrpprc lead to increase level of lactate.....94

Figure 19. Absence of Lrpprc leads to cerebellar developmental defects.....95

Figure 20. Absence of Lrpprc leads to loss of dopaminergic neurons in *substantia nigra* of newly born knockout pups.....96

Figure 21. Loss of Lrpprc did not lead to neuroinflammation.....98

Figure 22. Loss of Lrpprc did not lead to oxidative stress nor induction of the UPRmt pathway.....99

Figure 23. Loss of Lrpprc did not lead to increased autophagy in the brain of MCKO mice.....101

Figure 24. Loss of Lrpprc increased cell death in midbrain and cerebellum of newly born MCKO pups.....101

Figure 25. Cerebellar developmental delay in MCKO embryos.....103

Figure 26. Abundance of dopaminergic neurons in the substantia nigra of E15.5 MCKO embryos is not substantially changed when compared to controls.....104

Figure 27. Increased the number of apoptotic cells in midbrain (and cerebellum) of E15.5.....105

Figure 28. Primary cells culture suggests defects in dendrite and axonal growth of MCKO dopaminergic neurons.....106

Figure 29. Pedigree of three affected families and evolutionary conservation of the affected amino acids.....109

Figure 30. Decreased abundance of ELAC2 in patient fibroblasts do not lead to decrease of other proteins involved in mtRNA metabolism in fibroblasts of patients (Pt1, Pt3, Pt5) compared to controls (C1, C2).....110

Figure 31. Accumulation of unprocessed tRNAVAL precursor in patient fibroblasts.....111

Figure 32. Decreased abundance of ELAC2 in patient fibroblasts do not lead to decrease in abundance of different OXPHOS proteins in fibroblasts of patients (Pt1, Pt3, Pt5), compared to controls (C1, C2).....112

List of tables

Chapter I: Introduction

Table 1. Recapitulative table of genes involved in Leigh syndrome.....48

Table 2. Recapitulative table of LSFC variant mutations in different geographic regions.....51

Table 3. Recapitulative table of ELAC2 variant mutations in different geographic regions.....64

Chapter II: Materials and Methods

Table 4. List of primers used for mouse genotyping.....70

Table 5. PCR programs set up with different primers used for mouse genotyping.....71

Table 6. Primary and secondary antibodies used for immunostaining and SDS-PAGE.....80

Chapter III: Results

Table 7. Clinical features, brain MRI and biochemical analyses of the reported patients carrying *ELAC2* variants.....108

List of Abbreviations

ADHD: attention deficit/hyperactive disorder

ADP: adenosine di-phosphate

ANT: adenine nucleotide translocator

ATP: adenosine triphosphate

BG: Bergmann glia

BN-PAGE: blue-native polyacrylamide gel electrophoresis

BSA: bovine serum albumin

CI-CV : complex I-V

CI : NADH-dehydrogenase

CII : succinate dehydrogenase

CIII : cytochrome reductase

CIV : cytochrome oxidase

CV : ATP synthase

Calb: calbindin

cDNA: complementary DNA

COX: cytochrome *c* oxidase

CO2: carbon dioxide

CM: cardiomyopathy

CNS: central nervous system

CSF: cerebrospinal Fluid

DAB: diaminobenzidine

DAPI: 4',6-diamidino-2-phenylindole

DMEM: Dulbecco's modified eagle medium

DMSO: dimethyl sulfoxide

DNA: desoxyribonucleic acid

DNs: dopaminergic neurons

dNTP: Deoxynucleotide triphosphates

DRP1: dynamin-related protein 1

DTT: dithiothreitol

E0,5-19,5: embryonic day 0,5-19,5

EDTA: Ethylenediaminetetraacetic acid

EGL: external granular layer

ELAC2: ELAC Ribonuclease Z 2

EN1: homeobox engrailed 1 transcription factor

ER: endoplasmic reticulum

ETC : electron transport chain

EtOH : ethanol

FADH2: dihydroflavine-adenine dinucleotide, reduced form

FBS: fetal bovine serum

FGF: fibroblast growth factors

GABA: gamma-butyric acid

GBX2: gastrulation brain homeobox 2

GCPs: granule cell precursors

GFAP: glial fibrillary acidic protein

GTP: guanosine triphosphate

1H-RMN: proton magnetic resonance spectroscopy

H2O2: hydrogen peroxide

HBSS: Hanks' Balanced Salt Solution

HPLC-ESI-MS/MS: high-performance liquid chromatography/electrospray ionization MS/MS

HSP10,60: heat shock proteins 10, 60

HSP: heavy-strand promoter

i-AAA: intermembrane space ATPases Associated with diverse cellular Activities

IBA1: ionized calcium-binding adapter molecule 1

IGL: internal granular layer

IHC: immunohistochemistry

IMS: intermembrane space

iPSC: induced pluripotent stem cell

kb: kilobase

kDa: kilodalton

KI: knock-in

KO: knockout

LC-MS/MS: liquid chromatography-tandem mass spectrometry

LC3: microtubule-associated protein 1A/1B-light chain 3

LHON: Leber hereditary optic neuropathy

LMX1: LIM homeobox transcription factor 1 beta

LRPPRC: Leucine Rich Pentatricopeptide Repeats Containing

LS: Leigh syndrome

LSFC: Leigh syndrome, French-Canadian type

LSP: light strand promoter

LSU: large subunit

m-AAA: matrix ATPases Associated with diverse cellular Activities

MALDI-TOF: matrix-assisted laser desorption ionization–time of flight

MCKO: midbrain -and-cerebellum-specific Lrpprc knockout mouse model

MCU1,2: mitochondrial calcium uptake protein 1,2

MD: mitochondrial diseases

MELAS: mitochondrial encephalomyopathy with lactic acidosis and stroke-like episodes

MFN1-2: mitofusin 1-2

MgCl2: Magnesium chloride

MILS: maternally inherited Leigh syndrome

MLS: microphthalmia with linear skin defects syndrome

MPTP: 1-methyl-4-phenyl-1,2,3,6-tetrahydropyridine

MRI: magnetic resonance imaging

mRNA: messenger RNA

MRPL: mitoribosomal proteins of the large subunit

MRPP1-3 : mitochondrial RNase P Protein 1-3

MRPS: mitoribosomal proteins of the small subunit

MS-MS: tandem mass spectrometry

mt-: mitochondrial

mtPAP: mitochondrial polyA polymerase

MTS: mitochondrial targeting sequence

NADH: nicotinamide adenine dinucleotide, reduced form

NaOH: Sodium hydroxide

NARP: neurogenic muscle weakness, ataxia, and retinitis pigmentosa

NBT: nitroblue tetrazolium

NCR: non-coding region

NPCs: neural progenitor cells

nt: nucleotide

O2-: superoxide ion

OCT: optimal cutting temperature compound

OPA1: optic atrophy 1

OTX2: orthodenticle homeobox 2

OXPHOS: oxidative phosphorylation

Pax6: paired box protein 6

PBS: Phosphate-buffered saline

PBST: PBS containing 0,05% of Tween®

PCL: Purkinje cell layer

PCs: Purkinje cells

PCR: polymerase chain reactions

PDH : pyruvate dehydrogenase

PEO: external ophthalmoplegia

PFA: Paraformaldehyde

PGC-1 α: peroxisome proliferator activated receptor γ coactivator 1α

PLO: poly-L-ornithine

PMS: phenazine methosulfate

PNPase: polynucleotide phosphorylase

POLγ: DNA polymerase- γ

POLRMT : mitochondrial RNA polymerase

polyA : polyadenylation

PPARα: peroxisome proliferator activated receptor α

PPR : pentatricopeptide repeat

Pt1-5 : Patient 1-5

PTCD2-3 : pentatricopeptide repeat domain 2-3

PVDF : Polyvinylidene fluoride

RG: radial glia

RNA: Ribonucleic acid

RNase P: ribonuclease P

RNase Z: ribonuclease Z (ELAC2)

ROS: reactive oxygen species

rRNA: ribosomal RNA

SDH : succinate dehydrogenase

SDS: Sodium dodecyl sulfate

SHH: sonic hedgehog

SN: substantia nigra

SOD2: superoxide dismutase 2

SSB: the single strand binding

SSU: small subunit

TAE: Tris-acetate-EDTA

TCA: tricarboxylic acid

TEFM: transcription elongation factor

TES: targeted exome sequencing

TFAM: mitochondrial transcription factor A

TFB2M: mitochondrial transcription factor B2

TH: Tyrosine-Hydroxylase

TIM: translocase of the inner membrane

TOM: translocase of the outer membrane

TOP1mt: topoisomerase

Tris-HCl: Tris-Hydrochloric acid

tRNA: transfert RNA

TSS: transcription start site

UPR-mt: mitochondrial unfolded protein response

VAL: Valine

VDAC: voltage dependant anion channel

VTA: ventral tegmental area

WES: whole exome sequencing

WB: western blot

WGS: whole genome sequencing

WINT1: wingless-type MMTV integration site family

Chapter I: Introduction

I. Mitochondria

1. Structure and principal functions of mitochondria

Mitochondria are small semi-autonomous double membrane organelles that evolved from endosymbiosis between an archaebacteria and a prokaryote host 1.5 billion years ago (Sagan, 1967; Gray, 2012, 2017). They provide energy for the whole organism, producing adenosine triphosphate (ATP) by a process called oxidative phosphorylation (OXPHOS) under aerobic conditions.

Mitochondria possess a double membrane defining four distinct compartments: the outer membrane, the inner membrane, the intermembrane space, and the matrix. The matrix has a pH of 7.9 to 8 that allows the maintenance of a trans-membrane electrochemical gradient. In this compartment, we find mitochondrial DNA (mtDNA) molecules that are transcribed into mitochondrial (mt-) rRNAs, tRNAs and mRNAs, mitochondria-specific ribosomes, and proteins. Matrix is also the site of enzymatic reactions like the citric acid cycle that provides protons and electrons at the entries of the respiratory chain.

The inner membrane forms invaginations, cristae, protruding into the matrix space (Martin, Garg and Zimorski, 2015) where, in addition to protein complexes like the i-AAA and the m-AAA protease (Opalińska and Jańska, 2018), prohibitins (Tatsuta, Model and Langer, 2005), the TIM complex, OXA1 (Stuart, 2002) and lipid rafts (Sorice *et al.*, 2009), the enzymes of the oxidative phosphorylation system (OXPHOS) are embedded. The inner membrane is also traversed by channels like the adenosine di-phosphate (ADP)/ATP carriers known as adenine nucleotide translocator (ANT) (Pebay-Peyroula *et al.*, 2003) or selective ion channels that account for the electrochemical membrane potential of 180 mV (Kühlbrandt, 2015).
The intermembrane space (IMS) separates the inner membrane from the outer membrane. This compartment contains 5% of the mitochondrial proteome accounting for 53 proteins with a variety involved in import mechanism (Rath *et al.*, 2020). Among other proteins, we find hydrophilic carrier protein cytochrome c that shuttles electrons of the electron transport chain (ETC) from complex III (CIII) to complex IV (CIV) (Bernardi and Azzone, 1981; Kühlbrandt, 2015; Edwards, Eaglesfield and Tokatlidis, 2021). Hydrophilic regions of translocase proteins of the outer membrane and inner membrane, TOM and TIM, respectively, essential for import of nuclear encoded proteins in the mitochondrial matrix and inner membrane, are also found in the IMS (Neupert and Herrmann, 2007; Schmidt, Pfanner and Meisinger, 2010; Edwards, Eaglesfield and Tokatlidis, 2021).

The mitochondrial outer membrane is traversed by ions and small molecules through specific channels like porins, also called voltage dependant anion channel (VDAC), that among other functions, are coupled to inner membrane ANT, to release ATP in the cytosol (Allouche *et al.*, 2012). VDAC is also implicated in the control of cell death through apoptosis (Shimizu, Narita and Tsujimoto, 1999; Shi *et al.*, 2003), in autophagy (Sun *et al.*, 2012; Ham *et al.*, 2020), calcium homeostasis and connection of mitochondria to endoplasmic reticulum (Szabadkai *et al.*, 2006). Mitochondrially targeted proteins also require TOM-TIM translocation system to cross the mitochondrial double membrane and enter the matrix (Neupert and Herrmann, 2007; Schmidt, Pfanner and Meisinger, 2010).

Mitochondria are also dynamic organelles—they form a network and undergo fission (Frank *et al.*, 2001) and fusion (Cipolat *et al.*, 2004; Chen, McCaffery and Chan, 2007), two processes regulated by specific proteins found at the inner and outer membranes that allow maintenance of their shape, their distribution in the cell, thus their function in response to the cell requirements. Mitochondrial fission, regulated by GTPases dynamin-related protein 1 (DRP1), and the recruitment of Dynamin 2 is the process by which one mitochondrion is divided into two mitochondria. Mitochondrial fusion is a process by which two mitochondria get fused into one mitochondrion, mediated by Mitofusin 1 (MFN1) and Mitofusin 2 (MFN2) that allow fusion of the outer mitochondrial membranes, and the optic atrophy 1 (OPA1) protein that allows fusion of the inner mitochondrial membrane (Tilokani *et al.*, 2018). Therefore, mitochondria can be either fused with a tubular network appearance to ensure their survival against autophagy (Rambold *et al.*, 2011) or very fragmented with a round shape to allow mitochondrial dynamic, but also quality control since defective mitochondria can be easily degraded by autophagy (Otera, Ishihara and Mihara, 2013). The defects of these two processes have been associated to a range of mitochondrial diseases characterised by atrophy and degeneration of sensorimotor axons (Tilokani *et al.*, 2018).

Mitochondria are also involved in other cellular processes including cellular signalling, biogenesis of iron-sulphur clusters (Braymer and Lill, 2017), lipid synthesis (English and Voeltz, 2013), regulation of calcium homeostasis, different stress responses (Duchen, 2000, 2012; Schieber and Chandel, 2014; Chandel, 2015) as well as autophagy and apoptosis (Newmeyer and Ferguson-Miller, 2003).

ATP production is also accompanied by the generation of a basic level of reactive oxygen species like superoxide ion (O2-) as sub-products of the OXPHOS (CI and CIII) (Dröse and Brandt, 2012). The mitochondrial unfolded protein response (UPRmt) is a response to

mitochondrial stress caused by accumulation of misfolded proteins, leading to nucleus retro-signalling and activation of specific protective genes. It involves mitochondrial chaperone proteins like the heat shock proteins 10 or 60 (HSP10, HSP60). HSP60, commonly used as UPRmt marker, allows correct folding of the mitochondrial targeted proteins leading to reduction of mitochondrial stress (Zhao *et al.*, 2002; Mottis, Jovaisaite and Auwerx, 2014).

Finally, mitochondrial dysfunction and cellular stress dysregulation are involved in aging and human diseases (López-Otín *et al.*, 2013), aging being considered as a progressive impairment of physiological and vital functions often associated to pathologies like cardiovascular diseases, neurodegenerative disorders, diabetes, cancers, leading to death (Trifunovic *et al.*, 2004; Vermulst *et al.*, 2008; Quirós, Langer and López-Otín, 2015).

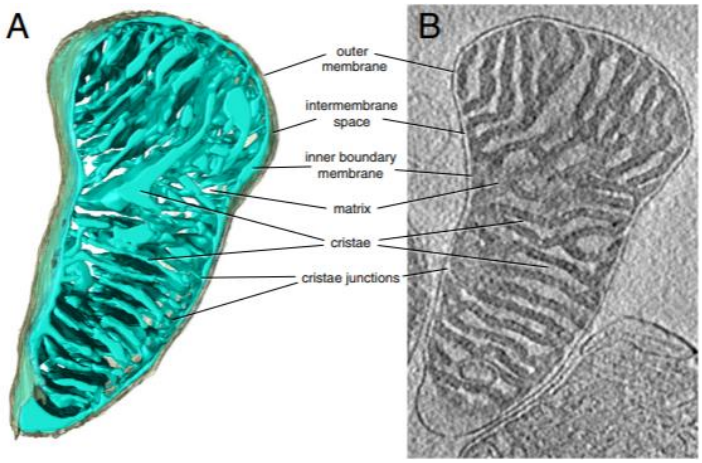


Figure 1. Mitochondrial compartmentalization (Kühlbrandt, 2015)***. A. 3D representation of a mouse mitochondrion. The inner membrane, in cyan, forms cristae protruding in the matrix, is surrounded by the outer membrane in grey. The intermembrane space represents the gap between both membranes. B. Tomography imaging of mouse mitochondrion. The matrix in light grey is traversed by cristae, invaginations of the inner membrane in dark grey. The intermembrane space appears like a clear line surrounding the inner boundary membrane. the outer membrane follows at about 20 nm.***

2. Mitochondrial DNA organisation

During evolution, mitochondria have retained their own genome. Consisting of a circular double-stranded DNA, localized in the mitochondrial matrix, mtDNA contains different number of genes and a different organisation in different species. In human, the mitochondrial genome of 16 kb does not contain any intronic regions, but a single long regulatory region called the D-loop that contains regulatory sequences for mtDNA replication and transcription.

Human mtDNA encodes 11 mRNAs translated into 13 proteins (2 mRNAs, ND4/ND4L and ATP6/ATP8, are bicistronic) that are core subunits of complexes I, III, IV and V forming the OXPHOS system, 2 rRNAs (12S and 16S) and 22 tRNAs required for synthesis of these subunits (Stewart and Chinnery, 2021).

The 37 genes are unevenly distributed across the double-stranded mitochondrial genome with a strand carrying most of the genes and a strand carrying one open reading frame for mt-ND6 and 8 tRNAs interspaced by non-coding regions.

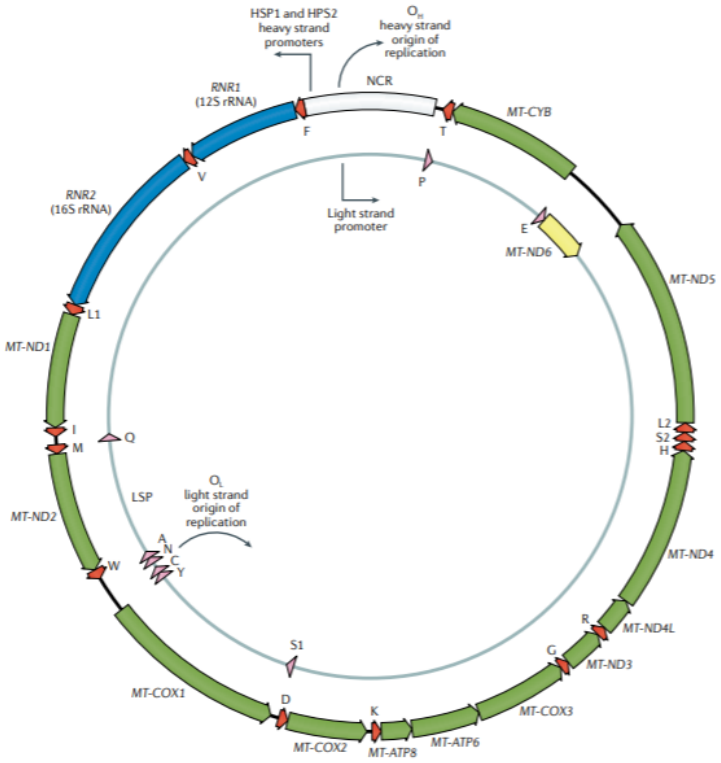


Figure 2. Map of the human mitochondrial genome (Stewart and Chinnery, 2021)***. The mtDNA is a circular double-stranded DNA molecule of 16 kb with a heavy strand, and a light strand. It encodes for core subunits of the most of OXPHOS complexes with MT-ND1 to MT-ND6 and MT-ND4L that belong to complex I, MT-CYB belonging to complex III, MT-CO1, MT-CO2 and MT-CO3 for complex IV, and MT-ATP6 and MT-ATP8 subunits of complex V. It also encodes for 22 tRNA and two rRNA genes. The noncoding region (NCR) includes the heavy strand origin of replication or displacement loop.***

2.1 Mt DNA replication

In human, mtDNA replication is carried out by a protein complex called the mitochondrial replisome, whose central component is the DNA polymerase- γ (POLγ), a trimer of one catalytic subunit (POLγA) and two accessory subunits (POLγB) that mediate interactions with DNA substrates (Fan L. et al., 2006). Other replisome proteins include the mtDNA helicase

TWINKLE, which unwinds the double-stranded mtDNA molecules at the replication forks (Garrido *et al.*, 2003) and the single strand binding (SSB) proteins responsible for maintaining the single strand conformation of the unwound mtDNA regions (Korhonen J.A. et al., 2004). The topoisomerases TOP1mt , TOP2α and TOP2β catalyse transient single-stranded and double-stranded mtDNA breaks and help relax the supercoiled DNA newly synthetised (Zhang *et al.*, 2001; H *et al.*, 2014). Finally, POLRMT, the mitochondrial RNA polymerase is also considered a replisome component and is responsible for syntheses of short RNA primers used to initiate mtDNA replication (Zhang *et al.*, 2001; Arnold *et al.*, 2012).

2.2 MtDNA transcription

MtDNA transcription starts in opposing directions from two strand-specific promoters located in the D-loop region, the light strand promoter (LSP) and the heavy-strand promoter (HSP). Transcription is carried out by the nuclear encoded mitochondrial RNA Polymerase (POLRMT). This enzyme contains a C-terminal catalytic domain and a N-terminal domain with a hairpin structure that has a role in separating RNA from DNA during transcription elongation. POLRMT also has a N-terminal extension with a pentatricopeptide repeat (PPR) domain known to bind RNA (Schwinghammer *et al.*, 2013). POLRMT, binding specifically to HSP and LSP, cannot initiate transcription efficiently without the help of the mitochondrial transcription factor A (TFAM) and mitochondrial transcription factor B2 (TFB2M) (Yakubovskaya *et al.*, 2014). TFAM can bind mtDNA without sequence specificity and plays a critical role in mtDNA compaction (Yakubovskaya *et al.*, 2014). During transcription, TFAM recruits POLRMT and TFB2M to the transcription start sites and creates a sharp U-turn in mtDNA to increase the contact (Ngo, Kaiser and Chan, 2011; Hillen *et al.*, 2017). TFB2M is part of the initiation complex and interacts with the promoter and POLRMT transiently before being replaced by the transcription elongation factor (TEFM) during transcript elongation (Sologub *et al.*, 2009; Hillen *et al.*, 2017).

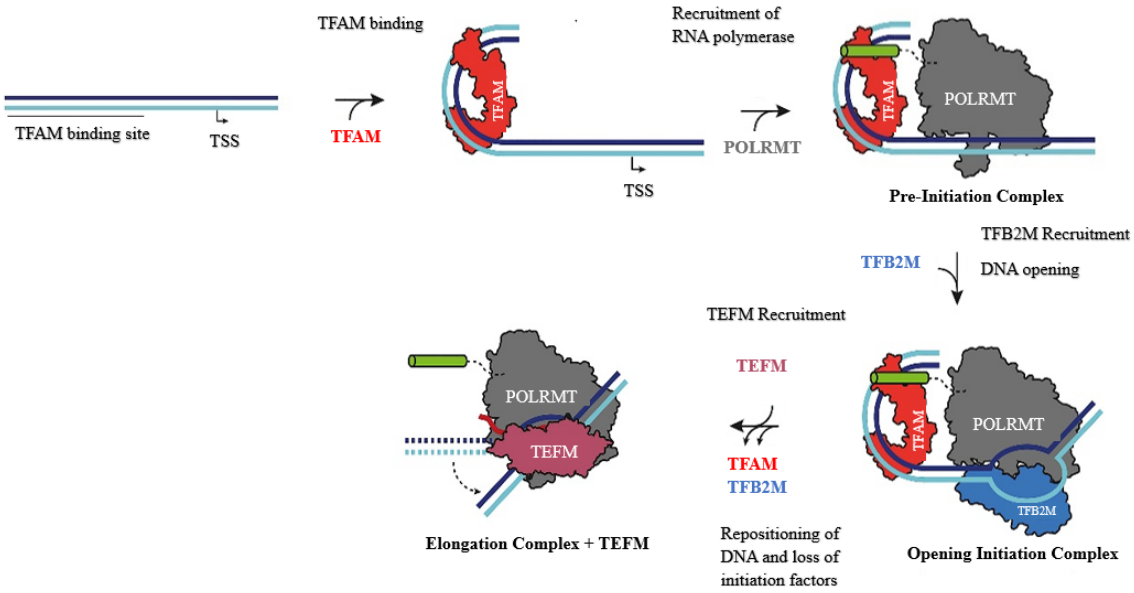


Figure 3. Initiation of mtDNA transcription adapted from (Hillen *et al.*, 2017). ***During transcription, TFAM (red) binds upstream of the transcription start site (TSS) and recruits POLRMT (grey) to form the pre-initiation complex and creates a U-turn in the mtDNA. Then TFB2M (blue) is recruited at the TSS to allow opening of mtDNA. The initiation complex transition into elongation complex with the release of TFAM et TFB2M, and the recruitment of TEFM.***

2.3 Transcript processing and maturation

MtDNA transcription from HSP- and LSP-promoters produces long polycistronic transcripts that are cleaved to produce mature mRNAs, tRNAs and rRNAs. Along the polycistronic transcripts, tRNAs are located between rRNAs and mRNAs. In addition, tRNAs 3'- and 5'-ends serve as nuclease recognition sites, according to the so-called "punctuation model for RNA processing". Thus, two ribonucleases intervene in transcript processing: the ribonuclease RNase P (composed of three subunits MRPP1, MRPP2 and MRPP3) cleaves the polycistronic precursor at its 5' end, while the ribonuclease RNase Z (ELAC2) cleaves at its 3' end, releasing tRNAs, rRNAs and mRNAs (Ojala, Montoya and Attardi, 1981). However, not all mRNAs are flanked by tRNAs. Such is the case for the mtND5-mtCYB, mtND4-mtND4L and mtCOX3-mtATP6-mtATP8. Maturation of mtND5 and mtCYB requires the involvement of pentatricopeptide repeat domain 2 (PTCD2) (Xu *et al.*, 2008). Releasing of the single mRNAs mtCOX3, mtATP6 and mtATP8 is made possible with of the involvement of PTCD3 homologue in yeast (Ellis *et al.*, 2004).

The mtDNA-encoded mRNAs do not contain any 5'-untranslated region (UTR) or they are very short as is the case of ATP6, as well as ATP8 (Temperley *et al.*, 2010). At their 3' ends, all mt-mRNAs except ND6, have a short a polyA tail (Temperley *et al.*, 2010; Ruzzenente *et al.*, 2012). These polyA tails of approximately 45 to 50 nt (Ojala, Montoya and Attardi, 1981) are synthesised by the mitochondrial polyA polymerase (mtPAP) (Tomecki *et al.*, 2004; Nagaike *et al.*, 2005) and may be involved in transcript stability or translation.

In addition, mitochondrial transcripts are subjected to other maturation events. For instance, they can undergo base and ribose modifications such as methylation or pseudouridylation that can affect their structure, function or stability (Suzuki and Suzuki, 2014). For tRNAs, the addition of three nucleotides CCA at their 3' ends, achieved by the CCA enzyme, is an important step for tRNAs biosynthesis and codon decoding process since CCA is the binding site of aminoacylation (Hou, 2010). Ribosomal RNAs can undergo methylations by various methyltransferases including TFB1M, NSUN4 (Metodiev *et al.*, 2014), RNMTL1, MRM1, and MRM2 (Lee et al., 2013), which can be essential for mitoribosomal assembly.

2.4 Mitochondrial translation

Mature mRNAs are translated in the mitochondrial matrix by a dedicated translation machinery giving rise to 13 proteins that are essential for the biogenesis of the OXPHOS system. These translation machineries include mitoribosomes and proteins directly involved in translation.

The mitoribosome is a complex formed by the small subunit (SSU) and the large subunit (LSU). The SSU contains the mitochondrial encoded rRNA 12S assembled with more than 29 nuclear-encoded proteins (MRPS). The LSU contains the 16S rRNAs assembled with 50 nuclear-encoded mitoribosomal proteins of the large (MRPL) subunit (Sharma *et al.*, 2003). Once fully assembled, SSU and LSU are connected by subunits that act as bridges. All protein components involved in mitochondrial translation like translation factors and MRP proteins are encoded by nuclear genes. Almost all tRNAs are mitochondrial encoded.

3. The oxidative phosphorylation (OXPHOS) system

Compared to glycolysis or fermentation, ATP production via OXPHOS inside mitochondria is the most efficient mechanism to produce energy for the cell (Bonora *et al.*, 2012). The OXPHOS system consists in five multi-subunits complexes (Complexes I through V) and is localized in the inner mitochondrial membrane. All complexes, except complex II that is entirely nuclear-encoded, contain both mtDNA- and nucleus encoded subunits. Thus, they have a dual genetic origin (Chaban, Boekema and Dudkina, 2014; Viscomi, 2016).

The flux of electrons generated by the release of two products from the TCA cycle, enter the ETC by the CI and CII respectively at the inner mitochondrial membrane. Then, this transfer of electrons from Complex I (CI) to Complex IV (CIV) (also forming the so-called respiratory chain) is coupled to proton pumping from the matrix to the intermembrane space by CI, CIII and CIV. This proton translocation generates a proton gradient on both sides of the inner mitochondrial membrane that is used by Complex V (ATP synthase or ATPase) to produce ATP.

Complex I (**CI**) is the first and the largest of the five OXPHOS complexes with an L shape extending into the matrix. It is also known as NADH-dehydrogenase, as it accepts pairs of electrons from NADH originating from Krebs cycle and transfers them to ubiquinone (Baradaran *et al.*, 2013). Complex I contains 45 different subunits (Khorsandi, Taanman and Heaton, 2017) including 7 subunits encoded by mtDNA (mtND1 to 6, mtND4L). At the level of CI, 4 protons are transferred across the inner membrane.

Complex II (**CII**) or succinate dehydrogenase is a secondary entry for electrons. Inside Krebs cycle, succinate dehydrogenase is essential for the oxidation of succinate involving FAD, to fumarate, with the release of $FADH_2$. Inside ETC, CII accepts pairs of electrons from $FADH_2$. Then, electrons generated from this reaction are transferred to ubiquinone CoQ_{10} at the limit of IMS. CII is composed of 4 subunits, (SDHA, SDHB, SDHC and SDHD), all of which are encoded by nuclear genes (Sun *et al.*, 2005; Bandara, Drake and Brown, 2021).

Complex III (**CIII**) (cytochrome reductase) accepts electrons from CII through the reduction of CoQ_{10}. It contains one subunit encoded by mtDNA, mtCYB, while the remaining subunits are encoded by nuclear DNA. CIII transfers the electrons to the electron shuttle cytochrome *c*, located in the intermembrane space. At this level, 4 protons are simultaneously transported across the inner membrane (Smith, Fox and Winge, 2012).

Complex IV (**CIV**) (cytochrome oxidase) is functional as a dimer and is composed of 13 subunits including COX1, COX2 and COX3 that are encoded by mtDNA (Capaldi, 1996; Shoubridge, 2001; Kadenbach, 2021). This complex accepts 4 electrons from the cytochrome *c* shuttle and transfer them through copper centres and heme groups to one molecule of oxygen (O_2). Simultaneously, 2 protons are pumped across inner membrane to intermembrane space. The transfer to oxygen produces 1 molecule of water (H2O), preventing the formation of intermediate reactive oxygen species (ROS): $2e^- + 2H^+ + 1/2O_2 = H_2O$

Complex V (**CV**) is composed of two functional subcomplexes: F_0, embedded in the mitochondrial inner membrane, and F_1, protruding in the mitochondrial matrix. The F_0 subcomplex forms a proton channel across the inner membrane, while the F_1 subcomplex is responsible for ATP phosphorylation. F_1 is found in the matrix, bound to F_0 by a subunit γ (that is involved in conformational changes of F_1). In the presence of proton gradient, three protons are returned to matrix through the F_0 channel, activating a rotation of the F_1 subunit that condenses ADP+Pi substrates (Boyer, 2000). Thus, newly synthetized ATP is released in the mitochondrial matrix. ATP molecules can pass through mitochondrial inner and outer membrane via specific channels (VDAC) and participate in cellular processes (Bonora *et al.*, 2012).

The consumption of one molecule of glucose in aerobic conditions contributes to the synthesis of 2 molecules of ATP during glycolysis, 2 molecules of ATP during Krebs cycle and 32 molecules of ATP during oxidative phosphorylation making OXPHOS the most efficient process to produce energy.

Mutations in either nuclear or mitochondrial genes can impair the assembly or function of the OXPHOS system and lead to the development of mitochondrial diseases (MD) in humans.

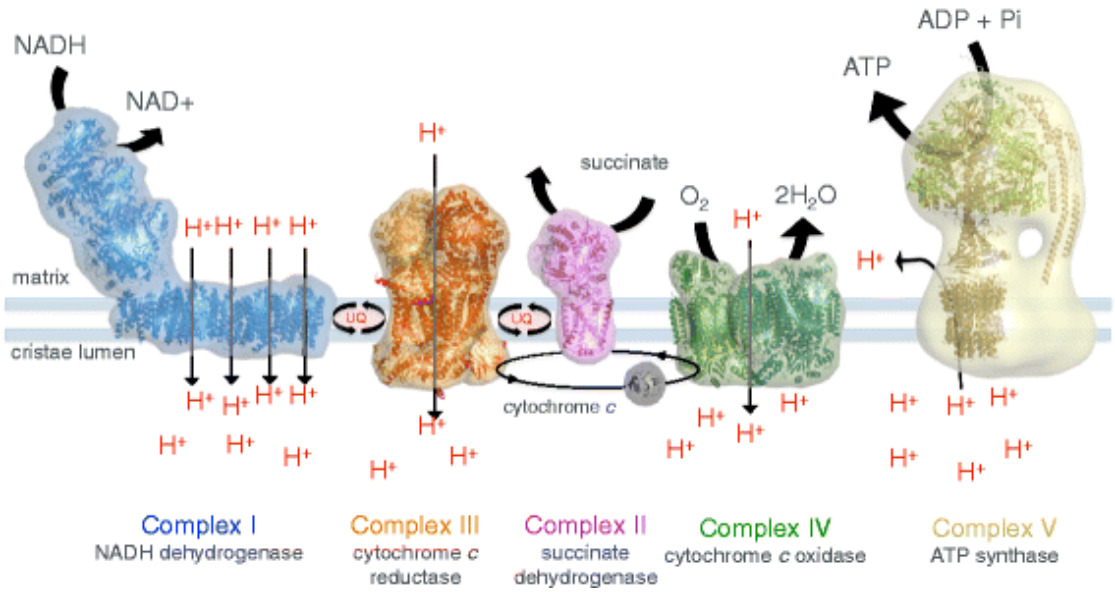


Figure 4. Schematic illustration of the oxidative phosphorylation system (OXPHOS) (Kühlbrandt, 2015)***. Electron transport chain (Complex I-IV) and Complex V or ATP synthase (light grey) form the OXPHOS system that provide energy, ATP, to the cell. Complex I or NADH dehydrogenase (blue) with its L-shape and Complex II or succinate dehydrogenase (pink), are the two entries for electrons, with the oxidation of NADH and $FADH_2$ respectively. Electrons are transferred to the different complexes via ubiquinone pools (UQ)between Complex I, Complex II and Complex III or cytochrome***

reductase (orange), and cytochrome shuttle between complex III and IV to its final acceptor, O_2, in complex IV or cytochrome c oxidase (green). As a result of the gradient of protons established by Complexes I, III and IV across inner membrane, 1 molecule of water is produced in complex IV. This gradient of proton finally drives the synthesis of ATP in complex V.

4. LRPPRC, an mRNA-stability factor involved in Leigh Syndrome

The Leucine Rich Pentatricopeptide Repeats Containing gene, *LRPPRC,* contains 38 exons, with a length of 100 kb (Gene ID: 10128, MIM 607544). It encodes for a 130 kDa protein located in mitochondrial matrix.

4.1 Structure

LRPPRC — with 35 amino acids repeat motif— belongs to the family of well conserved pentatricopeptide repeats (PPR) proteins, all of which carry a varying number of the so-called PPR motifs, that confers the ability of the family members to interact with nucleic acids. While more than 50 PPR proteins were found in plants, only 7 were reported in human. Human PPR proteins are all located in mitochondria where they are involved in various processes through their ability to interact with RNA, as exemplified by LRPPRC with 22 PPR domains or POLRMT with only 2 PPR repetitions (Lightowlers and Chrzanowska-Lightowlers, 2008, 2013).

4.2 Function of LRPPRC

LRPPRC, previously known as LRP130 was first described by Hou J., Wang F. and McKeehan W. L. in 1994. Working on HepG2 hepatoblastoma cells, initially to study liver heparin-binding fibroblast growth factors (FGF) receptors from 130 to 150 kDa, they observed a protein overexpressed in HepG2 cells at 130 kDa, (Hou, Wang and McKeehan, 1994). Hou and colleagues first produced specific Lrp-130 antisera in rabbit. Then, they prepared a HepG2 cDNA library inserted in *E.Coli*, and using the lysogenic capabilities of the transgenic expression vector phage λgtll. With an insertion of Lrp-130 cDNA in the expression cassette for the β-galactosidase, phage λgtll were used to screen the HepG2 cDNA containing -*E.Coli* library. The positive clones were able to produce fusion proteins β-galactosidase-Lrp-130 and to present antigens at their membranes; they were finally recognized by the antiserum Lrp-130 previously prepared in rabbit. They were finally able to determine a 4.7kb Lrp-130 cDNA clone encoding for a leucine-rich protein of 130 kDa. Southern, RACE-PCR and Northern hybridization analyses confirmed that the exact full-length of lrp130 cDNA was 4.8 kb, with 13% of its sequence occupied by leucine residues. They found LRP130 useful as a marker for

liver HepG2 cells detection (Young and Davis, 1983; Hou, Wang and McKeehan, 1994). Then, Ghiso and colleagues localised Lrp130 on the chromosome 2 (Ghiso and Lennon, 1994).

Then, the work of Mili S. and his team on ribonucleoprotein complexes involved in mRNAs maturation, highlighted 9 PPR motifs in lrp130 and confirmed an RNA-binding role via Matrix-assisted laser desorption ionization–time of flight (MALDI-TOF)-MS and MS-MS mass spectrometry analyses (Mili *et al.*, 2001). Tandem mass spectrometry (MS/MS) is a technique for analysing chemical, biochemical or biological samples by ionisation and separation of individual ions by weight and charge in two successive spectrometers for increased accuracy of identification. MALDI-TOF MS uses a laser to enable ionisation, to refine the analysis, in addition to its speed of analysis, which makes it very efficient.

Although previous work did not report LRP130 cDNA in murine tissues (Hou, Wang and McKeehan, 1994), Tsuchiya N. and his team performed northern blot analysis to redefine LRP130 mRNA expression in mouse and found strong expression in heart, liver and kidney, and weaker expression in the brain, skeletal muscle and testis. Using immunofluorescence, they were able to localize it at the perinuclear region, in the nucleus, and in the cytoplasm of NIH3T3 mouse fibroblasts (Tsuchiya *et al.*, 2002).

Lui L. and McKeehan W.L. reported 23 PPR motifs in LRPPRC by sequence homology analyses (Liu and McKeehan, 2002) and suggested, among others, a role in cytoskeletal networking and vesicles trafficking. Previous work did not report human LRP130 cDNA expression in other human tissues than hepatoblastomas (Hou, Wang and McKeehan, 1994). Northern analysis revealed human LRPPRC mRNA expression in all organs, although stronger in heart, skeletal muscle, kidney, and liver (Liu and McKeehan, 2002).

A study from Mili S. and Pinol-Roma S. co-localized LRPPRC with mitochondria, using immunofluorescence on Hela cells incubated with Mitotracker red, confirming a predominant localisation of LRPPRC in mitochondria (Mili and Piñol-Roma, 2003).

UV light-induced cross-linking experiment confirmed the RNA-binding function of LRPPRC previously established (Mili *et al.*, 2001). This experiment allowed to emphasize its role in mitochondrial RNA metabolism with an RNA-binding site localized at its C-terminal region.

With the advance in whole-genome datasets of RNA and protein expression, Mootha V.K. and his team discovered *LRPPRC* as the causing gene in Leigh syndrome, French-Canadian type (LSFC) (Mootha *et al.*, 2003).

In vivo studies also reported that LRPPRC acts as an RNA chaperon, allowing the folding of the mitochondrial transcripts. It has a vital role in the stabilization, polyadenylation, and translation of mitochondrial mRNAs. It is therefore necessary for regulation of mitochondrial gene expression, which is crucial to sustain OXPHOS and energy homeostasis (Ruzzenente *et al.*, 2012; Siira *et al.*, 2017).

Many of the molecular details of the function of LRPPRC were provided by the studies of patient skin fibroblasts carrying mutations in LRPPRC (Xu *et al.*, 2004; Sasarman *et al.*, 2010; Ruzzenente *et al.*, 2012; Burelle *et al.*, 2015; Oláhová *et al.*, 2015), or knockout (KO) mice (Ruzzenente *et al.*, 2012; Xu *et al.*, 2012; Cuillerier *et al.*, 2017).

Although LRPPRC is necessary for maintaining all mitochondrial mRNAs pools (Ruzzenente *et al.*, 2012), its defects in LSFC lead to combined CI+CIV deficiencies (Sasarman *et al.*, 2015)

LRPPRC also forms a complex with the stem-loop interacting RNA-binding protein (SLIRP) and they participate in mitochondrial mRNA polyadenylation (poly(A)) by maintaining poly(A) tail length. In KO mouse models of Lrpprc (Ruzzenente *et al.*, 2012; Cuillerier *et al.*, 2017), knockdown model of *LRPPRC* in Hela cells (Chujo *et al.*, 2012), mRNAs poly(A) tails were reduced. Although synthesis of poly(A) tails is mediated by mtPAP, the complex LRRPRC-SLIRP (Sasarman *et al.*, 2010) was proposed to allow recognition of mRNAs by mtPAP or to protect mRNAs from degradation by the polynucleotide phosphorylase (PNPase) (Chujo *et al.*, 2012; Ruzzenente *et al.*, 2012; Siira *et al.*, 2017). Further studies need to be achieved to confirm its exact role in poly(A) maintenance.

Finally, LRPPRC could be involved in tumorigenesis since Tian and colleagues work suggested downregulated apoptosis while LRPPRC level was increased in some tumours compared to normal tissues (Tian *et al.*, 2012). They also studied lung cancer samples and found activated caspase-3 positive cells with very low levels of LRPPRC. Thus, low levels of LRPPC down-regulated pro-survival Bcl-2 protein, key regulator of apoptosis (Tian *et al.*, 2012). LRPPRC also contributed to inhibition of mitophagy and autophagy, through interaction with mitochondrial membrane protein PARKIN, supporting its role in tumorigenesis (Zou *et al.*, 2014).

5. ELAC2, a protein with an RNase Z activity, involved in mitochondrial diseases

5.1 Structure of ELAC2

RNase Z or ELAC2 is a mitochondrial protein encoded by the nuclear gene, *ELAC2*, 25.6 kb localized on chromosome 17p12 (Gene ID: 60528, MIM 605367). This protein of 92 kDa and 826 amino acids is a mt-tRNA endoribonuclease, essential for mt-tRNAs maturation. First described in *E. coli* (S. Schiffer, S. Rosch, A. Marchfelder, 2002), RNAse Z, found in many eukaryotes, possess a metallo-beta-lactamase domain with a catalytic metal binding arm (de la Sierra-Gallay, Pellegrini and Condon, 2005), capable of hydrolysing phosphodiester bonds (Vogel *et al.*, 2002), essential for RNA processing. Thus, *Elac* genes are well conserved between species; they have been studied in yeast (*Saccharomyces cerevisiae*), flies (*Drosophila melanogaster*) and pigs (S*us domesticus*) (Takaku *et al.*, 2003; Dubrovsky *et al.*, 2004).

5.2 Function of ELAC2

Initially linked to prostate cancer (Rebbeck *et al.*, 2000; Tavtigian *et al.*, 2001), *ELAC2* encodes the protein ELAC2 involved in mitochondrial RNA processing (Takaku *et al.*, 2003; Dubrovsky *et al.*, 2004; Rossmanith, 2011). Notably, Nashimoto et al. suggested that the endoribonuclease activity of mammalian 3'tRNase allows cleavage of any RNA with a stem-loop structure and a "guide RNA" resembling the structure of the tRNA precursor (Nashimoto *et al.*, 1998). Thus, after purifying a pig liver 3'tRNase and submitting it to BLAST and GenBank, Takaku and colleagues were able to determine a 3'tRNase function for ELAC2. In an *in vitro* assay, they provided evidence that ELAC2, purified from a human testis cDNA library cloned in *E. coli*, was capable of cleaving the 3' downstream tRNA-Arginine precursor at a specific Guanine nucleotide (Takaku *et al.*, 2003).

Then, Rossmanith W., but also Brzezniak L.K. and colleagues, uncovered ELAC2 dual localization in cytoplasm and in mitochondria, by immunocytofluorescent experiments using EGFP-labelled ELAC2 in different human cells (Brzezniak *et al.*, 2011; Rossmanith, 2011). Rossmanith W. also identified an alternative initiation site for translation, 15 amino acids downstream from the first initiation site, responsible for a shortened ELAC2 (811 amino acids). This shorter ELAC2 was not able to localize to mitochondria anymore, suggesting the presence of a mitochondrial targeting sequence (MTS) in the first 15 amino acids.

The 16 kb mtDNA is transcribed into a long polycistronic precursor that is cleaved to allow the release of individual mRNAs, rRNAs and tRNAs, according to the so-called tRNA punctuation model, during RNA processing (Ojala, Montoya and Attardi, 1981). Specific endonuclease, RNase P, a complex of three nuclear encoded proteins, MRPP1, MRPP2, and MRPP3, first cleaves pre-tRNAs at 5' (Holzmann *et al.*, 2008). Brzezniak and colleagues showed that upstream tRNAs cleavage at 5' by the RNase P preceded downstream tRNAs cleavage at 3' by the tRNase activity of ELAC2 (Brzezniak *et al.*, 2011), allowing the release of individual mRNAs, rRNAs and tRNAs. Once trimmed, tRNAs undergo addition of CCA triplets to reach their mature form (Hou, 2010).

Finally, *ELAC2* mutations were recently associated to mitochondrial RNase Z defects, mainly leading to neurodevelopmental delay and cardiomyopathy associated to complex I deficiency (Haack *et al.*, 2013; Shinwari *et al.*, 2017; Saoura *et al.*, 2019). Interestingly , a transgenic *Drosophila melanogaster* model with specific mutations of *Elac2* already associated to cardiomyopathy in human (Migunova *et al.*, 2021), and a heart specific -conditional KO mouse model of Elac2 (Siira *et al.*, 2018) also led to cardiac hypertrophy, allowing to better understand its function, and highlighting the role of ELAC2/RNase Z in heart function in other species.

Additionally, *ELAC2* variants led to hereditary prostate cancer, with p.[Ser217Leu] and p.[Ala541Thr] being the variants leading to higher cancer risk (Rebbeck *et al.*, 2000; Tavtigian *et al.*, 2001; Xu *et al.*, 2010). Another study from Korver W. and colleagues predicted another tumorigenesis activity, and interaction with cytoskeletal protein gamma-tubulin. By overexpressing ELAC2 in Hela cells, they showed a delay in their cycle at G2, suggesting that down-regulation and mutations of ELAC2, may lead to tumour progression (Korver *et al.*, 2003).

II. Mitochondrial diseases

1. mitochondrial diseases definition

Mitochondrial diseases (MDs) are clinically, and genetically heterogeneous diseases with defects in OXPHOS and ATP production (Nunnari and Suomalainen, 2012; Ylikallio and Suomalainen, 2012). Mitochondrial diseases affect 1 in 5000 live births and are often associated with a negative prognosis in children (Tuppen *et al.*, 2010; Gorman *et al.*, 2015). They can occur in childhood or adulthood and mutations in many genes can cause mitochondrial diseases with similar or very different tissue-specific involvement. Typically, mitochondrial dysfunction affects tissues with high energy demand such as the brain, skeletal muscle and heart causing various neurological diseases, myopathy and cardiomyopathy; liver failure, nephropathies and even skin conditions have also been reported (Tuppen *et al.*, 2010; Duno *et al.*, 2013; Gorman *et al.*, 2015; Alston *et al.*, 2017; Craven *et al.*, 2017). To date, mutations in 338 nuclear and mitochondrial genes have been linked to mitochondrial diseases (Stenton and Prokisch, 2020).

2. Mode of inheritance

Mitochondrial diseases can be inherited as autosomal recessive, dominant and X-linked in the case of nuclear gene mutations or maternally for mtDNA mutations.

Autosomal dominant inheritance pattern requires only one mutant allele to cause the disease. It can affect males or females in different generations of the same family as exemplified by the type 1 Optic atrophy (OPA1), an autosomal dominant disease caused by mutations of the gene *OPA1* that encodes a mitochondrial inner membrane protein (Lefèvre *et al.*, 1998). Heterozygous mutations of *POLG1* and *POLG2*, coding for two subunits α and β of the DNA-polymerase POLG, are responsible for autosomal dominant progressive external ophthalmoplegia (PEO) and the onset of the disease is often in adulthood (Van Goethem *et al.*, 2001).

Autosomal recessive inheritance pattern requires that both alleles be mutants in order to cause a disease. In a family with an autosomal recessive inheritance mode, parents of an affected child (with two affected alleles) represent “healthy carriers” since each one carry only one mutant allele. This mode of inheritance is mostly seen in pediatric cases; for instance, mutations in *SURF1* encoding an assembly factor of the OXPHOS complex IV (Zhu *et al.*, 1998), mutations in *CARS2* encoding the mitochondrial cysteinyl-tRNA synthase gene (Coughlin *et al.*, 2015),

or mutations in *DARS2* coding for the mitochondrial aspartyl-tRNA synthetase (Stellingwerff *et al.*, 2021).

X-linked inheritance affects mainly male individuals from a family with no male-to-male transmission. Barth syndrome is the most frequent X-linked mitochondrial disease characterised by cardiomyopathy (CM), skeletal myopathy, growth delay, neutropenia and increased urinary excretion of 3-methylglutaconic acid (3-MGCA) (Bione *et al.*, 1996). Patients present mutations in *TAFAZZIN* gene encoding a mitochondrial transacylase that catalyzes remodeling of immature cardiolipin to its mature form. This is also the case for *NDUFA1* gene coding for a subunit of OXPHOS complex I located on the X chromosome whose mutations are known to lead to progressive neurodegeneration (Mayr *et al.*, 2011). The microphthalmia with linear skin defects syndrome (MLS) is also an X-linked disease caused by mutations in the gene *HCCS* that encodes the mitochondrial holocytochrome *c*–type synthase that is involved in precursors of soluble cytochrome *c* (Wimplinger *et al.*, 2006). Defects in the pyruvate dehydrogenase (PDH) complex caused by mutations in the X-linked pyruvate dehydrogenase (E1) subunit gene (*PDHA1*) are another manifestation of mitochondrial diseases in children and lead to primary lactic acidosis. Clinical symptoms are heterogeneous and can manifest as ataxia to a severe retardation, neurological defects, and early death (Lissens *et al.*, 2000).

Mitochondrial DNA mutations are maternally inherited. During fecundation, mitochondria from the male gamete are destroyed leaving only mitochondria from the female gamete. To date, we know more than 200 point-mutations in mtDNA leading to mitochondrial diseases (Wong, 2007). Mitochondrial encephalomyopathy with lactic acidosis and stroke-like episodes (MELAS) is an early-onset clinical presentation linked to the common point mutation (m.3243A>G) (Sproule and Kaufmann, 2008). Leber hereditary optic neuropathy (LHON) is another disease of maternal inheritance that affects adults and is characterized by a visual failure often leading to loss of acuity before 50 years of age. It is commonly caused by mtDNA mutations in *MT-ND1*, *MT-ND4* and *MT-ND6*, subunits of complex I. (Yu-Wai-Man and Chinnery, 1993). NARP, for neurogenic muscle weakness, ataxia, and retinitis pigmentosa, appears during childhood and stays stable for years. Two pathogenic variants, m.8993T>G and m.8993T>C are among the most common mutations in *MT-ATP6* associated to NARP (Holt *et al.*, 1990; Rantamäki *et al.*, 2005).

MtDNA mutations can be either homoplasmic, when all copies of mtDNA share the same genotype, or heteroplasmic when both wild type and mutant mtDNA molecules co-exist. In the

latter case, disease severity often correlates with the level of heteroplasmy (Hayashi *et al.*, 1991; Tuppen *et al.*, 2010; Craven *et al.*, 2017). However, although selections mechanisms allow to circumvent certain mutations (amino acid substitutions, selection against embryos with pathogenic tRNA mutations, decreased fertility in highly mutated female gametes), the bottleneck effect can surprisingly increase the mutation load in the offspring while the mother only carries mutations, leading to mitochondrial diseases in the next generation (Taylor and Turnbull, 2005).

For example, the heteroplasmy level defines severity of the phenotypes caused by mutations m.8993T>G/C in *MT-ATP6*: a heteroplasmy level with 70% to 90% of mutants will result in NARP, while a heteroplasmy with more than 90% of *MT-ATP6* variants will result in the more severe maternally inherited Leigh syndrome (MILS) (Uziel *et al.*, 1997; Claeys *et al.*, 2016).

MtDNA deletions (rearrangements) are also linked to mitochondrial diseases (Srivastava, 2017). The Pearson syndrome occurs during infancy and cause pancreatic insufficiency, anaemia, and bone-marrow defects, due to ubiquitous rearrangements in mtDNA, generally leading to early lethality (Rötig *et al.*, 1990).

Also due to rearrangements in mtDNA, Kearns-Sayre syndrome develops before adulthood and is characterized by progressive loss of visual acuity and retinopathy associated with a wide range of symptoms (cerebellar ataxia, deafness, cognitive impairment, cardiomyopathy, endocrinopathies and dysphagia) (Maceluch and Niedziela, 2006).

3. Diagnosis of mitochondrial diseases

Diagnosis of mitochondrial diseases relies on several techniques including clinical, biochemical, histological, enzymatic, imaging, and genetic investigations (Gorman *et al.*, 2015). Although it may remain difficult due to heterogeneity of symptoms from one patient to another, mitochondrial disease diagnosis attempts to ensure rapid and efficient recognition of the disease for patients and their families in most cases, and allows the best available counselling or treatments to be provided (Vento and Pappa, 2013; Avula *et al.*, 2014; Craven *et al.*, 2017)

3.1 Clinical presentation

Mitochondrial diseases can manifest at any age although they are most commonly present during infancy. They can affect any organ and system in the body (Fig. 5). Some clinical presentations are limited to a single organ like LHON disease, but most of patients present a multisystemic disease with the brain, muscles (including heart), liver and sensory organs (eyes and ears) being the most affected (Munnich and Rustin, 2001; Auré, Jardel and Lombès, 2005; McFarland, Taylor and Turnbull, 2010; Gorman *et al.*, 2016).

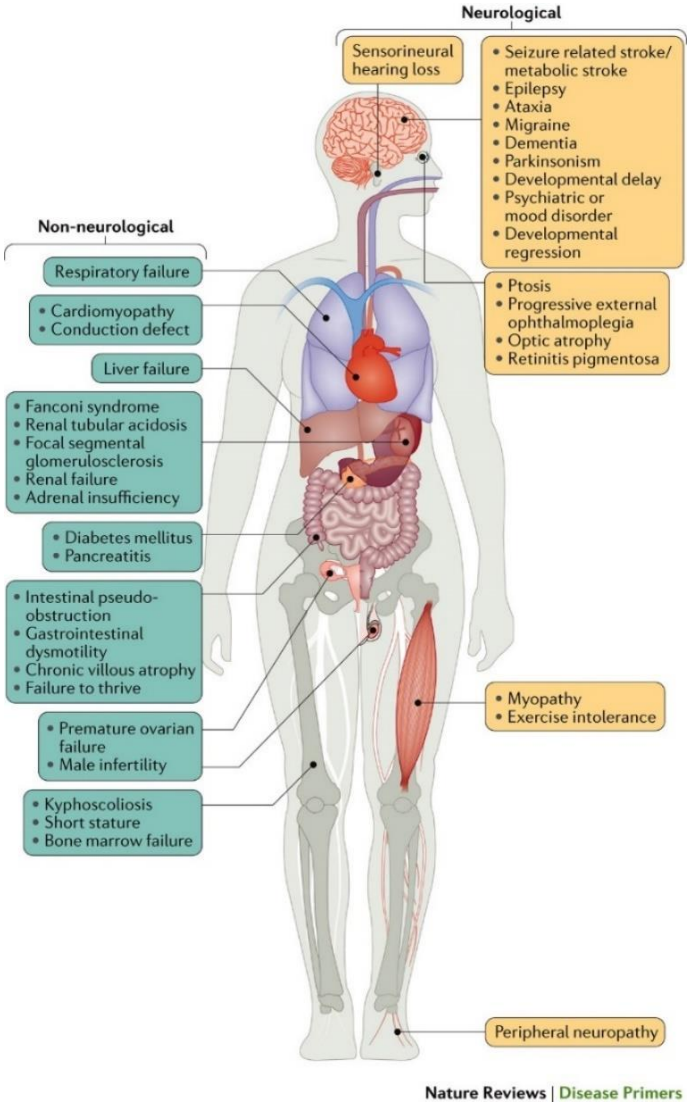


Figure 5. Clinical presentation of mitochondrial diseases, (Gorman *et al.*, 2016)***. Schematic image of mitochondrial disease associated to neurological and non-neurological clinical phenotypes.***

3.2 Biochemical analyses

Metabolic investigations are meant to reveal accumulation of substrates like lactate, TCA cycle intermediates, creatine kinase or amino acids in blood plasma, organic acids in urine (but also decrease of pyruvate) by mass spectrometry. High levels of lactate in plasma suggest an impairment of the OXPHOS system. Some mitochondrial diseases including Leigh syndrome are characterized by hyperlactatemia and hyperlactatorachia, although 10–20% of patients with mitochondrial disease have normal lactate levels. (Munnich *et al.*, 1996; Touati *et al.*, 1997; Debray *et al.*, 2011; Rodenburg, 2011; Semeraro *et al.*, 2018).

3.3 Histological analyses

In affected tissues, certain histochemical changes may be indicative of OXPHOS deficiency. From muscle biopsies, histological sections are obtained and stained with different techniques to identify underlying mitochondrial deficiencies. In patient's muscles, mitochondria may have an abnormal proliferation that give a ragged red fibres peculiar aspect after staining with modified Gömöri-trichrome (Pavlakis *et al.*, 1984; Velez-Bartolomei, Lee and Enns, 1993).

Another commonly used histochemical technique is the COX/SDH staining that allows the identification of cells with deficient cytochrome *c* oxidase (COX, complex IV) activity compared to succinate dehydrogenase (SDH, Complex II) activity. The catalytic site of COX is encoded by mtDNA while SDH is entirely made of nuclear encoded subunits, therefore defects in mtDNA, transcript processing and maturation do not affect integrity of CII. In this method, functioning COX is detected by a brown staining obtained by the electron donor diaminobenzidine (DAB) that will produce a brown saturated polymer in cristae. Functioning SDH is detected by the electron acceptor nitroblue tetrazolium (NBT), that will be reduced by CII and give a final blue stained product. If brown staining is decreased, it suggests a decreased activity of CIV. Usually, double staining with COX staining first, then SDH staining, allows a better location of isolated defective cells (Ross, 2011).

3.4 OXPHOS activity

Diagnostic tests include polarographic and spectrophotometric studies, each provides an independent clue towards the diagnosis of OXPHOS deficiency. Polarographic studies consist in measurement of oxygen consumption by mitochondria-enriched fractions, using a Clarke

electrode in the presence of various oxidative substrates (malate + pyruvate, malate + glutamate, succinate, palmitate, etc...) (Ogawa *et al.*, 2017) (Rustin *et al.*, 1994; Munnich and Rustin, 2001). Spectrophotometric studies involve isolated or combined respiratory enzyme assays, using specific electron donors and acceptors (Frazier and Thorburn, 2012).

3.5 Imaging analyses

Since many mitochondrial diseases are characterized by neurological symptoms, brain magnetic resonance imaging (MRI) constitutes a non-invasive procedure to diagnose such diseases. In some diseases, like Leigh syndrome (Leigh, 1951), characteristic lesions in specific regions of the brain allow to define a neuropathological profile and suggest specific OXPHOS complexes' defects or specific genes in cause (Lebre *et al.*, 2011; Bricout *et al.*, 2014). In the case of anormal lactatemia, specific proton magnetic resonance spectroscopy analysis (1H-RMN) allows to identify increased lactate level in specific regions of the brain (Lin, Crawford and Barker, 2003).

3.6 Genetic diagnosis of mitochondrial diseases

Genetic diagnosis of mitochondrial diseases is mainly done by next-generation sequencing technologies like whole genome sequencing (WGS), whole exome sequencing (WES), or targeted exome sequencing (TES), as well as gene panel screening (Carroll, Brilhante and Suomalainen, 2014). These approaches allow the detection of mutations by screening the whole genome, exome or targeted coding sequences (Bannwarth *et al.*, 2013; Carroll, Brilhante and Suomalainen, 2014).

The detection of mtDNA deletions is also carried out using long range PCR amplification of mtDNA for a rapid identification (Cortopassi and Arnheim, 1990). The detection and heteroplasmy quantification of MELAS mutation m.3243A>G for instance, has been carried out by using specific techniques based on PCR amplification and enzymatic digestion (Bannwarth, Procaccio and Paquis-Flucklinger, 2005).

4. Leigh syndrome

One of the most common clinical presentations of mitochondrial disease in paediatric patients is Leigh syndrome (LS) (Leigh, 1951; Hommes, Polman and Reerink, 1968; Willems *et al.*, 1977; Ruhoy and Saneto, 2014; Lake *et al.*, 2016a). . Initially depicted as a subacute necrotizing encephalomyelopathy (SNE), Leigh syndrome (LS) is a neurological disease (characteristic subacute attacks affecting the central nervous system) with an incidence of 1 in 40,000. Neuroimaging reveals characteristic lesions in basal ganglia and brainstem, but also in the cerebellum, in thalamus, white matter and spinal cord. With subacute deteriorations (attacks), followed by stabilization or mild improvement, Leigh syndrome is characterized by progressive loss of mental and motor abilities. These attacks often lead to death within early infancy, due to respiratory failure. Mutations in more than 75 genes, either nuclear or mitochondrial, that lead to defects in the OXPHOS system and ATP production, have been linked to LS (Gerards, Sallevelt and Smeets, 2016; Lake *et al.*, 2016b).

4.1 Clinical and biochemical characteristics of LS

More than 80% of patients develop symptoms of LS during infancy, with an average before the age of 2 (Thorburn, Rahman and Rahman, 1993; Sofou *et al.*, 2014). However, in some cases, the onset of the disease may also occur in adolescence or adulthood (McKelvie *et al.*, 2012). Infantile presentation includes neurodevelopmental delay or regression, with respiratory dysfunction, failure to thrive, vomiting episodes and hypotonia. Patients present with walking difficulties associated with dysarthria and dystonia (Baertling *et al.*, 2014; Ruhoy and Saneto, 2014). Later in childhood and adolescence, patients present progressive symptoms like respiratory dysfunction, rigidity, dystonia, and cerebellar ataxia but can remain stable for years (Huntsman *et al.*, 2005). Adulthood onset LS can have heterogeneous presentation with common symptoms of infant-onset LS, headaches accompanied with memory loss and ocular impairment, digestive, and respiratory troubles (McKelvie *et al.*, 2012).

Neurodevelopmental delay, hypotonia, dystonia, seizures, movement disorders, ataxia, hearing loss and dysphagia are related to the different areas affected in midbrain, basal ganglia, and cerebellum; brainstem involvement can manifest with respiratory and swallowing difficulties, but also with ophthalmological symptoms (ptosis, retinis pigmentosa and optic atrophy). The peripheral nervous system can also be involved with myopathy (Finsterer, 2008; Baertling *et*

al., 2014). Cardiomyopathy, liver failure, and renal symptoms are part of the multisystemic presentation that accompanies LS (Sofou *et al.*, 2014).

Biochemical analyses of most LS patients reveal high levels of lactate or alanine in blood or cerebrospinal fluid (Sofou *et al.*, 2014). Local increase of lactate in specific brain regions can also be detected by proton magnetic resonance spectroscopy (Baertling *et al.*, 2014). Histochemical analyses can reveal COX-defective fibres in muscle biopsies of LS patients while biochemical analyses detect isolated or multiple OXPHOS defects, typically CI or CIV deficiencies (Finsterer, 2008; Baertling *et al.*, 2014; Ruhoy and Saneto, 2014; Sofou *et al.*, 2014).

4.2 Genetics of LS

Development of NGS and exome/genome sequencing increased the pace of identification of new genes involved in LS. To date, known genes linked to LS include those encoding subunits of the OXPHOS system or assembly factors, mtDNA maintenance, mitochondrial translation, pyruvate, fatty acids or thiamine metabolism, TCA enzymes (Table 1).

Gene	**Function**	**Location**	**Reference**
BCS1L	Assembly factor of C III	Nuclear	(de Lonlay *et al.*, 2001)
C12ORF65	Mt translation release factor	Nuclear	(Antonicka *et al.*, 2010)
COX3	Subunit of CIV	Mitochondrial	(Tiranti *et al.*, 2000)
COX10	synthesis of human hemeA assembly of CIV	Nuclear	(Valnot *et al.*, 2000; Antonicka *et al.*, 2003)
COX15	synthesis of human hemeA assembly of CIV	Nuclear	(Oquendo *et al.*, 2004)
DLD	Pyruvate dehydrogenase, PDH (E3)	Nuclear	(Grafakou *et al.*, 2003)
ECHS1	Fatty acid beta-oxidation	Nuclear	(Ganetzky and Stojinski, 1993)
IARS2	Ile-tRNA synthetase	Nuclear	(Schwartzentruber *et al.*, 2014)
FOXRED1	Assemby and stabilisation factor of CI	Nuclear	(Calvo *et al.*, 2010)

GFM2	Mt ribosome recycling factor	Nuclear	(Fukumura *et al.*, 2015)
LIPT1	Lipoyltransferase, PDH metabolism	Nuclear	(Soreze *et al.*, 2013)
LRPPRC	Mt-RNA stability	Nuclear	(Merante *et al.*, 1993; Morin *et al.*, 1993)
MT-ATP6	Subunit of CV	Mitochondrial	(Tatuch *et al.*, 1992)
MT-ND1	Subunit of CI	Mitochondrial	(Moslemi *et al.*, 2008)
MT-ND2	Subunit of CI	Mitochondrial	(Ugalde *et al.*, 2007)
MT-ND3	Subunit of CI	Mitochondrial	(Taylor *et al.*, 2001)
MT-ND4	Subunit of CI	Mitochondrial	(Komaki *et al.*, 2003)
MT-ND5	Subunit of CI	Mitochondrial	(Taylor *et al.*, 2002)
MT-ND6	Subunit of CI	Mitochondrial	(Kirby *et al.*, 2000)
MRPS34	Protein of the small mitoribosomal subunit	Nuclear	(Lake *et al.*, 2017)
MTFMT	Mt-methionyl-tRNA formyltransferase	Nuclear	(Tucker *et al.*, 2011)
MT-TK	Mt tRNA-Lysine	Mitochondrial	(Shtilbans *et al.*, 2000)
MT-TL1	Mt tRNA-Leucine	Mitochondrial	(Vilarinho *et al.*, 1997)
MT-TV	Mt tRNA-Valine	Mitochondrial	(Chalmers *et al.*, 1997)
MT-TW	Mt tRNA-Tryptophan	Mitochondrial	(Santorelli *et al.*, 1997)
NARS2	Mt-asparaginyl-tRNA synthetase	Nuclear	(Simon *et al.*, 2015)
NDUFA1	Subunit of CI	Nuclear (X-linked)	(Fernandez-Moreira *et al.*, 2007)
NDUFA2	Subunit of CI	Nuclear	(Hoefs *et al.*, 2008)
NDUFA4	Subunit of CIV	Nuclear	(Pitceathly *et al.*, 2013)
NDUFA9	Subunit of CI	Nuclear	(van den Bosch *et al.*, 2012)
NDUFA10	Subunit of CI	Nuclear	(Hoefs *et al.*, 2011)
NDUFA12	Subunit of CI	Nuclear	(Ostergaard *et al.*, 2011)

NDUFAF5	Assembly factor of CI	Nuclear	(Gerards *et al.*, 2010)
NDUFAF6	Assembly factor of CI	Nuclear	(Bianciardi *et al.*, 2016)
NDUFS1	Subunit of CI	Nuclear	(Bénit *et al.*, 2001)
NDUFS3	Subunit of CI	Nuclear	(Bénit *et al.*, 2004)
NDUFS6	Subunit of CI	Nuclear	(Rouzier *et al.*, 2019)
NDUFS7	Subunit of CI	Nuclear	(Triepels *et al.*, 1999)
NDUFS8	Subunit of CI	Nuclear	(Loeffen *et al.*, 1998)
PDHA1	PDH subunit (E1α)	Nuclear (X-linked)	(Matthews *et al.*, 1993)
PDHB	PDH subunit (E1β)	Nuclear (X-linked)	(Quintana *et al.*, 2009)
PDHX	PDH subunit (E3BP)	Nuclear (X-linked)	(Schiff *et al.*, 2006)
PDSS2	Ubiquinone synthesis	Nuclear	(López *et al.*, 2006)
PET100	Biogenesis of CIV	Nuclear	(Lim *et al.*, 2014)
PNPT1	RNA-binding protein, PNPase	Nuclear	(Matilainen *et al.*, 2017)
POLG	Subunit of MtDNA polymerase (POLγ)	Nuclear	(Scalais *et al.*, 2012)
SCO2	Assembly factor of CIV	Nuclear	(Papadopoulou *et al.*, 1999)
SDHA	Subunit of CII	Nuclear	(Bourgeron *et al.*, 1995)
SDHAF1	Assembly of CII	Nuclear	(Ohlenbusch *et al.*, 2012)
SLC19A3	Thiamine transport	Nuclear	(Gerards *et al.*, 2013)
SUCLA2	TCA enzyme and Mt DNA maintenance	Nuclear	(Elpeleg *et al.*, 2005; Ostergaard *et al.*, 2007)
SUCLG1	TCA enzyme and Mt DNA maintenance	Nuclear	(Van Hove *et al.*, 2010)
SURF1	Assembly factor of CIV	Nuclear	(Tiranti *et al.*, 1998)
TACO1	Translational activator of CIV	Nuclear	(Weraarpachai *et al.*, 2009)
TPK1	Thiamine transport and metabolism	Nuclear	(Fraser *et al.*, 2014)

TRMU	Mt-specific tRNA-modifying enzyme	Nuclear	(Sala-Coromina *et al.*, 2021)
TSFM	Mt translation elongation factor	Nuclear	(Scala *et al.*, 2019)
TTC19	Assembly of CIII	Nuclear	(Atwal, 2013)
UQCRQ	Subunit of CIII	Nuclear	(Barel *et al.*, 2008)

Table 1. Recapitulative table of genes involved in Leigh syndrome. Genes linked to LS include those encoding subunits of the OXPHOS system or assembly factors, ubiquinone, mtDNA maintenance, mitochondrial translation processes, pyruvate metabolism, TCA enzymes as well as thiamine metabolism. The mode of inheritance is maternal, X-linked, or autosomal recessive. CI-CV, complex I-V; Mt, mitochondrial; PDH, pyruvate dehydrogenase.

4.3 LRPRPC and LS

The protein LRPPRC drew interest when it has been linked to Leigh Syndrome French Canadian variant (LSFC), using proteomic and transcriptomic technics. In a cohort of patients presenting with LS, V.K Mootha and colleagues mapped the LSFC gene to chromosome 2p16-21 (Mootha *et al.*, 2003). In this region, the authors identified 15 genes, 6 of which did not yet have a known function. Transcriptomic and proteomic analyses were used to identify a single gene candidate for LSFC—LRPPRC.

LSFC is an early-onset progressive neurodegenerative disorder with a distinct pattern of tissue involvement. In addition to the common neurological involvement observed in LS patients, affected infants present with liver failure and lactic acidosis, and mortality occurs after a fatal metabolic crisis (Merante *et al.*, 1993; Morin *et al.*, 1993). LSFC patients develop severe symptoms and face early lethality at a median age of 2.6 years old (Debray *et al.*, 2011).

The homozygous c.1061C>T, p.(Ala354Val) variant has been linked to LSFC. Due to a founder effect, this variant has an unusually high carrier frequency (1 in 23) in the Saguenay-Lac-Saint-Jean (SLSJ) population and affects 1 in 2000 births (Morin *et al.*, 1993). In addition, some patients also carried the C1277Xdel8 variant (Debray *et al.*, 2011).

At molecular level, LSFC patients present reduced abundance of LRPPRC, and exhibit CIV deficiency in fibroblasts and muscle biopsies (Xu *et al.*, 2004; Gohil *et al.*, 2010; Sasarman *et al.*, 2010, 2015; Debray *et al.*, 2011; Burelle *et al.*, 2015). A study of tissue-specific responses to the p.Ala354Val mutation in LSFC revealed a tissue-dependant modulation of CIV levels

(Sasarman *et al.*, 2015). Interestingly, by analysing complexes in their native form by Blue-native polyacrylamide gel electrophoresis (BN-PAGE), CIV defects appeared milder in heart compared to liver, although LRPPRC was decreased in all affected tissues. High levels of CI and CIII were detected in both organs, which probably represents a compensatory mechanism for CIV defects. These results suggest a specific adaptation of tissues towards LRPPRC mutations. To address this issue, mitochondria extracts were subjected to sucrose gradient fractionation, Sasarman and colleagues observed a decrease in small mitoribosomal subunits in liver of patients compared to the heart where both mitoribosomal subunits were increased, suggesting a compensatory mechanism aimed at overcoming the OXPHOS deficiency in the heart. A difference was also observed between immunoblot analyses of cultured patient fibroblasts, myoblasts and differentiated myotubes. Although LRPPRC was reduced to 20-30% in the three cell types, CIV subunits were more reduced in myoblasts. Myoblasts and myotubes cultures also showed a combined CI+CIV defects in BN-PAGE, compared to patients' fibroblasts with only CIV assembly defects.

Although they develop severe neurological disorders and liver failure, patients with LSFC usually die of a metabolic crisis and fatal lactic acidosis, probably due to these liver failures. During lactic acidosis, elevated lactate levels are associated with either increased production or decreased clearance by the liver or kidney, thus increasing the risk of mortality. If OXPHOS is defective, pyruvate enters the Cori cycle or lactic acid cycle, the alternative pathway (Cori, 1981; Soeters *et al.*, 2021), increasing lactate production by the more demanding peripheral organs. Excessive production can exceed the capacity of the liver and kidneys to absorb lactate and metabolise it into glucose (Foucher and Tubben, 2022).

In LSFC, among other organs, CIV activity is also decreased in brain and liver, leading to hepatopathy (steatosis) (Merante *et al.*, 1993). Thus, the inability of liver to process lactate could explain defects in lactate homeostasis resulting in metabolic crises and early lethality.

To date, more than 13 variants of LRPPRC, have been linked to Leigh syndrome. Regardless of the mutations, the patients present with severe lactic acidosis and early-onset neurodevelopmental problems, together with either cardiomyopathy, congenital malformations, or liver failure.

Variants	Geographic region, Country	Clinical features summary	References
homozygous c.1061C>T, p.(Ala354Val)	SLSJ, Canada	Developmental delay, ataxia, lactic acidosis, dysmorphic facial features, hypotonia, hirsutism, microvesicular steatosis	(Merante *et al.*, 1993; Morin *et al.*, 1993; Mootha *et al.*, 2003)
compound heterozygous c.1061C>T, p.(Ala354Val) / c.3830_3837del, p.(Cys1277*)	SLSJ, Canada	Developmental delay, failure to thrive, dysmorphic facial features, lactic acidosis, neurological acute crisis (Leigh syndrome and/or stroke-like episodes)	(Debray *et al.*, 2011)
homozygous c.3900+1G>T p.(Gly1050Argfs*4)	India, Pakistan	Microcephaly, coagulopathy, hypotonia, mild dysmorphic facial features with broad nasal bridge, mild hirsutism, failure to thrive, cardiac malformation, lactic acidosis with ketosis, micrognathia, polysyndactyly and hypospadias, renal impairment with raised creatinine , kidneys and intestinal dysfunctions	(Oláhová *et al.*, 2015)
compound heterozygous c.3147dupA / c.1582+7A>G	United Kingdom	Severe encephalopathy, seizures, hypotonia, lactic acidosis	(Oláhová *et al.*, 2015)
homozygous c.2726_2728delAGA	Iraq	Developmental delay, hypotonia, trunk ataxia, dysmetria, esotropia of the eye, motor regression, dysphagia, arterial hypertension, ventricular hypertrophy	(Oláhová *et al.*, 2015)
homozygous c.2595_2597delGGT	Turkey	Lactic acidosis, tachypnoea, hypotonia, dystonia, hypospadias, inguinal hernia, mild hypertrophic cardiomyopathy, acute respiratory failure	(Oláhová *et al.*, 2015)
compound heterozygous	China	Developmental delay, encephalopathy, hypotonia,	(Han *et al.*, 2017)

c.3130C>T / (p.Arg1044Cys) c.3430C>T / (p.Arg1144Cys) c.4078G>A (p.Ala1360Thr)		dystonia, brachycephaly, hypopigmented hair, swallowing dysfunction, reflux disease, orofacial and limb dyskinesias, refractory multifocal epilepsy, sleep apneas, mild intermittent metabolic acidosis	
compound heterozygous c.1921–7A > G / c.2056A > G (p. Ile686Val)	Italy	Bilateral adducted thumbs, dysmorphic facial features, right exophoria, mild diffuse cerebral atrophy, hypoplasia of the corpus callosum, cerebellar vermis hypoplasia and bilateral incomplete hippocampal inversion, hearing loss	(Piro *et al.*, 2020)

Table 2. Recapitulative table of LSFC variant mutations in different geographic regions. Most of the cases present developmental delay, lactic acidosis, dysmorphic facial features and hypotonia. SLSJ: Saguenay-Lac-Saint-Jean.

4.4 Brain structures involved in LS and their development

During embryogenesis, the ectoderm gives rise to the central nervous system (CNS). At early stage, the neural tube is divided into three distinct regions: the prosencephalon that will give the cerebral cortex, the mesencephalon that will give the midbrain and the rhombencephalon that will become the hindbrain (Ángeles Fernández-Gil *et al.*, 2010).

The prosencephalon is divided into telencephalon, where the cerebral hemispheres are located, and the diencephalon at posterior position. The hindbrain is divided into the metencephalon and the myelencephalon: The metencephalon is consisting of the *pons*, the cerebellum, and the intermediate structure of the fourth ventricle; the myelencephalon is comprising the lower part of the CNS, the *medulla oblongata*, and the lower part of the fourth ventricle. The midbrain is not divided into additional segments.

The brainstem constitutes the lower ventral part of the CNS, connecting the brain, the cerebellum and the spinal cord, and is composed of four structures: the diencephalon (basal ganglia, thalamus, and hypothalamus), the midbrain, the *pons* and the medulla oblongata.

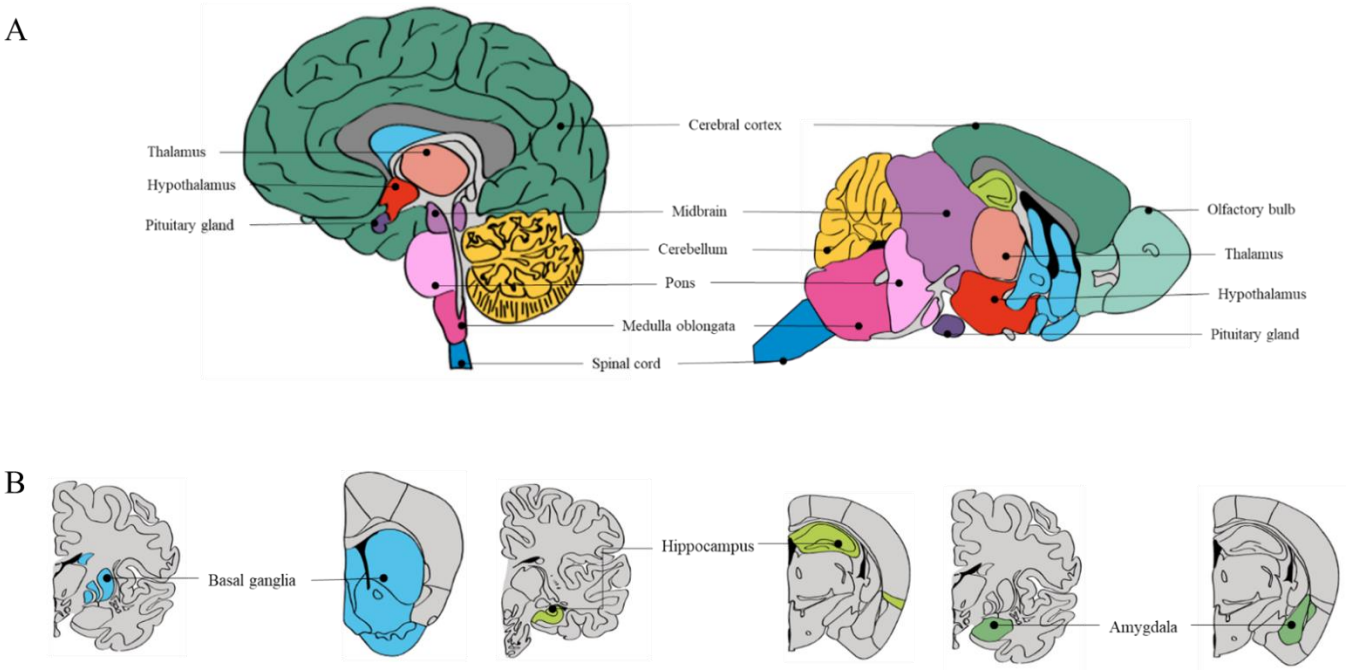


Figure 6. Comparative schematic representation of human and mouse brain structures adapted from (Sjöstedt *et al.*, 2020)***. (A) Panel A depict midsagittal representation of human (left) and mouse (right) brains. The human cortex region, with its gyri and sulci formations is more expanded than in mice, which exhibit a smooth cortical structure. Midbrain in mice is more developed than in human, as well as basal ganglia. Mice also present with a more prominent olfactory bulb located upfront of the cerebral cortex. In human, the olfactory bulb is smaller and located inferior. (B) Panel B images depict coronal representations to show internal structures in human and mouse brains.***

4.4.1 Brainstem formation, structure, and function

The brainstem is a major structure that connects the cerebral cortex, the cerebellum and the spinal cord. It is responsible for vital functions like breathing, heart blood pressure, movement, and control sleep and state of consciousness (Guyenet, 2006; Ángeles Fernández-Gil *et al.*, 2010; Del Negro, Funk and Feldman, 2018).

Inside the brainstem, grey matter is composed of neuronal bodies, assembled into clusters of cranial nerves and nuclei; the white matter is made of the many types of axons from the different neurons going upward or downward. The brainstem is also structured internally into 3 longitudinal segments called laminae, the tectum, the tegmentum, and the basis. The basis represents the most anterior segment and the site of motor pathways.

On the dorsal part of the tegmentum, located in between the basis and the tectum, are located all the cranial nerves nuclei that account for somatic and visceral motor and sensory pathways.

The ventral part of the tegmentum contains supplementary motor nuclei, localised in the midbrain, the substantia nigra (SN) and ventral tegmental area (VTA), rich of dopaminergic neurons (DNs) essential for movement, reward system and control of addiction, and the red nucleus (Nestler, 2005; Damasio and Carvalho, 2013; Grace, 2016) that account for motor functions (Lang and Lozano, 1998). The posterior part, the tectum contains very important structures, involved in control of gaze and movement called the superior and inferior colliculi (Nevue *et al.*, 2016; Ito and Feldheim, 2018).

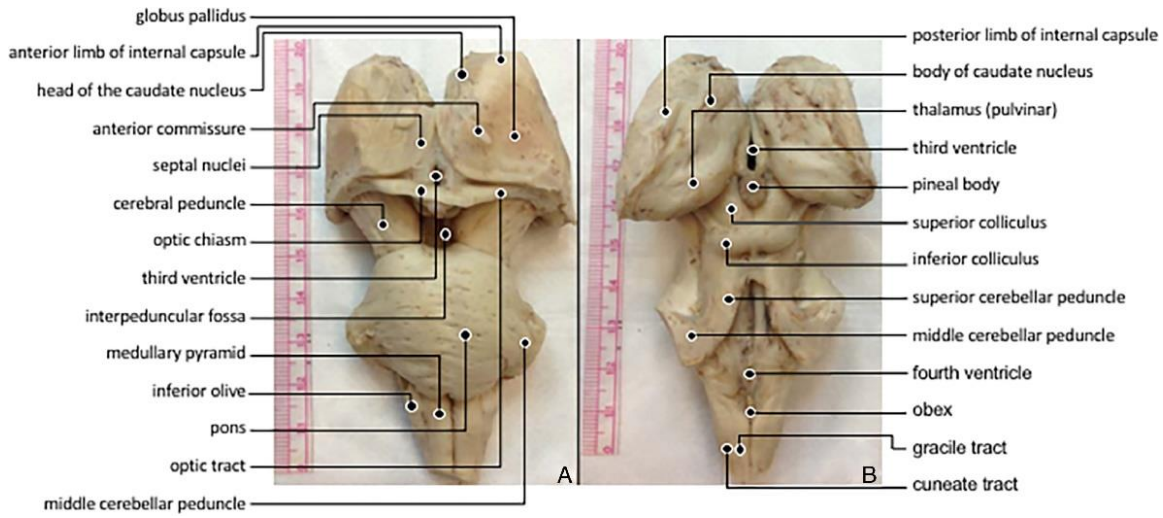


Figure 7. Dorsal and ventral overview of a human brainstem specimen from (Adil *et al.*, 2021)***. Adil and colleagues photograph dorsal and ventral view of post-mortem brainstem specimen after dissection, vascular flush and fixation. Specimen have been annotated to identify each structure.***

4.4.2 *Cerebellum formation, structure, and function*

The cerebellum, that comprises the cerebellar cortex and cerebellar nuclei, is part of the hindbrain and is characterized by a foliated structure with a central vermis flanked by two lateral hemispheres.

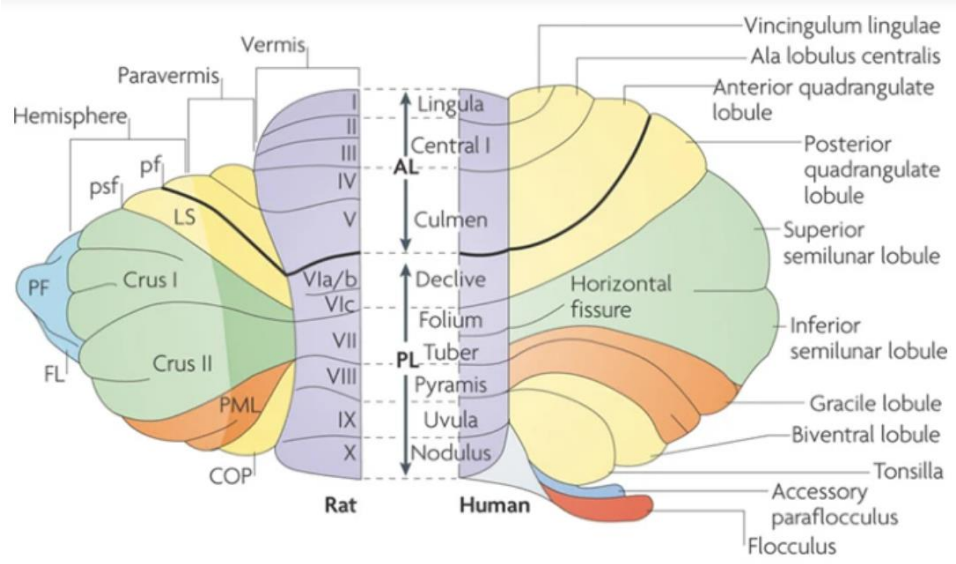


Figure 8. Murine and human cerebellar structure from (Apps and Hawkes, 2009)***. The dorsal view of both rat (left) and human (right) cerebellum is presented and annotated. The similar colours in rat and human represent the same structure. Longitudinally, the cerebellum is divided into 3 regions, the vermis, the paravermis and the hemisphere. On lateral plan, the vermis is subdivided into 11 lobules (I, II, III, IV, V, VI a/b, VI c, VII, VIII, IX, X). On the human side, the vermis is described with another nomenclature. The bold line, representing the primary fissure (pf), separates the anterior lobe (AL) from the posterior lobe (PL) just above the posterior superior fissure (psf). The posterior lobe comprises the lobulus simplex (LS), the ansiform lobule (Crus I and II) the paramedian lobule (PML) and the copula pyramidis (COP). The most lateral structures in rat brain are the paraflocculus (PF in blue) and the flocculus (FL in red). They are the most posterior structure in the human cerebellum.***

In the mouse embryo, the cerebellum is derived from the posterior midbrain-hindbrain boundary and the rhombomere 1 between embryonic day 10 and 13, thanks to the expression of many patterning genes at specific territories (Corrales *et al.*, 2004, 2006). The regional identity determinant orthodenticle homeobox 2 (Otx2) that intervenes in posterior midbrain-hindbrain patterning, acts concomitantly with the gastrulation brain homeobox 2 (Gbx2), the fibroblast growth factor 8 (Fgf8) activated by wingless-type MMTV integration site family (Wint1), the homeobox engrailed 1 transcription factor (En1) and the LIM homeobox transcription factor 1 beta (Lmx1) to allow the cerebellar development. Around embryonic day E17.5, sonic hedgehog (Shh) is expressed and induces the process of cerebellar foliation (Corrales *et al.*, 2004, 2006).

On a cellular level, the cerebellar cortex is structured into three layers, the external molecular layer with stellate and basket neural cells, the Purkinje cell layer (PCL) composed of the Bergmann glial (BG) and somas of Purkinje cells (Pcs) with highly arborized dendrites that

extend in the external layer, and the internal layer composed of granule cells, unipolar brush cells and Golgi cells (Fig. 9). During development, cerebellar expansion is enhanced by the rapid division of the granule cell precursors (GCPs) that are derived from Shh expression, induced by Purkinje cells (Fleming and Chiang, 2015).

Bergmann glia are unipolar cerebellar astrocytes arising from radial glial cells in the cerebellar ventricular zone at E10.5. Between E14.5 and E18.5 radial glia (RG) are differentiated into BG that maintain a basal radial glia activity but migrate their somas toward the external granular layer (EGL), while migrate Purkinje cells (Pcs), at the forming PCL around E17.5. They send their radial fibres to the EGL and are involved in inward granule cells (GC) migration after birth (Schilling, 2018). Purkinje cells, arising also from the ventricular zone around E10.5, undergo axon genesis at E12.5, reelin-dependent orientation changes between E13.5 and E14.5 and migrate their somas along the radial glia fibres to finally reach the forming PCL (Bellamy, 2006; Fleming and Chiang, 2015). Along their highly arborized dendrites directed toward the EGL, Pcs can control GCPs proliferation and migration through the secretion of the morphogen (mitogen)sonic hedgehog shh around E17.5 (Spassky et al., 2008; Miyata et al., 2010; Fleming and Chiang, 2015). After birth, GCPs initiate cerebellar foliation. At fissures sites they accumulate, following inward direction to allow invagination between folia. At the fissure sites, BG and PCs participate concomitantly to the formation of anchoring centres that are involved in the folding of the EGL (Sillitoe and Joyner, 2007; Sudarov and Joyner, 2007).

The cerebellar nuclei, which constitute the major output signal of the cerebellum, are located near to the roof of the fourth ventricle in the cerebellar white matter (Voogd and Glickstein, 1998; van Essen *et al.*, 2020). They are composed of inhibitory GABAergic interneurons that project in the inferior olive, part of the *medulla oblongata*, and glutamatergic excitatory neurons that project in several regions of the brain (Ruigrok, 1997; Uusisaari, Obata and Knöpfel, 2007; Uusisaari and Knöpfel, 2012).

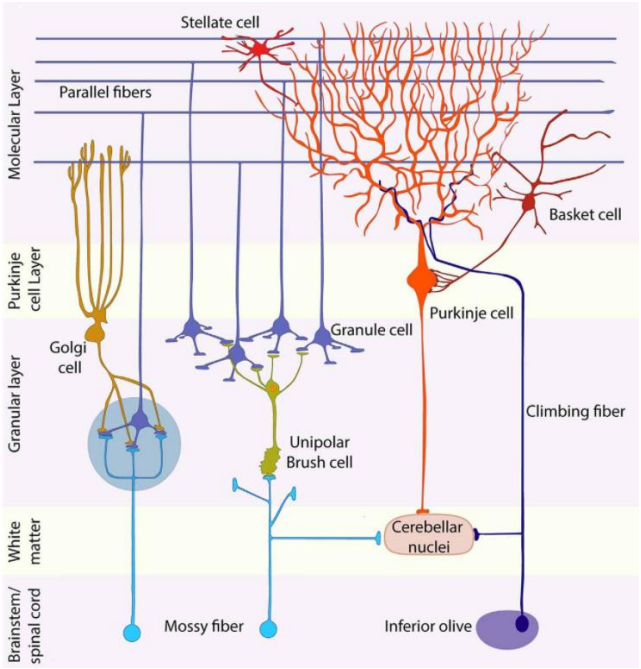


Figure 9. Cerebellar cortex cellular organisation. (Consalez *et al.*, 2021)***. Afferent inputs from the lower brainstem are transmitted via Mossy fibres and Climbing fibres. Basket cells, Golgi cells, Stellate cells, and Unipolar brush cells are interneuron subtypes. Purkinje cells in the Purkinje cell layer, project to cerebellar nuclei in the white matter. Granule cells received afferent inputs from the mossy fibres.***

Purkinje cells are the principal cells from cerebellum that exhibit a gamma-butyric acid (GABAergic) inhibitory response and project to the cerebellar nuclei. Basket cells, stellate cells, and Golgi cells are the other GABAergic interneurons. Granule cells, which represent 80% of all neurons in the entire brain are glutamatergic neurons, as well as, unipolar brush cells, and exhibit excitatory response after receiving input from afferent fibres. (Voogd and Glickstein, 1998; Kalinichenko and Okhotin, 2005; Sillitoe and Joyner, 2007; Sudarov and Joyner, 2007; Leto, Bartolini and Rossi, 2008; Leto and Rossi, 2012).

The cerebellum main function is motor coordination (Glickstein, 1993; Glickstein, Sultan and Voogd, 2011), but it also plays a role in language, sleep, emotional behaviour and attention (Leiner, Leiner and Dow, 1991; Schmahmann and Caplan, 2006).

5. Role of mitochondria in the neurogenesis and mature neurons

Mitochondria are suggested to play an important role in neural stem cell integrity and differentiation. Previously glycolytic, neural stem cells shift their metabolism to OXPHOS

when differentiating into neurons that become highly dependent on OXPHOS. In that respect, mitochondria, initially roundish, undergoes fusion. Their OXPHOS metabolism increases, mediated by an upregulation of tricarboxylic acid (TCA) cycle and an upregulation of peroxisome proliferator activated receptor γ coactivator 1α (PGC-1a) to increase mtDNA copy number (Varum *et al.*, 2011). The resulting maturing neuron also exhibits increased ROS production to allow differentiation (Brunetti *et al.*, 2021).

An article from Inak G. and colleagues published in 2021, highlighted mitochondrial contribution to substantia nigra neurogenesis. Using induced pluripotent stem cell (iPSC) and CRISPR-Cas9 techniques, they recapitulated Leigh syndrome (LS) caused by SURF1 and NDUFS4 mutations. Inak G. and colleagues generated mutant and control organoids enriched in Tyrosine-Hydroxylase (TH)-positive dopaminergic neurons, and glial cells to mimic the defect observed in the brainstem since these cell types are highly affected in basal ganglia phenotype of LS (Lake *et al.*, 2016a). They demonstrated that OXPHOS dysfunctions in neural progenitor cells (NPCs), due to SURF1 and NDUFS4 mutations, prevent their maturation (Inak *et al.*, 2021). Because of OXPHOS defects, SURF1- and NDUFS4-mutant NPCs were unable to do this switch. They remain mostly glycolytic with reduced axonal arborisation and synaptic wiring, preventing them to fully differentiate into neurons and establish networks. These defects may explain some phenotypes in LS patients like developmental delay, basal ganglia necrotizing or microcephaly. Hence, the earlier defects in neuronal morphogenesis are induced, the more immature the stage of NPCs, which prevents them engaging normally. This prevents normal brain development in early embryos and leads to early lethality (Inak *et al.*, 2021). Thus, mitochondria play an important role in neurogenesis.

Mitochondria also play specific roles in different neurons and glial cells. In an interesting study published in 2019, Fecher C. et al. determine a way to get specific cell-type-mitochondria from specific brain regions, tagging mitochondria with a specific marker, and using functional and proteomic analyses. From different cell types of the cerebellum, they sampled principal inhibitory neurons, Purkinje cells, principal excitatory neurons, Granule cells, and major glial cells, astrocytes. They showed diversity in their mitochondria (morphology, distribution), but also differentially regulated pathways, depending on the cell type, and they found specific markers to identify them. Fecher and collaborators also demonstrated that astrocytic mitochondria rely exclusively on lipid beta-oxidation to provide energy and support for neuronal cells. Proteomics analyses allowed to identify cell-type specific markers for mitochondria anchoring to other organelles: Pex11B was highly expressed in astrocytes and

played a role in peroxisome communication for lipid processing. Rmdn3, involved in mitochondria-endoplasmic reticulum communication for calcium signalling, was abundantly found in the rich dendritic Purkinje cells. Mitochondrial calcium uptake complex (MCU), mediated by mitochondrial calcium uptake protein 1 and 2 (MCU1, MCU2), the principal complex to regulate calcium in mitochondria, was highly expressed in Granule cells. Hence, mitochondria in cerebellum exhibit a great diversity in their signalling roles, regarding the cell type (Fecher *et al.*, 2019).

Mitochondria are also important for neuronal plasticity. Present in the soma of neurons, but also in areas requiring high demands of energy like synapses, dendrites or axons, mitochondria undergo dynamic transport along cytoskeleton of neurons. To be able to have such an important role in synapses (neurotransmitters releasing and uptake, vesicle recycling, repolarization, calcium buffering), mitochondrial fission and fusion events and mtDNA maintenance, occur away from the nucleus, in the axons and dendrites (Amiri and Hollenbeck, 2008). This is possible because neurons are able to compartmentalise protein synthesis in their distal regions, which enables mitochondrial function in axons and synapses, and thus accounts for synaptic plasticity. (Lee and Hollenbeck, 2003). Synaptic impairment and neurodegeneration are deeply linked to defects in synaptic mitochondria (Devine and Kittler, 2018).

6. Mechanism of neurodegeneration

Neurodegeneration refers to severe conditions where neurons from specific regions are affected and die, gradually impairing brain cognitive and motor functions. Mitochondria are involved in neuronal death during programmed cell death. Indeed, some triggering events common to neurodegenerative diseases such as stroke or Alzheimer's disease led to excessive activation of glutamate receptors that induce calcium ion excitotoxicity (Mattson, 2000). Since they can no longer be regulated by the homeostasis of the endoplasmic reticulum, calcium ions flow abundantly into the cytosol but also into the mitochondria via the activation of specific effectors (Bax). In mitochondrial matrix, calcium ions participate in the increase of oxidative stress, leading to the opening of the permeability transition pores, and the escape of cytochrome *c* into the cytosol. In the cytoplasm, cytochrome *c* binds to apoptotic protease-activating factor 1 (Apaf-1) and caspase-9 to trigger caspase-3. (Mattson, 2000; Friberg and Wieloch, 2002; Rizzuto, Duchen and Pozzan, 2004).

Although glial cells, that act as support for neural cells, rely first and mostly on glycolysis as an energy supply (Bélanger, Allaman and Magistretti, 2011; Calì, Tauffenberger and Magistretti, 2019), neurons depend on OXPHOS. In case of OXPHOS impairment, neurons have no capacity to regulate their energy supply and therefore get highly vulnerable (Herrero-Mendez *et al.*, 2009; Duchen, 2012; Verkhratsky and Nedergaard, 2018).

7. Mitochondrial cardiomyopathies

Cardiomyopathy is a common manifestation of mitochondrial diseases because heart, like brain or muscle, requires high mitochondrial metabolism to ensure contraction and circultation of oxygenated and oxygen-depleted blood into the whole organism (Munnich *et al.*, 1996). Mitochondrial cardiomyopathies are characterised by typical defects in heart structure and function, such as hypertrophic cardiomyopathy, arrythmias and heart failure. The disease presentation can be mild to severe (heart failure and arrythmias), leading to a poor prognosis in affected children, concomitantly to metabolic crisis. The cellular phenotype of mitochondrial cardiomyopathy describes large fusiform myocytes with larger mitochondria, cytoplasm clearing and granulation, increased glycogen concentrations associated to lipid accumulation (Holmgren *et al.*, 2003; Meyers, Basha and Koenig, 2013).

Myocardium relies principally on glucose and lactate during embryogenesis to produce ATP, due to poor oxygen input (Patterson and Zhang, 2010). A metabolic switch occurs at birth during which fatty acids, highly present in circulating blood, become the main provider of energy for cardiomyocytes through fatty acid oxidation. During this metabolic transition, glycolytic proteins drop while PGC-1α (peroxisome proliferator activated receptor γ coactivator 1α) and PPARα (peroxisome proliferator activated receptor α), involved in mitochondrial biogenesis and fatty acid metabolism, increase (Patterson and Zhang, 2010; Ritterhoff and Tian, 2017).

In case of mitochondrial hypertrophic cardiomyopathy, the energy metabolism reverts to an embryonic profile, where the heart relies on glycolysis, with general reduction of oxidative metabolism and energy supply, and a resulting increase in glucose uptake (Dorn, Vega and Kelly, 2015; Ritterhoff and Tian, 2017). Progressively, these changes will lead to reduction of cardiac energy and worsening of the disease.

8. ELAC2 and mitochondrial diseases

8.1 Clinical and molecular phenotypes associated with *ELAC2* variants

Initially associated to higher prostate cancer risk, several recent studies have associated *ELAC2* mutations to mitochondrial RNase Z defects, mainly leading to developmental delays, and infantile hypertrophic cardiomyopathy (Haack *et al.*, 2013; Shinwari *et al.*, 2017; Saoura *et al.*, 2019).

Performing WES, Haak T. and colleagues identified *ELAC2* as the disease-causing gene in five patients. Two siblings of unrelated German parents carried compound heterozygous mutations (c.[631C>T]; [559C>T], p.[Arg211∗]; [Thr520Ile]), one infant of consanguineous Arabic parents harboured a homozygous mutation (c.[460T>C], p.[Phe154Leu]) and two siblings born from consanguineous Turkish parents carried a homozygous mutation (c.[1267C>T], p.[Leu423Phe]). All five patients presented with infantile hypertrophic cardiomyopathy associated to lactic acidosis and OXPHOS complex I deficiency (Haack *et al.*, 2013). By the time of the study, three infants died prematurely from heart failure although they received dedicated medication and care. The different *ELAC2* variants and associated clinical features have been listed in table 3.

Quantitative real-time PCR and RNA-sequencing from patients' fibroblasts and muscle biopsies revealed increased levels of unprocessed tRNA precursors but no accumulation of immature mt RNAs. Immunoblotting analysis of patient fibroblasts and muscle biopsies showed a decrease in the steady-state level of OXPHOS proteins and a decrease in OXPHOS complex I, respectively, confirming that major decrease of ELAC2 levels lead to defects in mitochondrial translation and OXPHOS. An exogenous *ELAC2* cDNA complementation rescued the cellular phenotype, confirming that *ELAC2* was the disease-causing gene (Haack *et al.*, 2013).

Then, a study from Shinwari et al. have performed WES and mutation screening in Arabic families to finally identify the previously known p.Phe154Leu missense homozygous mutations of *ELAC2* in 16 infants that died prematurely from severe hypertrophic cardiomyopathy, lactic acidosis and OXPHOS complex I deficiency (Shinwari *et al.*, 2017).

Kim et al., also identified one heterozygous variant c.[95C>G]; p.[Pro32Arg] in a 5-month infant born to non-consanguineous parents of Korean origin with encephalopathy, epilepsy and hyperlactatemia who died prematurely. The second variation could not be identified. No cardiac involvement was reported in this patient (Kim *et al.*, 2017).

Interestingly, another study by Akawi et al. presented a consanguineous Pakistani family with five individuals carrying a homozygous splice site mutation of *ELAC2* (c.[1423 + 2 T > A]) that generally presented with milder cardiomyopathy and lactic acidosis, and mostly neurodevelopmental delay. Three teenagers presented with microcephaly and severe developmental delay. Quantitative real-time PCR and immunoblotting analyses from one patient's fibroblasts revealed an increase of uncleaved pre-tRNAs correlated to a reduced level of ELAC2. Thus, none of the patients died from cardiac complications, and this family's phenotypes expanded the clinical and molecular phenotypes associated to *ELAC2* mutations (Akawi *et al.*, 2016).

Paucar and colleagues reported compound heterozygous mutations (c.[394G>A]; [1040C>T], p.[Gly132Arg]; [Ser347Phe]) in a 69-year-old patient of Assyrian origin. With a mild cardiac involvement, this patient showed chorea and apraxia, involuntary movements disorders, accompanied with dystonia and atrophy of hand muscle, confirmed by muscle histological analyses (negative COX staining and presence of ragged red fibres), suggesting a demyelinating polyneuropathy and myopathy. Immunoblotting analyses from patient fibroblasts revealed an increase of unprocessed tRNA but muscle biopsy did not reveal any OXPHOS deficiency. Brain MRI revealed abnormalities in the insula, responsible for olfactory hallucinations in addition to bilateral atrophy of frontal cortex and temporal lobe. The patient was also diagnosed with an attention deficit/hyperactivity disorder (ADHD), and acanthocytosis, a defect in red blood cells' shape due to membrane lipids accumulation, characteristic of neuroacanthocytosis syndromes. Thus, *ELAC2* mutations spectrum also expends with movement disorders and psychiatric disorders (Paucar *et al.*, 2018).

Finally, while screening 13 patients by WES and TES, Saoura M. and colleagues reported 16 novel mutations in *ELAC2* associated with hypertrophic cardiomyopathy, lactic acidosis and OXPHOS deficiency (Saoura *et al.*, 2019)(Table 3). Three patients carried the same homozygous mutation (c.[460 T>C] ; p.[Phe154Leu]) reported previously (Haack *et al.*, 2013; Shinwari *et al.*, 2017). One patient harboured a splice site mutation (c.[1423 + 1 G>A]) at the

same position as the mutation of Pakistani patients (Akawi *et al.*, 2016). Moreover, study of patients' fibroblasts showed an increase of unprocessed tRNA, in concordance with previous studies, confirming the implication of the novel variants in the observed clinical phenotype. Interestingly, the substitution p.[Arg781His], previously identified in prostate cancer patients (Tavtigian *et al.*, 2001), has been reported in three patients from this study with heterozygous mutations, harbouring hypertrophic cardiomyopathy and mitochondrial pre-tRNA cleavage deficiency. The authors suggest that mitochondrial impairment may be implicated in the occurrence of prostate cancer.

8.2 ELAC2 mutations recapitulative table

To date, 19 pathogenic variants of *ELAC2* have been identified. For most of the variants, patients present with fatal hypertrophic cardiomyopathy, developmental delays, and lactic acidosis.

Variants	Origin	Clinical features summary	References
Compound heterozygous c.631 C>T ; p.Arg211∗ c.1559 C>T ; p.Thr520Ile	German	Hypertrophic cardiomyopathy, OXPHOS CI deficiency, psychomotor and growth retardation, muscular hypotonia, microcephaly, dysphagia, lactic acidosis, sensorineural hearing impairment, hyperintensities in basal ganglia at age 3 months	(Haack *et al.*, 2013)
Homozygous c.460 T>C ; p.Phe154Leu	Arabic	Hypertrophic cardiomyopathy, OXPHOS CI deficiency, intrauterine growth retardation, lactic acidosis, cardiac failure, normal muscle biopsy findings	(Haack *et al.*, 2013; Shinwari *et al.*, 2017; Saoura *et al.*, 2019)
Homozygous c.1267 C>T ; p.Leu423Phe	Turkish	Hypertrophic cardiomyopathy, OXPHOS CI deficiency, neurodevelopmental delay, muscular hypotonia, cardiac failure	(Haack *et al.*, 2013)
Homozygous c.1423+2 T>A	Pakistani	Intellectual disability, mild septal hypertrophy	(Akawi *et al.*, 2016)

Compound heterozygous c.95C>G ; p.Pro32Arg and unknown variant	Korean	Intrauterine growth retardation, Encephalopathy, cardiac anomaly, early lethality	(Kim *et al.*, 2017)
Compound heterozygous c.394G>A; p.Gly132Arg c.1040C>T; p.Ser347Phe	Assyrian	Mild cardiac involvement, ADHD disorder, acanthocytosis, chorea and apraxia, dystonia, atrophy of hand muscle, ragged-red fibres and COX-deficient, brain MRI abnormalities in the insula, bilateral atrophy of frontal cortex, olfactory hallucinations	(Paucar *et al.*, 2018)
Compound heterozygous c.1478 C>T; p.Pro493Leu c.202 C>T; p.Arg68Trp	-	Hypertrophic cardiomyopathy, OXPHOS CI+CIV deficiencies, lactic acidosis, muscle weakness, ragged-red fibres, and COX deficient/SDH- hyperreactive fibres, early lethality	(Saoura *et al.*, 2019)
Compound heterozygous c.2009del; p.Cys670Serfs*14 c.1423 + 1 G>A	-	Lactic acidosis, developmental delay, ataxia, microcephaly, constipation, cerebellar vermis hypoplasia and prominent posterior fossa on brain MRI	
Compound heterozygous c.297–2_297delinsTG c.2342 G>A ; p.Arg781His	-	Hypertrophic cardiomyopathy, OXPHOS complex CI deficiency, intrauterine growth retardation, elevated blood lactate level (normal serum levels), developmental delay	
Compound heterozygous c.2186 A>G ; p.Tyr729Cys c.2342 G>A ; p.Arg781His	-	Hypertrophic cardiomyopathy, OXPHOS CI deficiency, lactic acidosis, cardiovascular collapse, early lethality	
Compound heterozygous c.798–1 G>T c.1690C>A; p.Arg564Ser	-	Cardiomyopathy, OXPHOS CI deficiency, lactic acidosis, developmental delay, fatal infantile cardiomyopathy	
Compound heterozygous c.1979A>T ; p.Lys660Ile c.2039 C>T ; p.Ala680Val	-	Hypertrophic cardiomyopathy, OXPHOS CI+CIV deficiencies, elevated blood lactate level, cardiac transplant (3.8 years)	

Compound heterozygous c.245 + 2 T>A c.1264 C> ; p.Leu422Val	-	Cardiomyopathy, OXPHOS CI deficiency, lactic acidosis, early lethality	
Homozygous c.1163 A>G; p.Gln388Arg	-	Hypertrophic cardiomyopathy, OXPHOS CI deficiency, lactic acidosis, psychomotor retardation, fatigability, peripheral neuropathy	
Compound heterozygous c.457delA; p.Ile153Tyrfs*6 c.2342 G>A ; p.Arg781His	-	Hypertrophic cardiomyopathy, OXPHOS CI deficiency, Developmental delay, hypotonia, gastrointestinal dysmotility, cardiac transplant at age of 10 months	
Compound heterozygous c.297–2_297–1delinsT c. 2245 C>T ; p.His749Tyr	-	Hypertrophic cardiomyopathy, OXPHOS CI+CIV deficiencies, lactic acidosis, global developmental delay, hypotonia, cardiac transplant at the age of 10 months but early lethality	

Table 3. Recapitulative table of ELAC2 variant mutations in different geographic regions. Most of the cases present hypertrophic cardiomyopathy, developmental delay, and lactic acidosis. Adapted from (Haack *et al.*, 2013; Akawi *et al.*, 2016; Kim *et al.*, 2017; Shinwari *et al.*, 2017; Paucar *et al.*, 2018; Saoura *et al.*, 2019)***. ADHD: Attention deficit/hyperactive disorder; CI: Complex I; CIV: Complex IV.***

Objectives

Mitochondrial diseases are characterized by a huge clinical heterogeneity and tissue-specific involvement while they are due to mutations in ubiquitously expressed genes. These diseases are often associated with a poor prognosis and are incurable. The lack of MD cure(s) is, in part, a result of (1) our poor understanding of their pathomechanisms and (2) the lack of suitable animal models recapitulating the complexity of MD.

This PhD thesis project focused on two MD-causing genes, *LRPPRC* and *ELAC2*, encoding proteins involved in mitochondrial RNA metabolism. Mutations in the mitochondrial mRNA stability and polyadenylation factor LRPPRC invariably cause neurological disease, most often progressive necrotizing encephalopathy, Leigh syndrome (LS), accompanied with hepatopathy (LSFC) or cardiomyopathy. Mutations in *ELAC2*, encoding a mitochondrial tRNA ribonuclease, are known to cause mainly hypertrophic cardiomyopathy, neurodevelopmental delay, and lactic acidosis.

Objective I

The molecular function of LRPPRC has been studied using animal and cellular models. However, the mechanisms by which its loss results in tissue-specific clinical presentations affecting a few organs remains unknown. The first objective of my thesis project was to characterise a midbrain -and-cerebellum-specific Lrpprc knockout mouse model (MCKO) that could shed light on how loss of Lrpprc in these brain structures affects their function and development. This was important because midbrain and cerebellum are typical brain regions affected in the development of LS.

MCKO mice were generated by crossing conditionally targeted Lrpprc mice ($Lrpprc^{LoxP/LoxP}$) with mice expressing Cre recombinase under the control of the En1 promoter. The latter restricts Cre-expression to the midbrain and cerebellum thereby ablating Lrpprc only in these structures.

The characterisation of this mouse model that recapitulates LSFC main phenotypes appears crucial for a better understanding of LS and more specifically of the consequences of *LRPPRC* mutations in various neurological cellular types. Indeed, characterising this new mouse model will allow to expend our knowledge on tissue and specific cells mostly impacted by LRPPRC defects. Finally, it is a milestone to better define treatments options and provide a cure capable of targeting more precisely the defective cells.

Objective II

ELAC2 is another gene involved in mitochondrial RNA metabolism but variants of this gene result in another clinical phenotype mainly characterized by hypertrophic cardiomyopathy and lactic acidosis. Heterogeneous clinical phenotypes, with abnormal movements and psychiatric disorder, or mild cardiac impairment with microcephaly have also been reported.

Characterization of patients' fibroblasts represent a first step for understanding the consequences of *ELAC2* variants. Thanks to the diagnosis activity in the Necker-Enfants Malades hospital, I was able to access fibroblasts of three unrelated patients with *ELAC2* variants. The second aim of my thesis was to characterise the fibroblasts of these unrelated patients and determine if their study allow to expand the spectrum of clinical, biochemical, and molecular phenotype associated to *ELAC2* variants.

The characterisation of these mutant fibroblasts can be a milestone to better understand the function of the protein, and to propose new experimental *in vivo* models, key step to develop new treatments for hypertrophic cardiomyopathy, the most severe pathological features.

Chapter II: Materials and methods

I. Generation of mouse model and mouse breeding

Cerebellum and Midbrain-specific knockout mice were generated by crossing *Lrpprc*$^{Lox/Lox}$ with transgenic mice expressing Cre recombinase under the En1 promoter (Plummer et al.,2017), followed by crossing *Lrpprc* $^{Lox/+,En1\text{-}Cre}$ with *Lrpprc* $^{Lox/Lox}$ mice (Figure 7), adapted from (Ruzzenente *et al.*, 2012).

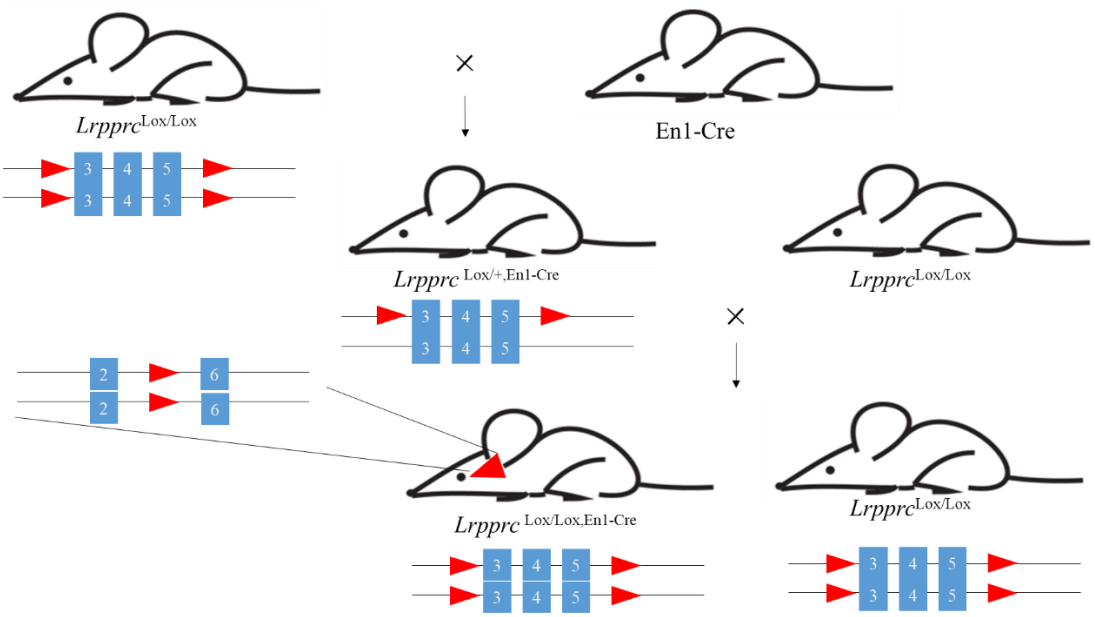


Figure 10. Generation of the cerebellum and midbrain knockout mouse model. Lrpprc $^{Lox/Lox}$ mice were breed with transgenic mice expressing Cre recombinase under Engrailed-1 promoter* (En1) *to finally obtain control and conditional knock-out mice respectively, Lrpprc $^{Lox/Lox}$ and Lrpprc $^{Lox/Lox,\ En1\text{-}Cre}$.

Additionally, *Rosa26* ^{tdTomato} mice (Madisen *et al.*, 2010) were also used to obtain control mice expressing Cre-inducible fluorescent protein Tomato cells with active En1 promoter.

All mice were maintained in the C56Bl6/N background.

II. Mouse genotyping

Genotyping was carried out on genomic DNA extracted from tails biopsies. 75µl of extraction buffer (25mM NaOH, 0,2mM EDTA) was added to the tail biopsies and was incubated at 95°C for 45 minutes to lyse the tissue and cells and release the DNA. Next, the tubes were incubated on ice for 5minutes and 75µl of neutralization buffer (40mM of Tris-HCl at pH 7.8) were added.

Lysates were vortexed quickly and centrifuged for 10 minutes at 14000-15000 rpm to pellet debris before storage at +4°C.

Specific primer sequences were used to genotype the different mouse models:

Primers	Sequence	Purpose	Size of PCR product
LRP A LRP B	GGAGAACAGGCCGCATCACAA TGCCTTCCACCTCAGCTTACCACT	Detection of floxed allele	Floxed allele: 520 bp Wt allele: 420 bp
LRP A LRP D	GGAGAACAGGCCGCATCACAA GTAACCCCACCCCCTTATGT	Detection of knock-out allele	Ko allele: 300 bp
CRE A-F CRE B-R	GAACCTGATGGACATGTTCAGG AGTGCGTTCGAACGCTAGAGCCTGT	Detection of Cre	Cre: 350 bp
TOM 1 TOM 2 TOM 3	CCCAAAGTCGCTCTGAGTTGTTATC GAAGGAGCGGGAGAAATGGATATG CCAGGCGGGCCATTTACCGTAAG	Detection of Tomato	Wt allele: 650 bp Tomato allele: 350 bp

Table 4. List of primers used for mouse genotyping.

Polymerase chain reactions (PCR) amplifications were performed using GoTaq® DNA Polymerase (5u/µl) (Promega, M300A), 1X (1.5mM MgCl2) of 5X GoTaq® green buffer, Promega, M791A), 0.125mM each dNTP from a PCR nucleotide mix (Invitrogen, 10297117), 0.5µM of forward and reverse primers, and less than 0.01µg/µl of template DNA and nuclease-free water to reach final volume.

The following PCR programs were used to amplify the different allele and transgenes:

primers	PCR program	
LRP A-LRP B LRP A-LRP D CRE A-F-CRE B-R	92°C	2 min
	92°C	15 sec
	60°C	15 sec
	72°C	20 sec 30 cycles
	72°C	7min

primers	PCR program	
TOM 1-TOM 2-TOM 3	94°C	2 min
	94°C	20sec
	61°C	20sec
	72°C	45sec 35 cycles
	72°C	7 min

Table 5. PCR programs set up with different primers used for mouse genotyping

PCR products were loaded on 2% agarose gel, containing 0.5 µg/ml ethidium bromide in TAE buffer (40 mM Tris base, 20 mM acetic acid, 1 mM EDTA, pH 8) and migrated at 80 to 110 volts. PCR products were visualized using an ultraviolet lamp.

III. Tissue processing for immunostaining

Freshly explanted brains from embryos at E15.5 and from newly born mice were fixed with 4% PFA in PBS for 2h and overnight, respectively, (CliniSciences, AR1068). Next, the samples were washed 3 times with PBS (Gibco, 14190-094), and cryoprotected by incubation with 30% sucrose (Sigma, S0389) in PBS solution, under agitation at +4°C for overnight. Finally, the samples were embedded in OCT matrix (CellPath, KMA-0100-00A) into square moulds and frozen using a liquid nitrogen-precooled metal block. The samples were stored at -80°C.

IV. Immunostaining in mouse tissues

10µm midsagittal or midcoronal sections, were equilibrated at room temperature for 30min to 1 hour and OCT was removed by 5 min incubation in PBS. Next the sections were blocked and permeabilized in 0.5%Triton X100 + 3% goat serum in PBS for 1h at room temperature and incubated with primary antibodies diluted in 0.1%Triton X100 + 3% goat serum in PBS overnight at 4°C. The following day, the sections were washed with PBS, three times for 10 min, and incubated with a secondary antibody for 2 hours at room temperature. Primary and secondary antibodies that were used are listed in the Table 6 at the end of Materials and Methods. Next, the sections were washed with PBS, three times for 10 min, and finally mounted using mounting media Prolong ™ Gold Antifade reagent with DAPI (Thermo Fisher scientific, P36931).

In the case of hybridization with antibodies anti-Calbindin the procedure was modified: sections were permeabilized with 0.5% Triton X-100 in PBS for 10 min at room temperature, rinsed 3 times with PBS 1X and blocked with 2 drops of Mouse-On-Mouse blocking reagent (Vector laboratories, MKB-2213) diluted into 2ml of PBS for 1h.

For the hybridization with antibody anti-Cherry the blocking was performed using 5% Bovine serum albumin (BSA) (Sigma, A9418) diluted in PBS.

V. Histochemistry

1. Nissl staining

According to (Kádár *et al.*, 2009) with modifications, freshly explanted mouse brains were embedded in a 5% low melting agarose square mold and 80µm midsagittal sections were obtained using a vibratome (Leica VT1000 S). The sections were dried overnight at room temperature on a glass and, next, were incubated in a 1:1 absolute ethanol/chloroform solution overnight. After rehydration for 10 min in 100% Et0H, 10min in 95% ethanol and 10min in H2O, the sections were incubated in Nissl solution (10mg/ml of cresyl violet acetate (Sigma, C5042) dissolved in deionized water, 3µl/ml of glacial acetic acid were added to the solution just before use) for 10min at room temperature. After a rinse in deionized water, the samples were incubated in 95% ethanol for 30 min, and dehydrated in 100% ethanol two times for 5 min. Finally, the sections were washed 2 times with xylene for 5 min and mounted using permanent using anhydrous Neomount® mounting media (Merck Millipore, 109016). The slides were scanned using the Nanozoomer 2.0 HT by Hamamatsu™.

2. Haematoxylin Eosin staining

Freshly explanted mouse brains from embryos at E15.5 and from newly born mice were fixed with 4% PFA in PBS for 2h or overnight, respectively, at 4°C under slow mechanical agitation. After 3 washes with PBS, the tissues were transferred at the histology platform from the SFR Necker in slotted cassettes (3 × 2.5 × 0.4 cm) and stored in 50 % ethanol. As described by (Fischer *et al.*, 2008), mouse brains were embedded in mid-sagittal orientation into paraffin and 4 µm-thick slices obtained from a microtome (HM 340E, Microm France) were used for

Haematoxylin-Eosin staining with a multistainer (ST5020-CV5030, Leica). The slides were scanned using the Nanozoomer 2.0 HT by Hamamatsu™.

3. COX/SDH staining

Adapted from (Ross, 2011), freshly explanted brains from newly born pups were incubated in pre-freezing buffer (30%sucrose, 1%DMSO (Sigma, C6164) in PBS) under agitation at +4°C. Next, the brains were embedded in OCT and frozen using a liquid nitrogen-precooled metal block, stored at -80°C or cut immediately using a cryostat (20µm midsagittal sections). Slides were equilibrated to room temperature for 1 hour before 150µl of COX solution, prepared with cytochrome c at 0.1mM (Sigma, C3131), 3,3'-Diaminobenzidine (DAB) at 4mM (Sigma, D8001) and a few flakes of bovine catalase (Sigma, C1345) in phosphate buffer 0.1M PH 7, were added and slides were incubated for 10-20min in a 37°C-incubator with humidified atmosphere. Next the samples were washed with PBS, 4 times 10 min, and incubated for 10-20 min as above in 150µl of SDH solution prepared with sodium succinate at 130mM (Sigma, 14160), PMS at 0.2mM (Sigma, P9625), sodium azide at 1mM, and NBT at 1.5mM in phosphate buffer 0.1M Ph 7. Excess of SDH solution was washed away, 4 times 10min, in PBS. Finally, the slides were dehydrated by sequential two-minute-incubations in baths with increasing ethanol concentrations (70%,70%,95%,95%,99.5%), before a final 10 min incubation in 99.5% ethanol followed by a 10 min incubation in xylene. The slides were mounted using anhydrous Neomount® mounting media (Merck Millipore, 109016) and allowed to dry overnight in a ventilated hood. The slides were scanned at the histology platform of SFR Necker using the Nanozoomer 2.0 HT by Hamamatsu™. COX and SDH staining can also be performed on different slices.

VI. Primary cell culture of ventral mesencephalon

According to (Gaven, Marin and Claeysen, 2014) with modifications, primary cell cultures from mouse embryonic mesencephalon at E13.5 and E14.5 were established by mating *Lrpprc*$^{LoxP/LoxP}$ and *Lrpprc*$^{LoxP/+,}$ *Cre* mice. Plug-check was carried out and positive mice—assumed embryo stage as E0.5—were monitored by regular measurements of their body weights, which were expected to increase if the mice were pregnant. In the meantime, 15mm diameter autoclaved coverslips, fitted in the wells of a 12-well plate, were coated with 20µg/mL of Poly-L-ornithine (PLO, Sigma, P4957) in deionized water for 2 hours in 37°C incubator;

rinsed in autoclaved deionized water and finally incubated in 10 µg/mL natural mouse laminin (Invitrogen, 23017-015) diluted in deionized water for 2h to overnight at 37°C and stored at +4°C; the laminin solution was removed prior to using of the glass slides. At E13.5 or E14.5, the pregnant mice were sacrificed by cervical dislocation and intact uteri were recovered in pre-cooled Hank's balanced salt solution (HBSS) (Gibco, 14175-095). Each embryo was extracted from the placenta and its brain explanted using sterilized dissecting instruments under a stereomicroscope; its mesencephalon was excised and incubated in pre-cooled dissection buffer prepared with 3.6mg/ml of D-glucose (Sigma, G8270), 200U/ml of Penicillin, 200µg/ml of Streptomycin (Thermo Fischer scientific, 15140122), HBSS 1X and 0.2mM of ascorbic acid (Sigma, A4034) added before use. A tail biopsy was kept for DNA extraction and PCR genotyping. For each embryo, mesencephalon was digested using trypsin 0.05%. Neutralizing buffer (F12 medium 1X (Gibco, 10565018), supplemented with 10% of heat-inactivated fetal bovine serum (FBS) (Gibco, 10438), and 0.2mM of ascorbic acid added just before use) was added to inhibit trypsin, and the tissue was carefully homogenized using a fire-polished Pasteur pipet. Tubes were centrifuged for 5min at 200 x g. The supernatant was carefully aspirated, and remaining cell pellet was resuspended into maturation medium (Neurobasal medium 1X (Gibco, 21103-049 L-glutamine 1X (Thermo Fisher Scientific, 25030-081), B-27 Supplement 1X (Thermo Fisher Scientific, 17504-044), B-27 Plus Supplement 1X (Thermo Fisher Scientific, A3582801), FBS 1X, and 0,2mM of ascorbic acid (Sigma, A4034). Using Kova™ glasstic™ Slide 10 with grids (KOVA, 87144) for cell counting, 900 000 and 600 000 cells per well were seeded onto the pre-coated coverslips. Maturation media was changed by semi-filling every other day. Cells were put to grow for 9 to 11 days in a humidified incubator, at 37°C, 5% CO2, before fixation using 4% PFA in PBS and immunostaining was finally achieved using specific antibodies towards different cell types.

VII. Immunostaining in primary cells

After 9 days of differentiation, adapted from (Gaven, Marin and Claeysen, 2014), primary neuronal cells were gently washed with PBS (Gibco, 14190) and fixed with 4% pre-heated PFA in PBS for 10 min. Next, the cells were rinsed 3 times with PBS and incubated in blocking/permeabilization medium (PBS/0.05% Triton X-100/20% goat serum) for 30 min at room temperature, before incubation with primary antibodies diluted in PBS/0.05% Triton X-100/1% goat serum, overnight at 4°C. After washing 3 times with PBS, the cells were incubated

with secondary antibodies diluted in PBS/0.05% Triton X-100/1% goat serum for 2 hours at room temperature, protected from light. Finally, coverslips were washed 3 times with PBS and mounted on Superfrost® plus slides (Thermo Fisher scientific, J1800AMNZ), using Prolong ™ Gold Antifade reagent with DAPI (Thermo Fisher scientific P36931). Slides were stored at 4°C.

VIII. Confocal microscopy

Images were captured using a Zeiss LSM 700 or Leica SP5 confocal microscopes with x10, x20, x40 or x63 objectives and standard wave lengths and filters.

IX. Image processing

For figures, confocal multi-stacking images were merged using Z project function in Image J software (Schindelin J. et al., 2012). Brightness and contrast were adjusted equally between control and KO images. Background was removed and a scale bar was applied to each image.

X. Fibroblasts culture

Control and patient fibroblasts cells were cultured according to (Barcia *et al.*, 2020) in T75cm² flasks in DMEM-GlutaMAX I medium 1X (Gibco, 31966-021) supplemented with 10% of FBS (Gibco, 10438), 100U/ml of Penicillin, 100µg/ml of Streptomycin (Thermofischer scientific, 15140122), non-essential amino acids 1X (Thermofischer scientific, 11140050) and 50µg/ml uridine (Sigma, U3003) in a humidified incubator, at 37°C, 5% CO2 until they reach 80-100% confluency. Cells were maintained in culture by passaging at a ratio 1:3 or 1:4. For long-term storage, cells were frozen in 10% DMSO in FBS at -80°C and stored at -150°C. For experiments, 80-90% confluent cells were collected by trypsinization, washed with PBS, frozen in liquid nitrogen, and stored at -80°C until needed.

XI. RNA extraction and Northern blot

Total RNA was isolated from control and patient fibroblasts frown to 80-90% confluence in T75 flasks using the miRNeasy mini kit (Qiagen, 217004), according to (Ruzzenente *et al.*, 2012). After DNAse treatment, 2µg RNA was mixed at a 1 to 1 (vol/vol) ratio with NorthernMax™ Gly sample loading Dye Ambion® (ThermoFischer scientific, AM8551), denatured for 45 min at 50°C and loaded on a 1.2% agarose gel prepared with Gel prep/gel running buffer Ambion® (ThermoFischer scientific, AM8678). RNA was blotted onto a nylon membrane Amersham hybond-XL (Merck, GERPN303S) by capillary transfer for 2 h using the NorthernMax™ transfer buffer Ambion® (ThermoFischer scientific, AM8672). Next, RNA was crosslinked to the membrane using an Uvitec crosslinker at 120 Jules. The membranes were prehybridized with Perfect Hyb Plus Hibridization buffer (Sigma, H 7033) for 1h and hybridized overnight with a γ-32P-ATP radiolabeled oligonucleotide complementary to $tRNA^{Val}$ (5' TGGTCAGAGCGGTCAAGTTAAGTT-3'). Radioactive signals were detected by autoradiography using a BAS-IP Imaging plate (Amersham).

XII. Protein extraction from mouse tissues

Cortex, midbrain, cerebellum and brainstem were dissected from freshly explanted brains from control and knockout mice, flash-frozen in liquid nitrogen and stored at -80°C. Each sample was powdered using a pestle and a liquid-N_2-precooled mortar. Adapted from (Ruzzenente *et al.*, 2012), the powders were resuspended in RIPA buffer (Thermo Fisher scientific, 89900), supplemented with 1X protease inhibitor cocktail (Roche, 48047900), and incubated on ice for 20 min. The lysates were cleared by 45 min centrifugation at +4°C and the supernatants were transferred to new tubes.

Alternatively, the different brain structures were placed in Lysing Matrix D tubes (MP Biosciences, 11422420) containing RIPA buffer (Thermo Fisher scientific, 89900) supplemented with 1X protease inhibitor cocktail (Roche, 48047900). Tissues were disrupted using the FastPrep-24™ Classic (MP Biosciences) bead grinder for 45 second with speed 6.5 m/s. Supernatants were transferred to 1.5ml Eppendorf tubes and centrifugated at maximum speed for 45 minutes at +4°C. Finally, the supernatants were transferred to new Eppendorf tubes and stored at -80°C. Protein concentrations were determined using Bradford reagent assay (Sigma, B6916).

XIII. Protein extraction from human fibroblasts

Control and patients' cell pellets were grown in T75 flasks and were processed according to (Ruzzenente *et al.*, 2018), once reaching 80-90% of confluence. They were trypsinized with 0.05% trypsin-EDTA 1X (Gibco, 25300-054) and incubated in a humidified incubator, at 37°C, 5% CO2, before inhibition of the trypsin by adding culture media with FBS (Gibco, 10438). Cells were collected centrifuged for 10 min at 2500 rpm, and supernatant were discard using vacuum and Pasteur pipet. After rinsing with PBS 1X, cell pellets were homogenised and transferred to a 1.5ml eppendorf tube and centrifuged once again for 10 min at 2500 rpm. Supernatant was finally fully discarded to keep a dry cell pellet that was snap-frozen in liquid nitrogen and stored in -80°C until use.

Cell pellets were resuspended in 120µl of lysis buffer (RIPA buffer and protease inhibitor cocktail 1X) added to each sample, then incubated 20 minutes on ice. Samples were sonicated to disrupt nuclear membrane integrity for a few seconds, before undergo centrifugation at 15,000 × g for 30 minutes. Protein concentration was finally determined using Bradford reagent (Sigma, B6916) and a Victor ® Nivo™ plate reader.

XIV. SDS-PAGE

30 µg of proteins were prepared in Laemmli Buffer 1X (1% SDS, 10% glycerol, 10mM Tris-HCl, pH 6.8, 1mM EDTA) (Biorad, 1610747) supplemented with 100mM Dithiothreitol (DTT, Merck, 10708984001). Protein samples were loaded either on 12% mini-PROTEAN TGX precast gel (4561043), 4-15% gradient (5671084), Any kD (5678124), 10% (5671034) criterion TGX precast gels, 12% Criterion™ XT Bis-Tris Protein (3450118) Gel membranes (Biorad).

1. Semi-dry transfer

Semi-dry blotting was carried out using the Transblot Turbo v1.02 (Biorad) transfer system and Trans-blot turbo RTA transfer kit (Biorad, 1704275) according to manufacturer's instructions. After transfer, the membranes were rinsed with water, fixed in absolute ethanol, and rehydrated prior to staining with Ponceau-S solution (Sigma, P7170) to visualize the proteins.

2. Immunodetection

According to (Metodiev *et al.*, 2009; Barcia *et al.*, 2020), PVDF membranes were either dried or directly blocked with 5% non-fat dry milk in PBST, PBS containing 0,05% of Tween (Sigma, P1379), under agitation at room temperature. Next, the membranes were hybridized for 1h at room temperature with primary antibodies in LiCor Intercept® Protein-Free Blocking buffer in PBS (LI-COR, 927-90001, diluted 1:5 with PBST). After 2 washings with PBST for 15 min, the membranes were incubated for 1h at room temperature with secondary antibody diluted at 1/10000 in PBST in a lightproof container. Next, the membranes were washed two times for 15 min in PBST and scanned using the Odyssey CLx infrared scanner (LI-COR). Images were processed and quantified in Image Studio Lite (LI-COR) and Excel (Microsoft). The antibodies used are listed in Table 6 at the end of the Materials and Methods.

XV. Lactate in brain tissues measurement by liquid chromatography-tandem mass spectrometry (LC-MS/MS)

Midbrain and cerebellum were homogenized in 200µl of pre-cooled RNAse free water using a clean Dounce homogenizer, snap-frozen in liquid nitrogen and stored at -80°C before processing. Prior to measurements, the samples were slowly thawed on ice and centrifuged at 15000 rpm for 10 min at 4°C. The resulting supernatant was divided into two tubes of 85µl. One tube was used for lactate measurements by liquid chromatography-tandem mass spectrometry (HPLC-ESI-MS/MS (QqQ) (ABSciex, Shimadzu 8060 ™) in collaboration with the mass spectrometry platform of Saint-Antoine hospital (CRSA) according to (Desmons *et al.*, 2020). From the other half, 20µl were used to determine the sample concentration by Bradford assay while the remaining 65 µl was snap-frozen in liquid nitrogen, alongside the pellets, and stored at -80^{o}C.

XVI. Statistics

Statistical significance was determined using Student's T test in Microsoft Excel or Anova 2-ways in GraphPad Prism. Significance intervals were as follows: *, $p<0.05$; **, $p<0.01$; ***, $p<0.001$; ****, $p<0.0001$.

XVII. Table 6. Primary and secondary antibodies used for immunostaining and SDS-PAGE

Type	Name	Species	Supplier	Cat.nb.	Application /dilution
Primary	Anti-Calbindin	mouse	Swant	CB300	IF 1:100
	Anti-Pax6	rabbit	Millipore Merck	AB2237	IF 1:500
	Anti-Glial Fibrillary Acidic Protein (GFAP)	rabbit	Millipore Merck	AB5804	IF 1:100
	Anti- GFAP	rabbit	Proteintech	16825-1-AP	IF 1:200 WB: 1:1000
	Anti-Thyrosine Hydroxylase (TH)	rabbit	Millipore Merck	AB152	IF 1:100 W: 1:1000
	Anti-Cleaved Caspase 3	rabbit	Cell Signalling Technology	9661S	IF 1:100
	Anti-IBA1	rabbit	Wacko	019-19741	IF 1:100 WB: 1:3000
	mCherry	goat	Sicgen antibodies	AB0040-200	IF 1:200
	LRPPRC	rabbit	Proteintech	21175-1-AP	WB: 1:1000
	LRPPRC (F-7)	mouse	Santa cruz biotechnology	sc-166178	WB: 1:500
	NDUFA13/ grim19 (CI)	mouse	Abcam	110240	WB: 1:1000
	SDHA (CII)	mouse	Abcam	14715	WB: 1:1000
	UQCRC2/ Core2 (CIII)	mouse	Abcam	14745	WB: 1:1000
	COX II (CIV)	rabbit	Proteintecih	55070-1-AP	WB: 1:1000
	COX IV (CIV)	rabbit	Proteintech	11242-1-AP	WB: 1:500
	ATP5a (CV)	mouse	Abcam	14748	WB: 1:1000
	HSP60-B-9	mouse	Santa Cruz Biotechnology	sc-271215	WB: 1:1000
	SOD2/MnSOD	rabbit	Abcam	ab13533	WB: 1:5000
	LC3B rabbit		Abcam	ab51520	WB: 1:3000
	MRPP2/HSD1 7B10	rabbit	Sigma	HPA001432	WB: 1:1000
	ELAC2	rabbit	Proteintech	10071-1-AP	WB: 1:30000
	Beta-actin	rabbit	Proteintech	20536-1-AP	WB: 1:1000
	Alpha-tubulin	mouse	Proteintech	66031-1-Ig	WB: 1:500
	Vinculin	mouse	Proteintech	66305-1-Ig	WB: 1:1000
Secondary	Alexa Fluor 568	Goat-anti-mouse	Thermofischer scientific	A-11004	IF: 1:1000

	Alexa fluor 488	Goat anti-rabbit	Thermofischer scientific	A-32731	IF: 1:1000
	Alexa fluor 488	Goat-anti-mouse	Thermofischer scientific	A-32723	IF: 1:1000
	Alexa fluor 568	Rabbit anti-goat	Thermofischer scientific	A-11079	IF: 1:1000
	IRDye® 680RD	Donkey anti-rabbit	Li-Cor	926-68073	WB: 1:10000
	IRDye® 800CW	Donkey anti-mouse	Li-Cor	926-32212	WB: 1:10000

Table 6. Primary and secondary antibodies used for immunostaining (IF) and SDS-PAGE (WB).

Chapter III: Results

I. Characterisation of midbrain-and-cerebellum specific Lrpprc knock-out mice (MCKO)

To generate ***Lrpprc*** $^{Lox/Lox,\ En1\text{-}Cre}$ ***knock-out mice,*** we crossed conditionally targeted *Lrpprc*$^{Lox/Lox}$ with mice expressing Cre recombinase under the control of En1 promoter. This promoter regulates the Engrailed homeobox 1 gene (*EN1*) specifically expressed during embryogenesis starting from embryonic day E9.5 across the midbrain and the cerebellum (Wurst, Auerbach and Joyner, 1994; Györfi *et al.*, 2021).

1. Expression pattern of the EN1-driven Cre recombinase

To better define the cells in which En1-Cre is expressed in the brain, Rosa26 tdTomato mice were crossed with En1-Cre mice (Wurst, Auerbach and Joyner, 1994; Madisen *et al.*, 2010). Immunofluorescent staining with antibody against mCherry, marker of the tdTomato fluorescent protein, confirmed the expression pattern of the promoter En1, across midbrain and cerebellum in the newly born En1-Cre/Rosa26 tdTomato mice. However, from these analyses it was also evident that tdTomato was not expressed in all cells from the two regions (Fig. 11).

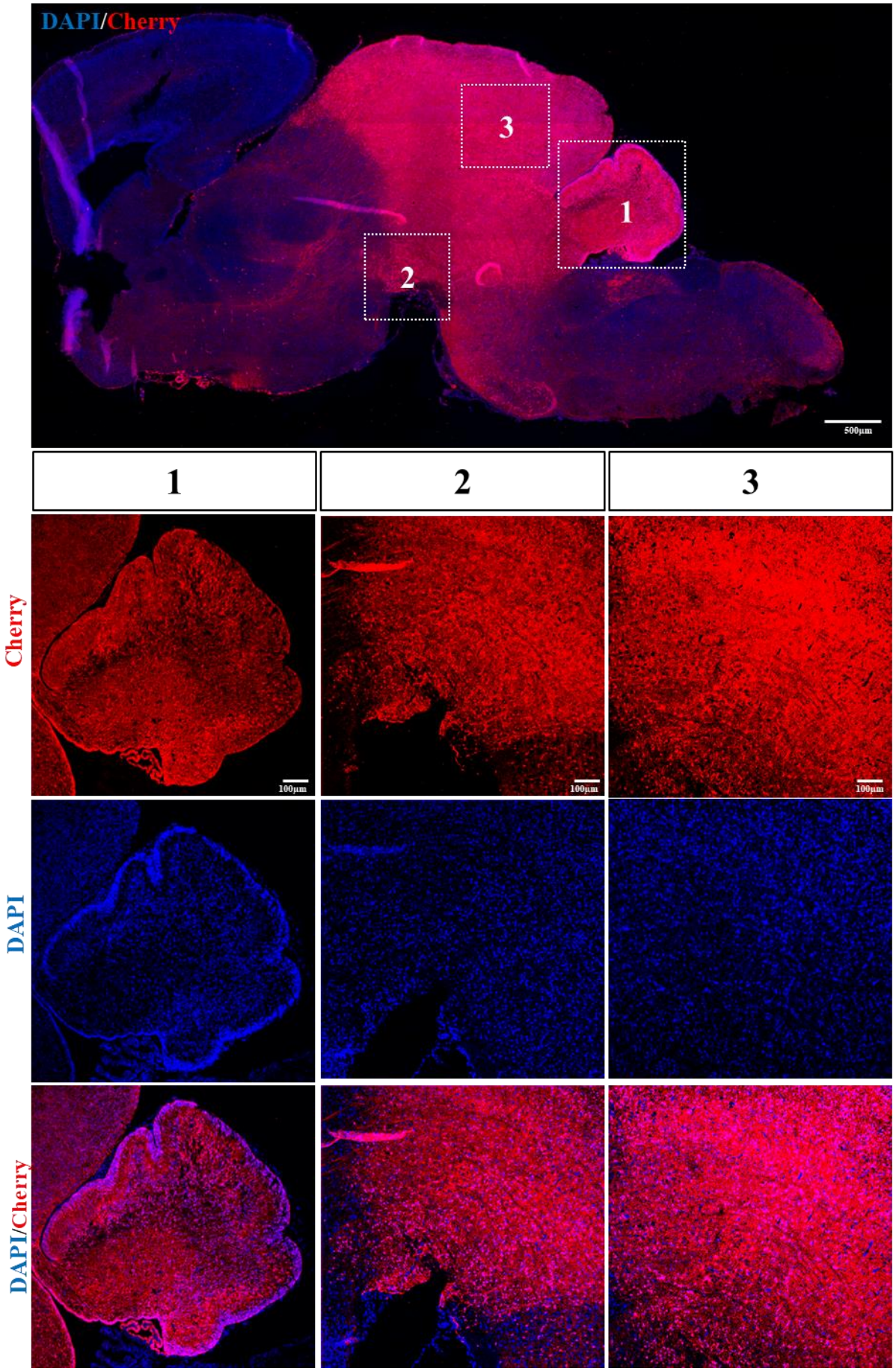

DAPI/Cherry
3
1
2
500μm
1
2
3
Cherry
100μm
100μm
100μm
DAPI
DAPI/Cherry

Figure 11. Expression pattern of En1 promoter was detected in the midbrain and cerebellum of newly born En1-Cre/Rosa26 tdTomato mouse. Immunofluorescent analysis of whole-brain sagittal sections (upper panel), the cerebellum (1) and midbrain (2,3) (lower panels). Expression of the tdTomato protein was detected using an mCherry-specific antibody (red). Dapi staining was used to stain all nuclei (blue). Representative images from a single experiment are shown. Upper panel was generated using Nanozoomer 2.0 HT (Hamamatsu) whereas the images of specific regions are taken using the SP5 confocal microscope. The different regions shown to the lower panels are indicated as white numbers on the full sagittal view of the mouse brain. Upper panel, scale bar was 500µm; remaining panels, scale bar was 100µm.

In addition, co-labelling of sagittal sections from newly born En1-Cre/Rosa26 tdTomato mouse with antibodies against Calbindin and Pax6 in the cerebellum, and TH in the midbrain, respectively marking Purkinje cells, Granule cell precursor cells, and dopaminergic neurons, revealed a clear colocalization with the mCherry fluorescence, confirming that Cre is expressed in these cell types (Fig 12). Thus, our analyses show that En1-driven Cre expression occurs in both DNs regions, ventral tegmental area (VTA) and substantia nigra (SN) (Fig.12). (Since En1 expression occurs in the nucleus and TH, marker of domapinergic neurons is expressed in the cytosol, the colocalization does not appear completely yellow).

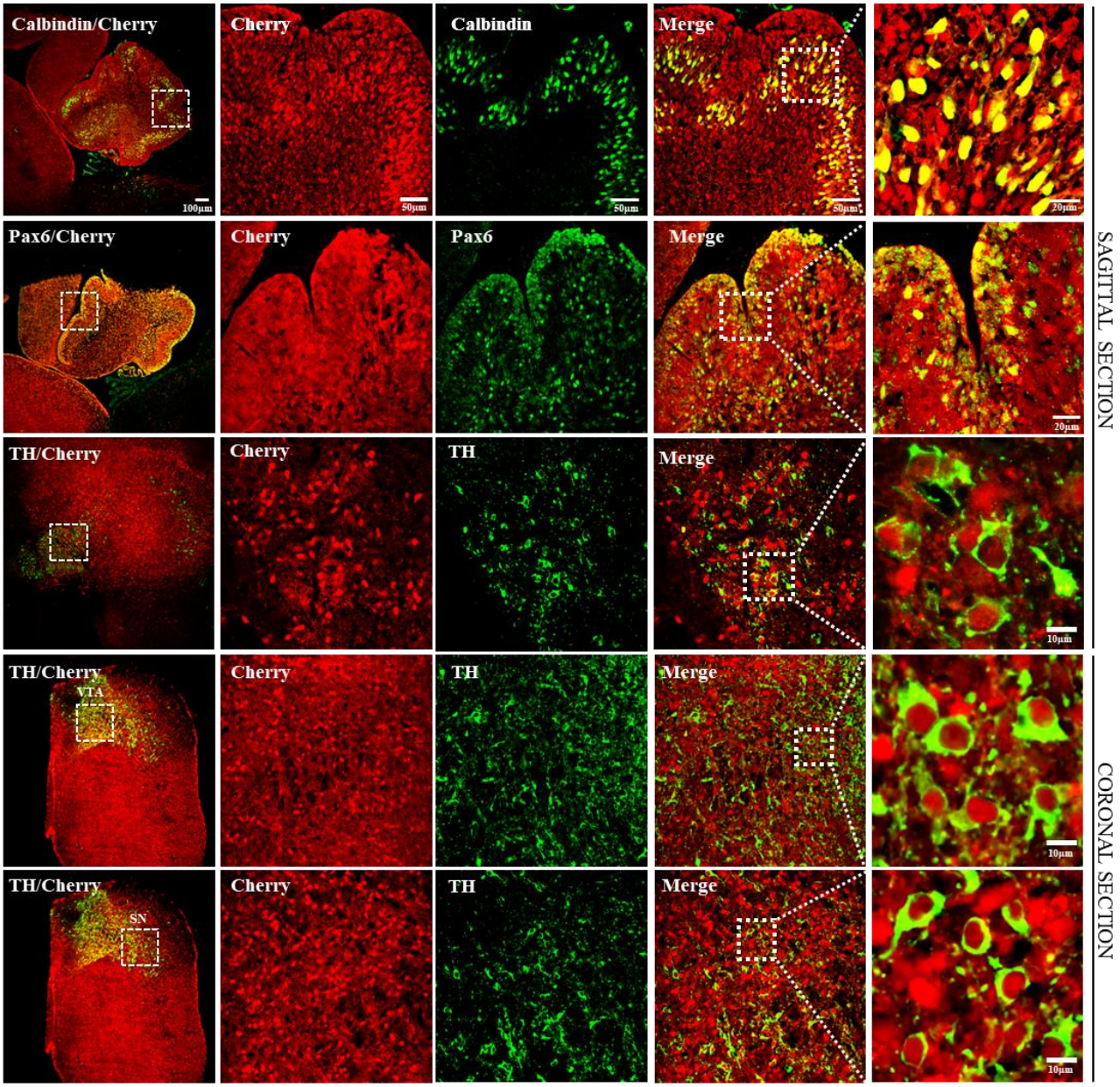


Figure 12. En1-driven Cre expression detected in Pcs, GCPs and DNs from newly born En1-Cre/Rosa26 tdTomato mouse. Immunofluorescent analysis of sagittal (three upper panels) and coronal (two lower panels) brain sections. dtTomato (red) was detected as in Figure 11. Pcs were detected using antibody against Calbindin (green), GCPs with antibody against Pax6 (green), and DNs with antibody against TH (green). Left-hand panels, scale bar was 100µm; magnification panels: scale bar from the two upper panels showing Pcs and GCPs was 20µm, scale bar from the middle panel in sagittal section showing DNs was 10µm, scale bar from the tow lower panels in coronal section showing DNs from the ventral tegmental area (VTA, upper) and substantia nigra (SN, bottom panel) was 10µm; remaining panels, 50µm. Representative images from a single experiment are shown.

2. Specificity of En1-driven Lrpprc knockout

In addition to midbrain and cerebellum, En1 mRNA [Gene ID-2019] was also reported to be expressed in other tissues, such as skeletal muscle and skin, although transiently during embryonic development (Wurst, Auerbach and Joyner, 1994; Digre and Lindskog, 2021; Györfi *et al.*, 2021). Therefore, Lrpprc expression was assessed by immunoblotting of skin protein extracts from newly born control and MCKO mice. This analysis revealed that no significant differences in Lrpprc expression were noted between control and MCKO mice (Fig.13).

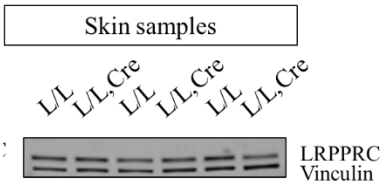


Figure 13. MCKO mice did not exhibit loss of Lrpprc skin tissues. Immunoblot analysis of skin protein extracts from newly born controls (n=3) and MCKO (n=3) mice, using antibody against Lrpprc and, as loading control, antibody against Vinculin.

3. Loss of Lrpprc in the midbrain and cerebellum causes early postnatal lethality

MCKO mice were born with Mendelian distribution comprising approximately 25% of all newly born pups (Fig.14 A). At birth, they appeared undistinguishable from their littermates despite having a slightly reduced weight (Fig.14 B) and a tendency for a smaller milk spot (Fig.14 C). However, they died soon after birth and none of the pups survived to P1.

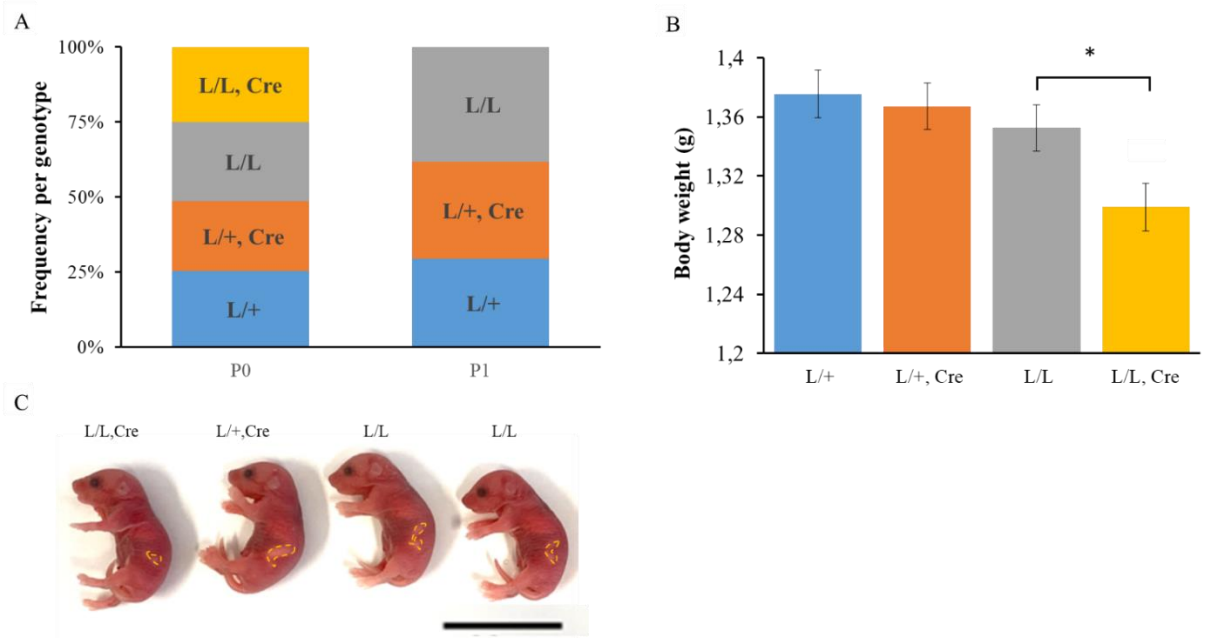


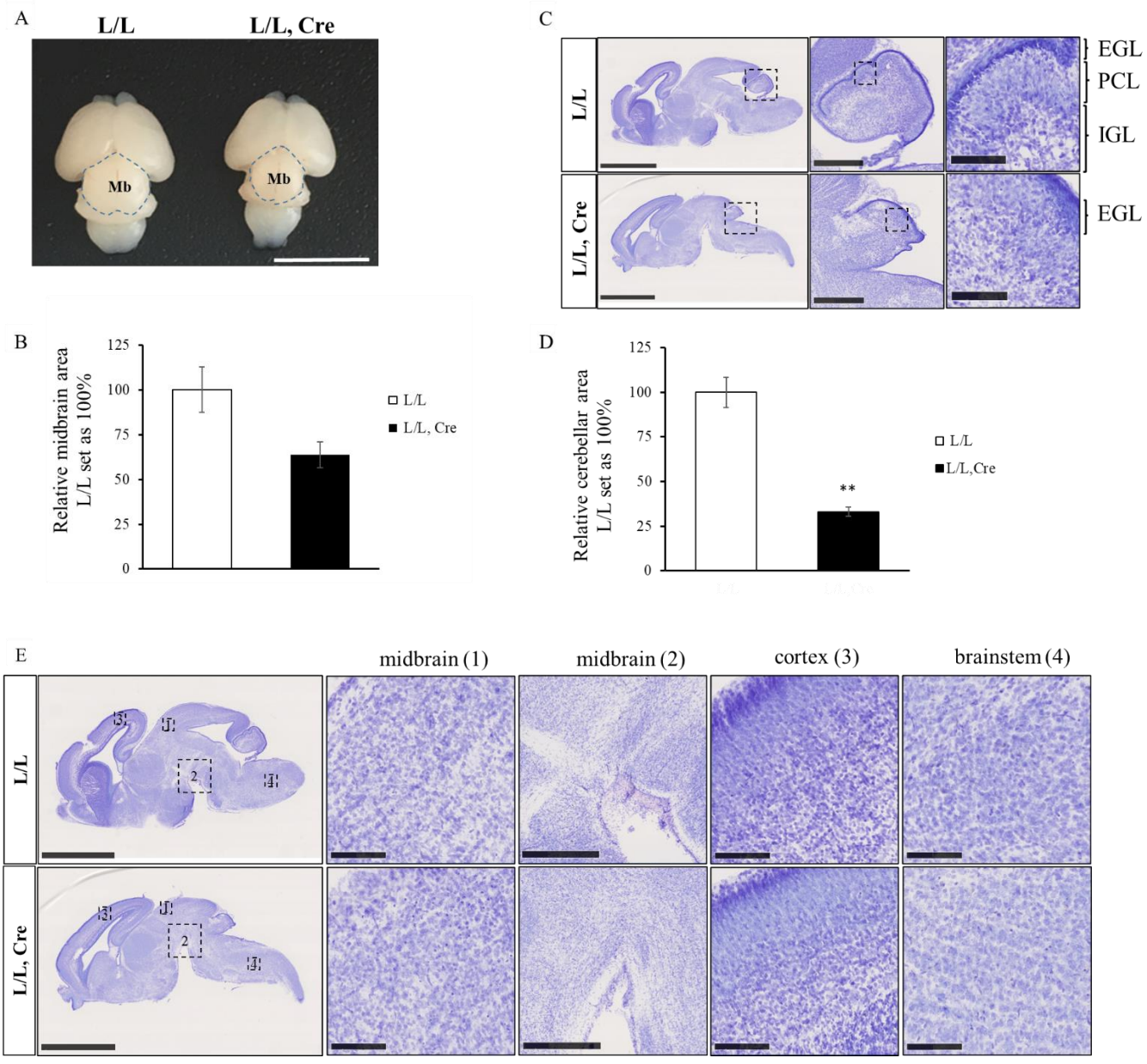
Figure 14. Early postnatal lethality of MCKO mice. (A) Relative distribution of the genotypes at birth and P1 in litters originating from mating *Lrpprc*$^{Lox/Lox}$ and *Lrpprc*$^{Lox/+,\ En1\text{-}Cre}$ mice. L/L, *Lrpprc*$^{Lox/Lox}$; L/+, *Lrpprc*$^{Lox/+}$; L/+, Cre, *Lrpprc*$^{Lox/+,En1\text{-}Cre}$; L/L, Cre, *Lrpprc*$^{Lox/Lox\ ,En1\text{-}Cre}$; Cre, En1-Cre. At P0, n=403 (L/L, n=102; L/+, n=94; L/+, Cre, n=106; L/L, Cre, n=101). Number of pups at P1=34 (L/L, n=10; L/+, n=11; L/+, Cre, n=13; L/L, Cre, n=0). (B) Decreased body weight of newly born MCKO pups compared to their littermates. n=404 (L/L, n=105; L/+, n=105; L/+, Cre, n=115; L/L, Cre, n=79). Data are plotted as the mean ± standard error of the mean. Body weight data from newly born L/L and L/L, Cre mice were analysed using Student's t-test. *, $p<0.05$. (C) Representative images of newly born pups with different genotypes illustrating the visible area of their milk spots (dashed line). Scale bar was 2cm.

4. Delayed development of cerebellar and midbrain regions showed in absence of Lrpprc

Morphometric comparison of explanted brains from newly born control and MCKO mice revealed underdeveloped midbrain and cerebellum in knockout mice (Fig.15 A). Dorsal view measurement of the midbrain area revealed a slight decrease in MCKO mice compared to controls (Figure 15 B).

To understand in further detail the nature of this developmental defect, we carried out a histochemical Nissl and haematoxylin-eosin staining on sagittal brain sections. This analysis corroborated our observation that loss of *Lrpprc* results in underdeveloped midbrain and revealed a severe cerebellar foliation defect with a drastic decrease (75%) of the cross-sectional cerebellar area in knockout mice (Fig. 15 C, D). Furthermore, Nissl staining, showed no significant changes in cortex and brainstem, as the majority of cells in these regions do not express Cre recombinase (Figs. 11 and 15 E).

Haematoxylin-eosin staining corroborated the above findings, but also revealed a complete disorganization of the different cerebellar cellular layers (Fig.15 F) and absence of clearly delineated internal granular (IGL) and Purkinje cell layers (PCL) in MCKO mice, suggesting importance of Lrpprc for cerebellar foliation and organization.



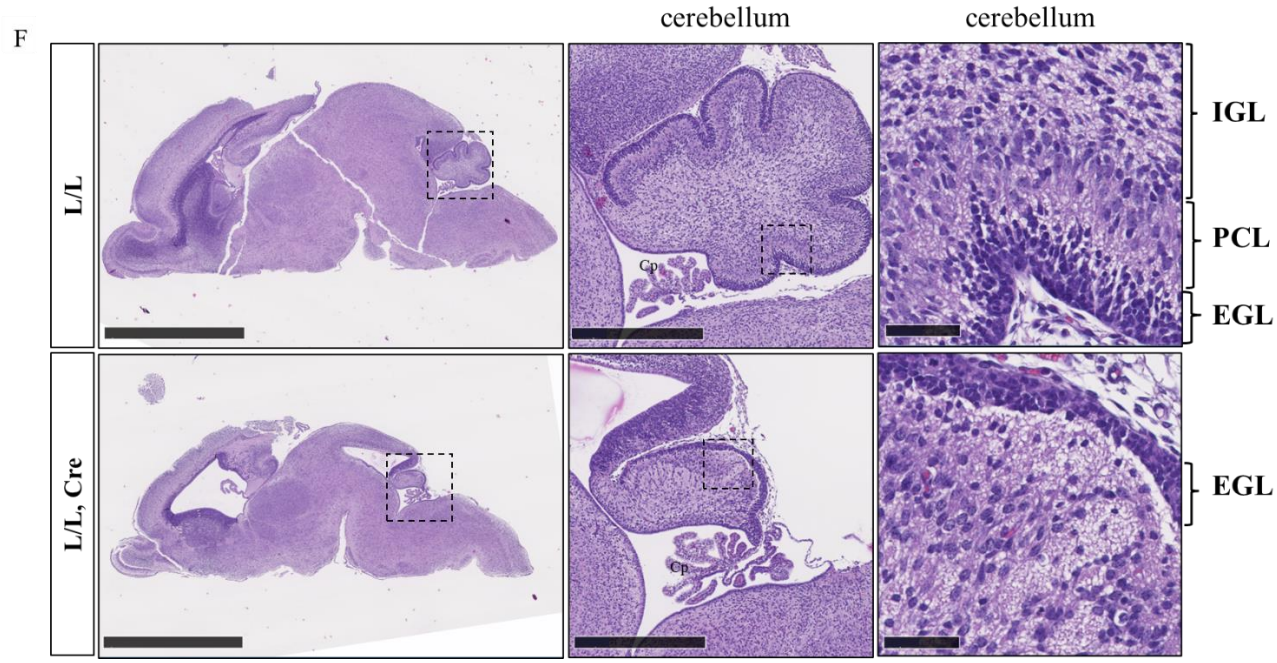
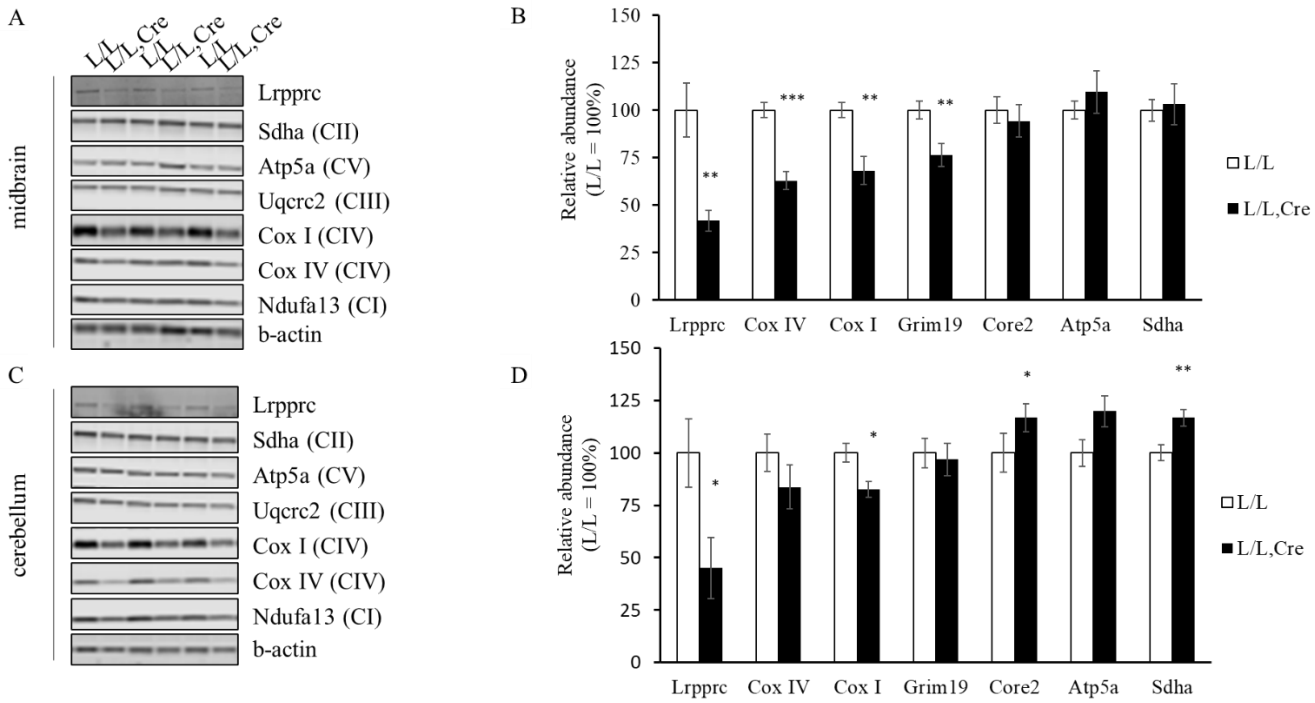


Figure 15. Loss of Lrpprc in cerebellum and midbrain alters the development of these two brain regions as visualised by morphometric analysis and Nissl staining. (A) Representative images of brains explanted from newly born control L/L (n=4) and MCKO L/L, Cre (n=4) mice. Blue dashed lines mark midbrain (Mb) visible area, red dashed lines mark cerebellum (Cb) visible area. Scale bar was 5mm (B) Measurement of the visible midbrain area from stereomicroscope images of newly born control, L/L (n=3) and MCKO L/L, Cre (n=3) mice. Data are plotted as the mean ± standard error of the mean and were analysed using Student's t-test. (C) Nissl staining of sagittal sections from newly born control and MCKO mice. Representative images from 4 independent experiments are shown. In the first panel, scale bar was 2,5 mm; second panel: scale bar was 500µm; magnification panel, scale bar was 100µm. IGL: internal granular layer; PCL: purkinje cell layer; EGL: external granular layer. (D) Cerebellar area analysis from Nissl staining sagittal sections of newly born control (n=4) and MCKO (n=4) mice. Data are plotted as the mean ± standard error of the mean and were analysed using Student's t-test; **, $p<0.01$. (E) Nissl staining of sagittal sections from newly born control and MCKO mice. Representative images from 4 independent experiments are shown. Scale bars: first left-hand panel 2.5mm; third panel, 500µm; remaining panels,100µm. (F) Haematoxylin-Eosin staining of sagittal sections from newly born control and MCKO mice showing disorganization of the different cerebellar cellular layers. Representative images from 3 independent experiments are shown. Scale bars: first left-hand panel, 2.5mm; second panel, 100µm; magnification panel, 50µm. IGL: internal granular layer; PCL: Purkinje cell layer; EGL: external granular layer; Cp: choroid plexus.

5. OXPHOS deficiency in midbrain and cerebellum of MCKO mice

Loss of Lrpprc in other mouse models resulted in decreased OXPHOS abundance and activity (Ruzzenente *et al.*, 2012; Cuillerier *et al.*, 2017), therefore, immunoblotting was performed to determine the abundance of LRPPRC and individual OXPHOS proteins, in four different brain regions: cortex, midbrain, brainstem and cerebellum. This analysis revealed that Lrpprc protein level was significantly reduced in midbrain and cerebellum of MCKO pups compared to controls. Concomitantly, abundance of the OXPHOS proteins Ndufa13 (Complex I), COXI and COXIV (Complex IV) was also decreased in midbrain (Fig.16 A, B) and cerebellum (Fig.16 C, D) from MCKO mice. The Complex II subunit Sdha, the Complex III subunit Uqcrc2 (Core2) and the complex V subunit Atp5a were unchanged or slightly upregulated in midbrain or cerebellum, respectively (Fig16. C, D). The decreased abundance, rather than complete absence, of Lrpprc in midbrain and cerebellum is consistent with the diverse cellular composition of these brain structures and the fact that some cell types do not express the En1-driven Cre recombinase. In cortex (Fig.16 E, F) and brainstem (Fig.16 G, H), which do not express Cre, Lrpprc level in MCKO mice was similar to control littermates.



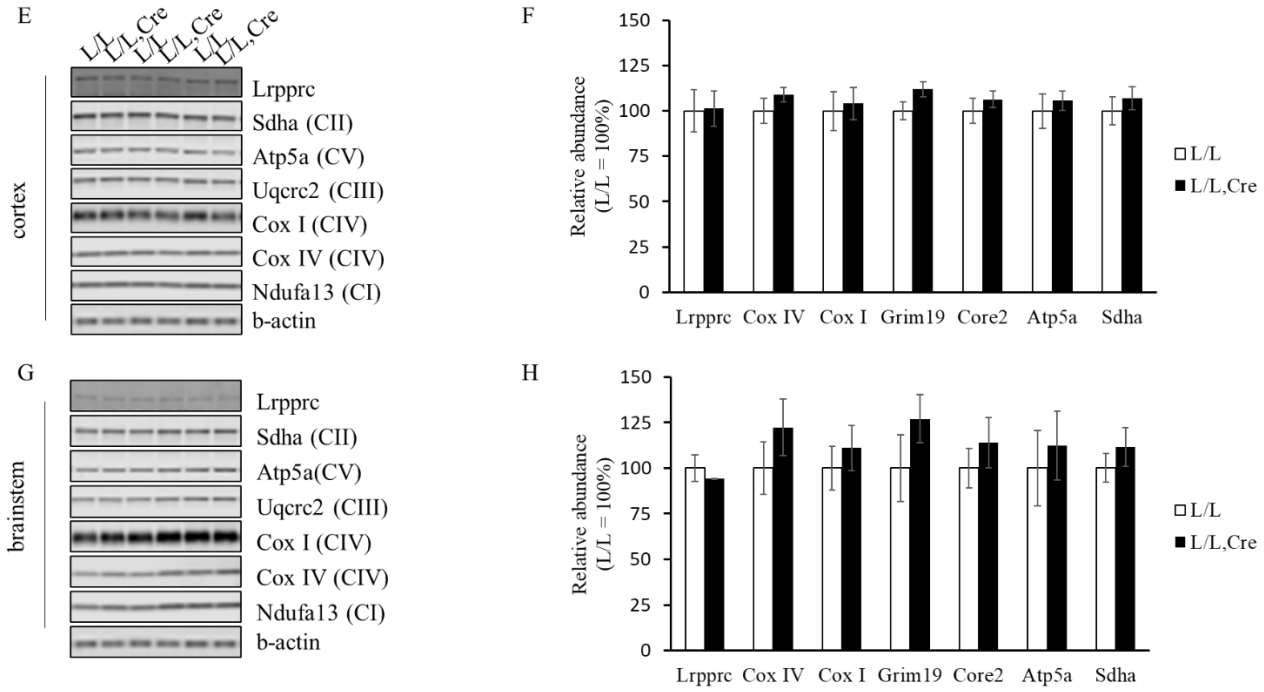


Figure 16. Abundance of different OXPHOS proteins in L/L and L/L, Cre mice in different brain regions at P0. Immunoblot analysis of whole-cell lysates from midbrain (A), cerebellum (C), cortex (E) and brainstem (G) explanted from newly born L/L (n=7) and L/L, Cre (n=8) mice using antibodies against Lrpprc and different OXPHOS proteins, and as loading control, β-actin-specific antibody. Three couples from the entire immunoblot are shown. (B, D, F, H). Quantification of the immunoblots in panels A, B, C, E and G. Data are plotted as the mean ± standard error of the mean and were analysed using Student's t-test: *, $p<0.05$; **, $p<0.01$; ***, $p<0.001$.

Next, cryoprotected sagittal sections of brains from newly born control and MCKO mice were subjected to COX/SDH enzymatic staining revealing a clear decrease of complex IV-activity throughout the midbrain and cerebellar regions of MCKO mice (Fig.17). As expected, cortex and brainstem did not show any OXPHOS activity defect.

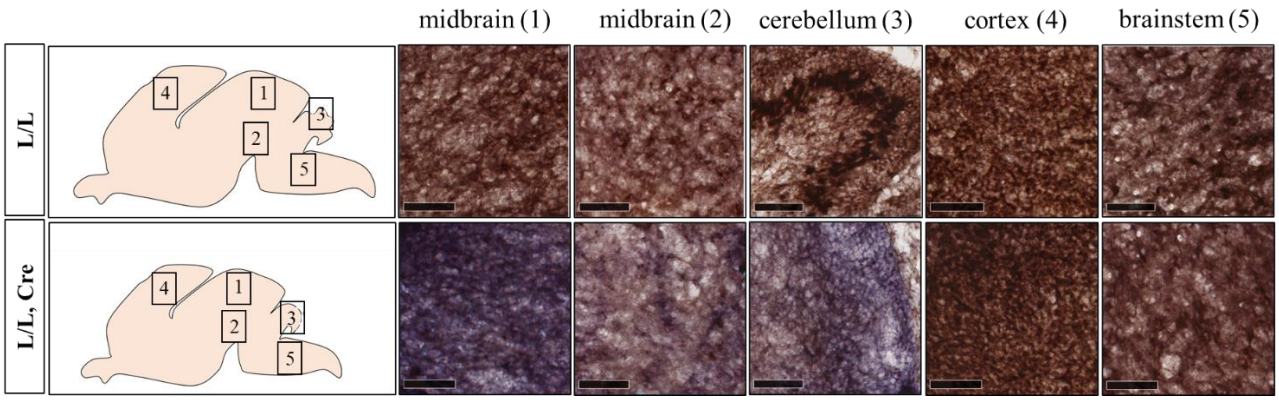


Figure 17. Loss of Lrpprc leads to complex IV deficiency in MCKO mice. Double COX/SDH staining of different brain regions from newly born control L/L (n=2) and MCKO L/L, Cre (n=2) mice. Representative images of 2 independent experiments are shown. The different regions shown to the right are indicated as numbered squares on the schematic mouse brains. Scale bar was 50 μm.

6. Lactate level in brain tissues

High levels of lactate in plasma and cerebrospinal fluid suggest an impairment of the OXPHOS system and is frequently observed in patients with mitochondrial diseases. Most patients with LSFC were diagnosed with elevated levels of lactate and some develop lactic acidosis leading to fatal crises (Morin *et al.*, 1993; Burelle *et al.*, 2015). Therefore, lactate level was assessed in tissue extracts from cerebellum and midbrain by liquid chromatography-tandem mass spectrometry (LC-MS/MS) analysis. This analysis showed a slight increase of lactate in the cerebella of MCKO mice (Fig. 18 A), and a significant increase of lactate in midbrain of MCKO mice (Fig.18 B) compared to controls, suggesting that loss of Lrpprc lead to elevated lactate concentration.

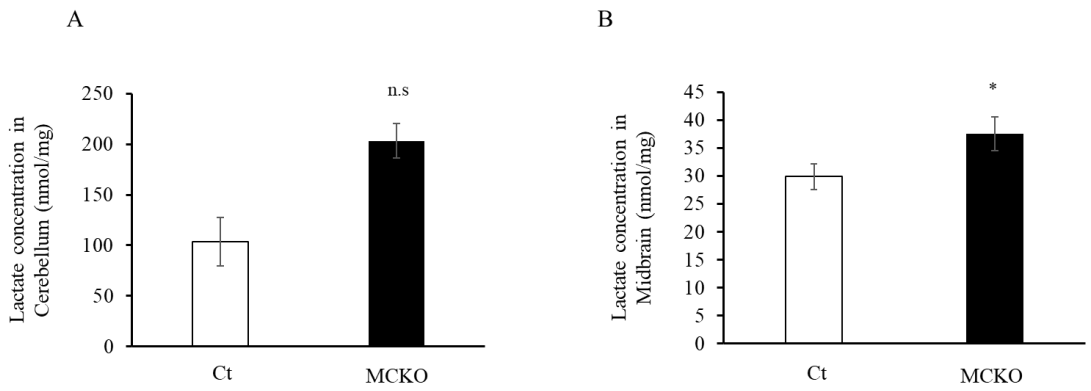
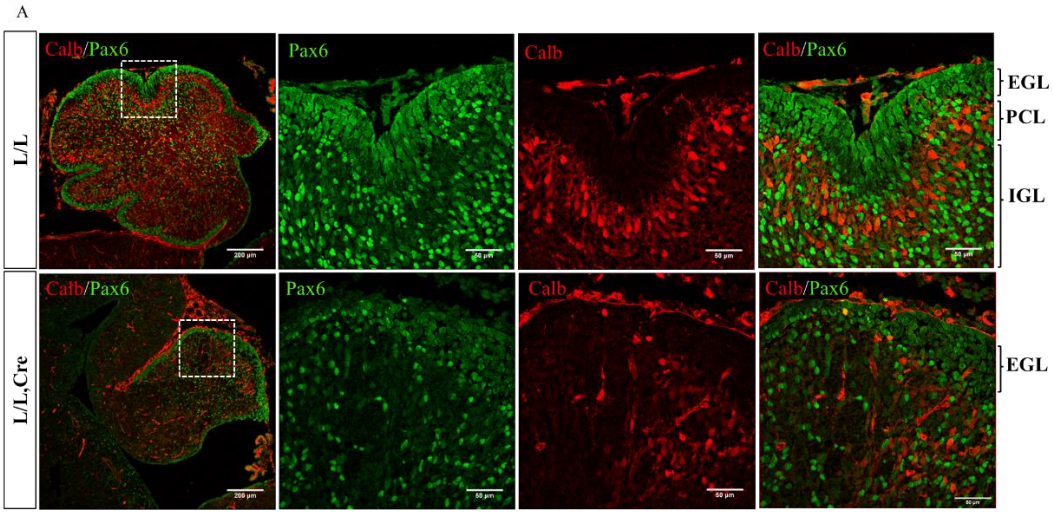


Figure 18. Loss of Lrpprc lead to increase level of lactate. (A) Lactate concentration (nmol/mg) in cerebellum from homogenates samples of newly born MCKO mice (n=6) compared with control mice (n=6). (B) Lactate concentration (nmol/mg) in midbrain from homogenates samples of newly born MCKO mice (n=7) compared with control mice (n=6). Data are plotted as the mean ± standard error of the mean and were analysed using Student's t-test; *, $p<0.05$; ns means not significant.

7. Loss of Lrpprc causes cerebellar disorganization and underdeveloped Purkinje cell dendrites

To assess how loss of Lrpprc affects individual cell populations within the cerebellum, immunohistochemistry (IHC) was carried out using specific cell type markers. Immunofluorescent staining with Calbindin and Pax6 antibodies, markers for Pcs and the GCPs in the EGL, respectively, confirmed the previously observed cerebellar foliation defect and revealed a complete disorganization of the different cellular layers in cerebella of knockout mice. In the latter, GCP cells formed a less defined layer in the EGL and failed to migrate properly in the IGL, their final location under normal conditions (Fig.19 A). Moreover, in MCKO cerebella, Pcs showed a reduced density and had poorly developed dendrites (Fig.19 B). These results suggest that proper mitochondrial function is essential for cerebellar layer establishment and Pcs development.



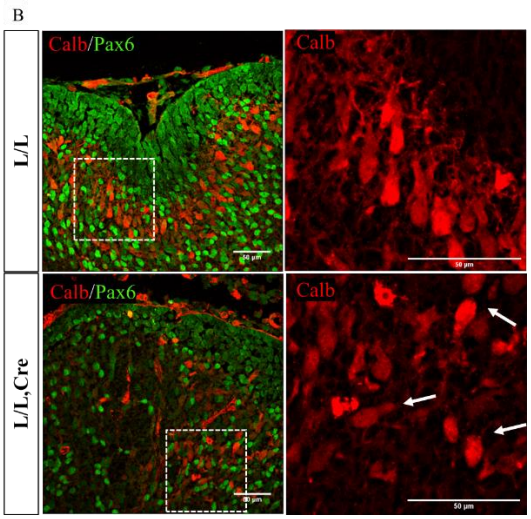


Figure 19. Absence of Lrpprc leads to cerebellar developmental defects. (A) Immunofluorescent analysis of sagittal cerebellar sections from newly born control and MCKO mice. Purkinje cells were detected using antibody against Calbindin (red) while the outer molecular layer and dividing cell are detected using antibody against Pax6 (green). Scale bars: 200µm and 50µm. (B) Magnification of the images in (A). White arrows indicate Pcs bodies. Representative images from 3 independent experiments are shown. Scale bars, 50µm. EGL: external granular layer; PCL: Purkinje cell layer; IGL: internal granular layer.

8. Dopaminergic neurons of the substantia nigra are sensitive to loss of Lrpprc

Substantia nigra and ventral tegmentum area are two close but different sources of dopaminergic neurons, part of the basal ganglia, one of the brain regions impaired in LS. Involved in motor function, behavior, as well as control of emotions and motivation, these cells are of major importance regarding the diseases related, thus a vulnerable cell type. Previous mouse models of LS have also described defects in dopaminergic neurons (Lagrue *et al.*, 2009), therefore, these neurons were assessed using immunofluorescent analysis. Staining of sagittal and coronal sections with tyrosine hydroxylase (TH) antibody, marker of DNs, revealed that this neuronal population was severely decreased in MCKO mice (Fig.20 A). Coronal sections revealed a more severe decrease in substantia nigra compared to the ventral tegmental region in MCKO indicating a location-specific sensitivity of DNs to the loss of Lrpprc (Fig.20 B). These data were corroborated by immunoblot analysis of midbrain extracts which also showed a decrease in TH levels in MCKO mice (Fig.20 C, D).

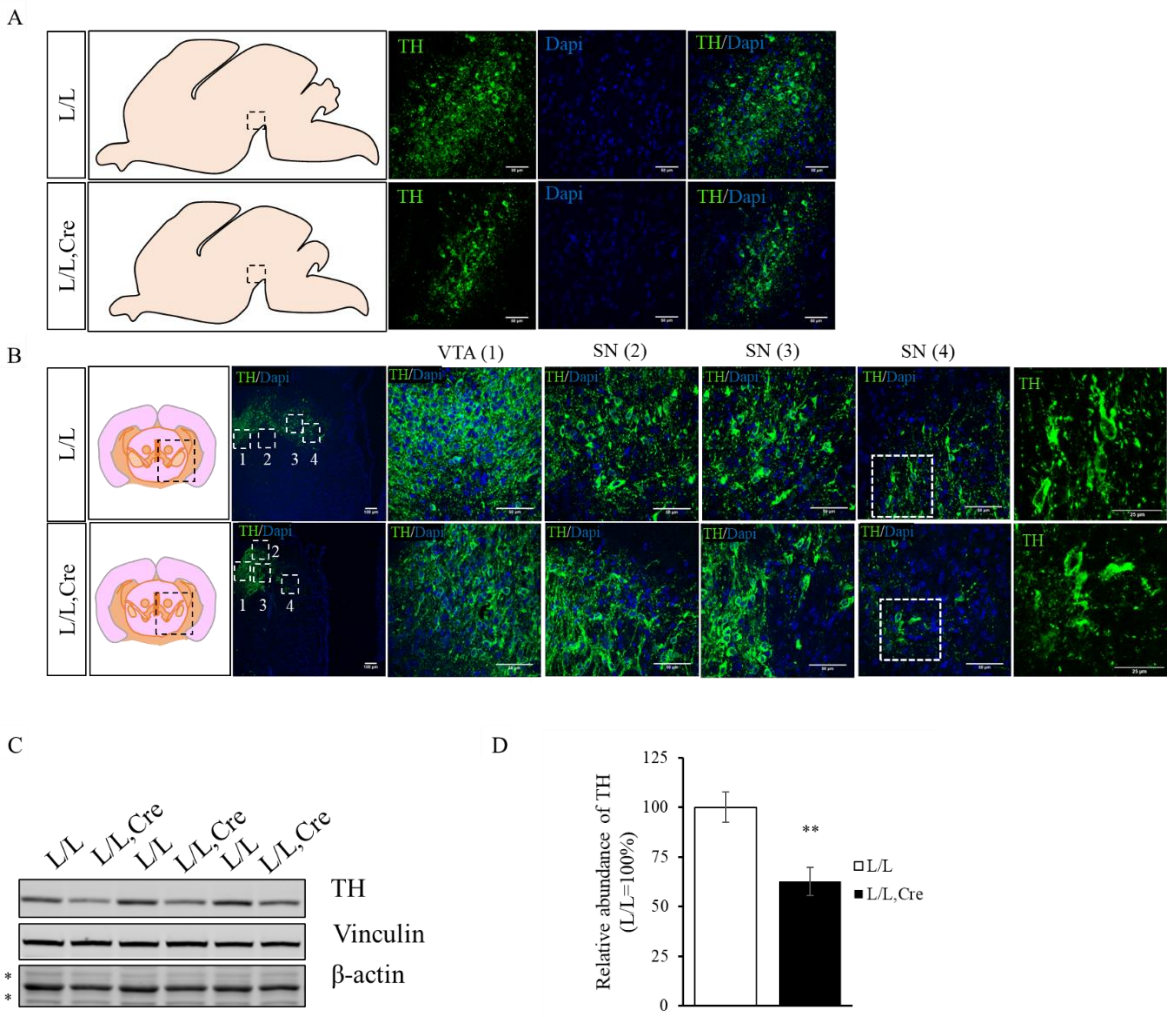


Figure 20. Absence of Lrpprc leads to loss of dopaminergic neurons in *substantia nigra* of newly born knockout pups. (A) Immunofluorescence analysis of sagittal sections across midbrain region from newly born L/L and L/L, Cre pups, hybridized with anti-TH antibody (green); Dapi counterstains all nuclei in blue. Representative images from 3 independent experiments are shown. Scale bar, 50µm. (B) Immunofluorescence analysis of coronal sections across midbrain region from newly born control and MCKO as in (A). Representative images from 3 independent experiments are shown. Scale bars: first left-hand IF panel, 100µm; magnification panel, 25µm; remaining panels, 50µm. (C) Immunoblot analysis of tissue lysates from newly born L/L (n=6) and L/L, Cre (n=6) pups, using anti-TH, and as loading controls, Vinculin and β-actin-specific antibodies. Three couples from the entire immunoblot are shown. (*) indicates cross-reacting bands. (D) Quantification of the immunoblots in panel C. Data are plotted as the mean ± standard error of the mean and were analysed using Student's t-test: **, $p<0.01$.

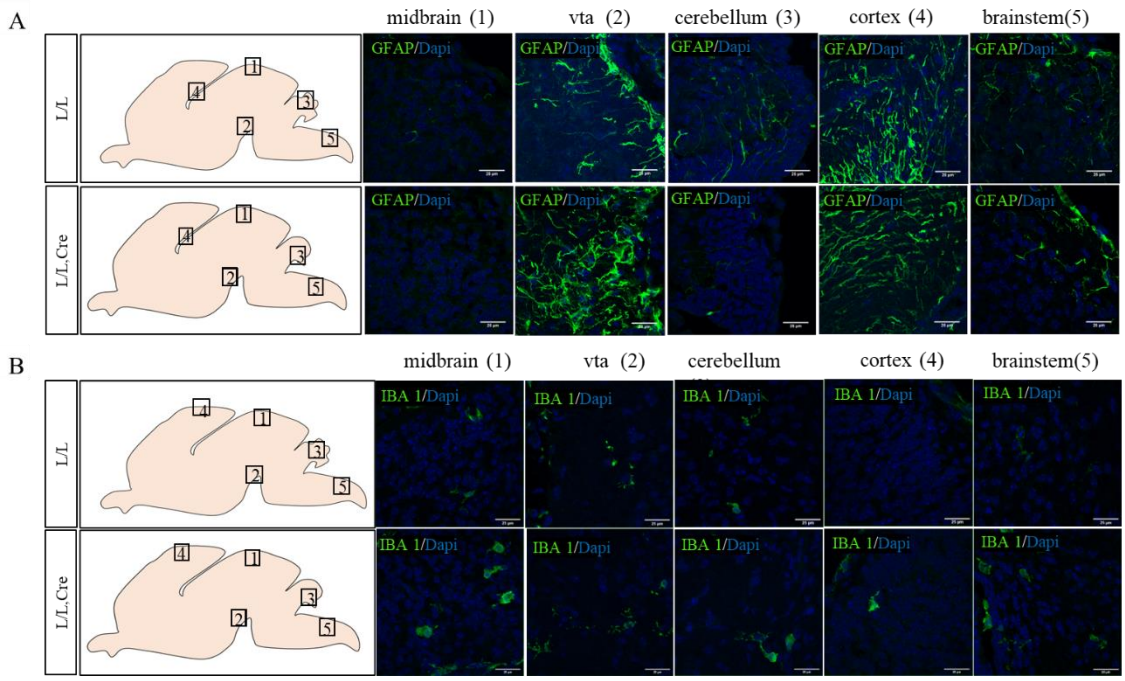
9. Response to mitochondrial dysfunction caused by loss of Lrpprc.

Loss of Lrpprc leads to mitochondrial dysfunction that could induce neuroinflammation, oxidative stress, mitochondrial unfolded protein response (mt-UPR), autophagy and/or apoptosis. Molecular markers characteristic of these responses were evaluated using immunoblotting and immunofluorescence.

a. Neuroinflammatory response

Neuroinflammatory response can arise as a result of various stressors including neurological diseases, physical trauma etc. During this response, microglia and astrocytes, the immune cells in the brain, are activated and proliferate, which promotes pro-inflammatory cytokines release, leading to neuronal death. Mitochondrial dysfunction have been previously shown to induce neuroinflammation in LS mouse models (Sörensen *et al.*, 2001; Quintana *et al.*, 2010; Bolea *et al.*, 2019).

Neuoinflammation was assessed using staining of sagittal sections from newly born control and MCKO mice with the antibodies anti-GFAP (Fig.21 A) and anti-IBA1 (Fig.21 B), which revealed neither significant increase in astrocyte activation nor reactive gliosis in MCKO midbrains and cerebella. Similarly, immunoblotting using GFAP and IBA1 antibodies (Fig.21 C, D) confirmed the absence of neuroinflammatory response in newly born MCKO mice.



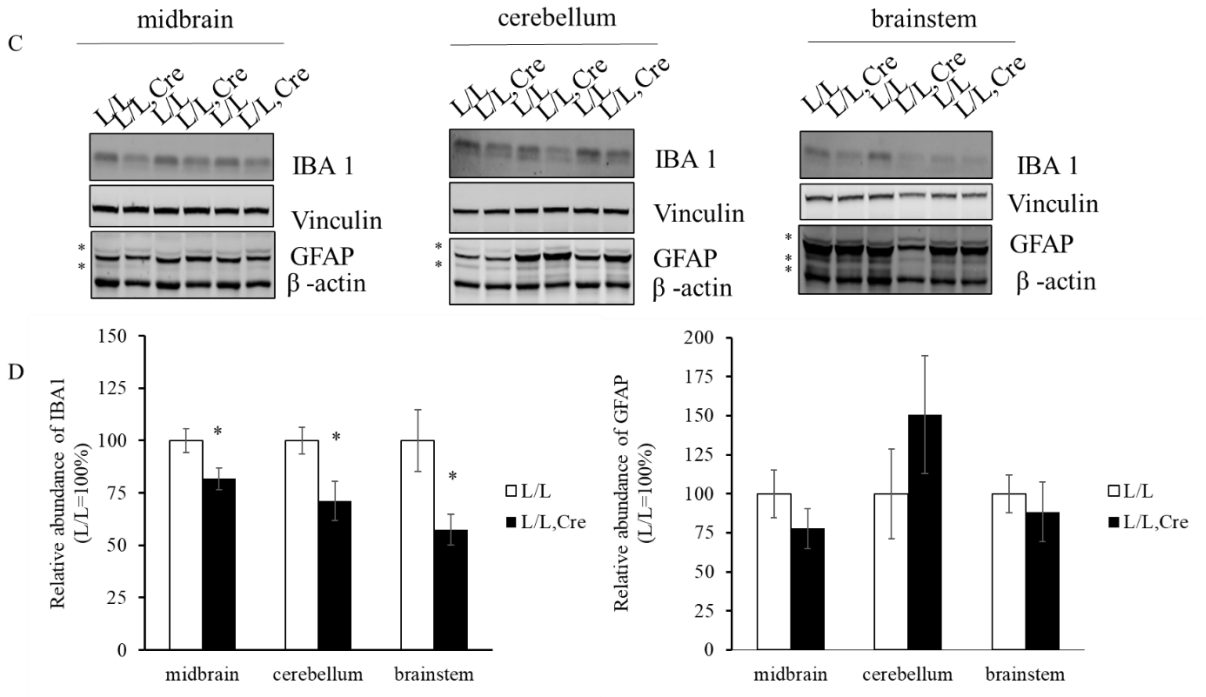


Figure 21. Loss of Lrpprc did not lead to neuroinflammation. (A) Immunofluorescence analysis of sagittal sections across different brain regions from L/L and L/L, Cre pups at P0, hybridized with antibody against GFAP (green). Dapi counterstains nuclei in blue. Representative images from 4 independent experiments are shown. Scale bar, 25µm. (B) Immunofluorescence analysis of brain sections as in (A) but hybridized with antibody against IBA1 (green). Dapi counterstains nuclei in blue. Representative images from 3 independent experiments are shown. Scale bar, 25µm. (C) Immunoblot analysis of tissue lysates from different brain regions of newly born L/L (n=6) and L/L, Cre (n=6) mice, using antibodies against GFAP, IBA1, and as loading controls, vinculin, and β-actin. Three couples from the entire immunoblot are shown. * indicates cross-reaction bands. (D) Quantification of the immunoblots in C. Data are plotted as the mean ± standard error of the mean and were analysed using Student's t-test; *, $p<0.05$.

b. Oxidative stress and UPRmt

ATP production is accompanied by the generation of a basic level of reactive oxygen species like superoxide ion (O2-) produced by the OXPHOS (CI and CIII) (Dröse and Brandt, 2012). However neurodegenerative diseases can exhibit an excessive generation of reactive oxygen species (ROS) (Hayashi and Cortopassi, 2015). In mitochondria, the enzyme superoxide dismutase 2 (SOD2) can further react with O2- to produce the more stable hydrogen peroxide (H2O2) and thus control ROS production (Flynn and Melov, 2013).

Excessive release of ROS can tax SOD2 scavenging role and cause irreversible damage to the neural cells at many levels: impairment of protein functions and degradation, altered

cytoplasmic and mitochondrial membrane integrity, nuclear and mitochondrial DNA mutations, decreased ATP production, induction of apoptosis, autophagy, and necrosis (Burchell *et al.*, 2010). Then, ROS excess leads to neuroinflammation and cell death via different signaling pathways, that are highly involved in progression of neurodegeneration (Burchell *et al.*, 2010).

The mitochondrial unfolded protein response (UPRmt) is a response to mitochondrial stress caused by accumulation of misfolded proteins, leading to nuclear retrograde signalling and activation of specific protective genes (Mottis, Jovaisaite and Auwerx, 2014; Fiorese and Haynes, 2017). It involves mitochondrial chaperones proteins like the heat shock proteins 10 or 60 (HSP10, HSP60) or the proteases ClpP and LONP1, overactivated by the induction of the transcription factors ATF5 CHOP. HSP60, upregulated in UPRmt is commonly used a marker of this stress response (Mottis, Jovaisaite and Auwerx, 2014; Fiorese and Haynes, 2017).

To determine the increase of oxidative stress, we tested the abundance of SOD2 by immunoblotting of protein extracts from different brain regions of newly born controls and MCKO mice. These analyses revealed no significant increase in the abundance of SOD2 and HSP60 (Fig.22 A, B) suggesting that loss of Lrpprc did not lead to oxidative stress nor UPRmt.

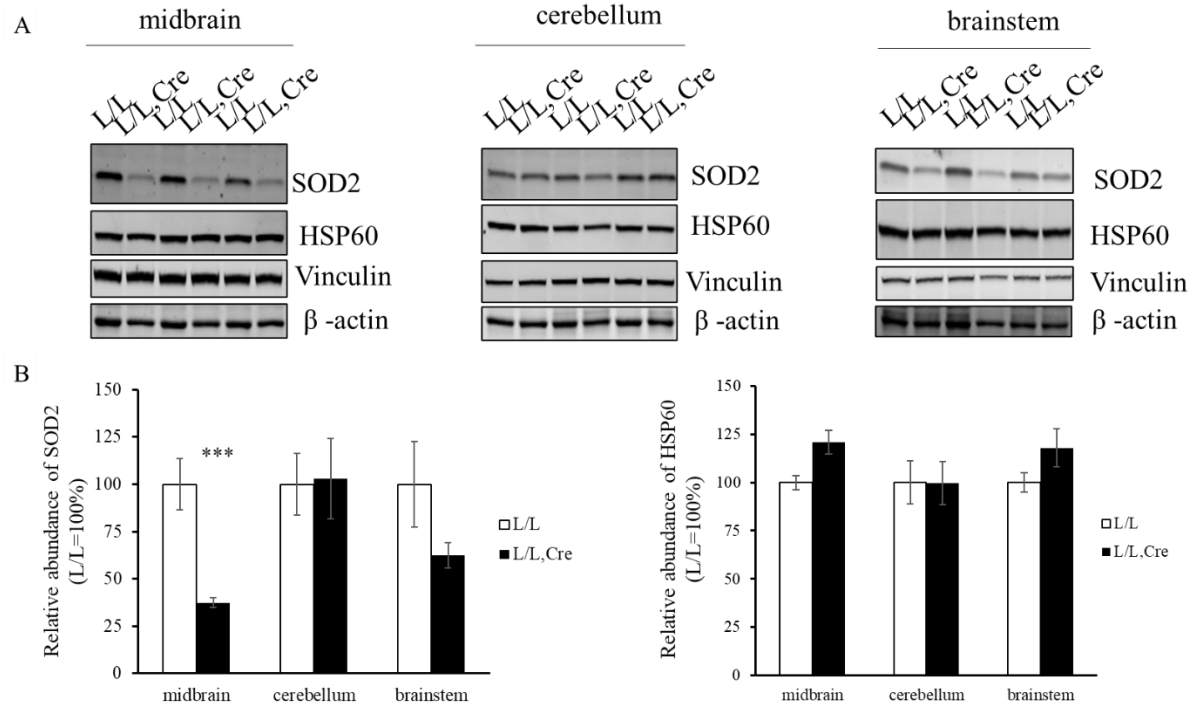


Figure 22. Loss of Lrpprc did not lead to oxidative stress nor induction of the UPRmt pathway. (A) Immunoblot analysis of tissue lysates from newly born L/L (n=6) and L/L, Cre (n=6) mice, using antibodies against SOD2, HSP60. Antibodies against vinculin and β-actin were used as loading controls. Three couples from the entire immunoblot are shown. (B) Quantification of

the immunoblots in (A). Quantification of the immunoblots in C. Data are plotted as the mean ± standard error of the mean and were analysed using Student's t-test; ***, p<0.001.

c. Autophagy

Autophagy is a process by which impaired cellular components like proteins or organelles are degraded. It requires autophagosomes that capture the impaired components by engulfment, and after fusion with lysosomes, form autolysosome vesicles that degrade the sequestered components. Autophagy is a key mechanism to maintain homeostasis in cells and autophagy defects contribute to neurodegenerative diseases (Son *et al.*, 2012). It involves the recruitment of the microtubule-associated protein 1A/1B-light chain 3 or LC3. LC3 is found soluble as LC3-I in the cytosol or as hydrophobic LC3-II once it is conjugated to phosphatidylethanolamine in autophagosome membrane during autolysosome formation. In the autolysosome, LC3-II is degraded and ,therefore, the increased LC3-II/LC3-I ratio is a marker for increased autophagy (Randow and Youle, 2014).

Immunoblotting with antibodies against LC3B, which detects the two forms LC3-I and LC3-II, was carried out from lysates from midbrain, cerebellum, and brainstem. However, LC3-I and LC3-II abundance showed no significant change in MCKO pups (Fig.23 A) and the LC3-II/LC3-I ratio did not increase in the different brain structures of MCKO pups compared to controls (Fig.23 B). Thus, loss of Lrpprc in midbrain and cerebellum did not lead to increased autophagy.

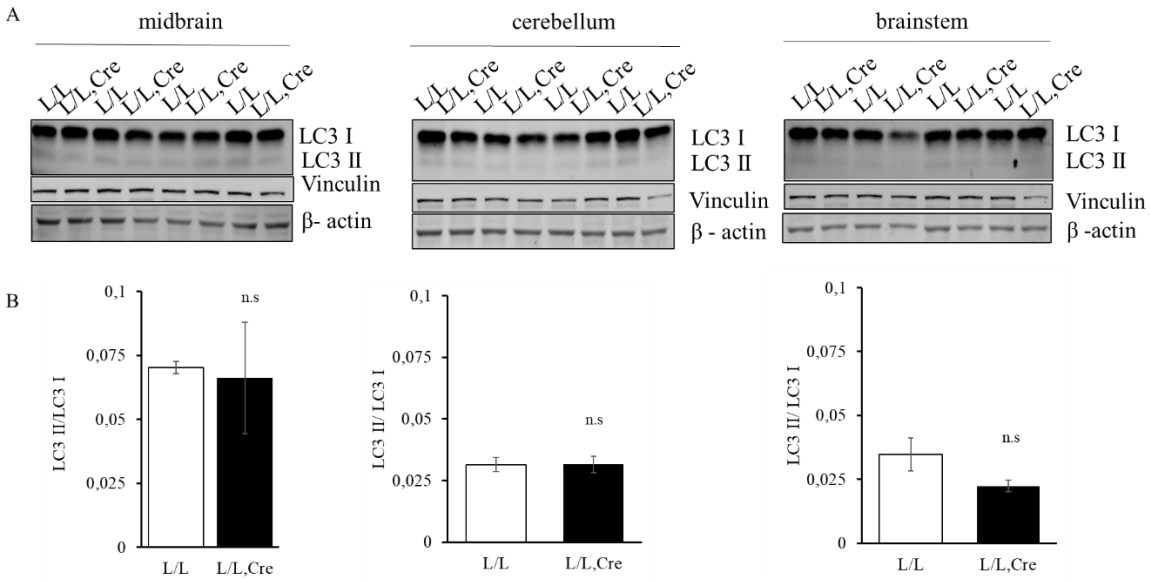


Figure 23. Loss of Lrpprc did not lead to increased autophagy in the brain of MCKO mice. (A) Immunoblot analysis of tissue lysates from newly born L/L (n=4) and L/L, Cre (n=4) mice, using antibody against LC3B, and as loading controls, antibodies against vinculin and β-actin. (B) Quantification of the immunoblot in A. Data are plotted as the mean ± standard error of the mean and were analysed using Student's t-test; ns means not significant.

d. Apoptosis

The caspase-3 cascade can be activated, through OXPHOS deficiency, accumulation of ROS, increase of lactate level and calcium uptake, triggering Bax/Bcl2 pro-apoptotic family, causing cytochrome *c* escape in the cytoplasm via the formation of the permeability transition pore (Mattson, 2000). The complex formed by cytochrome *c* with apoptotic protease-activator and caspase-9 would finally lead to the activation of the effector caspase-3, which would activate other apoptotic signals leading to cell phagocytosis by microglia and astrocytes (Mattson, 2000). Therefore, apoptosis or programmed cell death was assessed by the detection of antibodies against activated caspase 3. Immunofluorescence analysis using antibody against activated caspase 3 in different regions was assessed in newly born control and MCKO mice. Positive cells in midbrain and cerebellum of MCKO pups suggested an increase in apoptosis. (Fig.24).

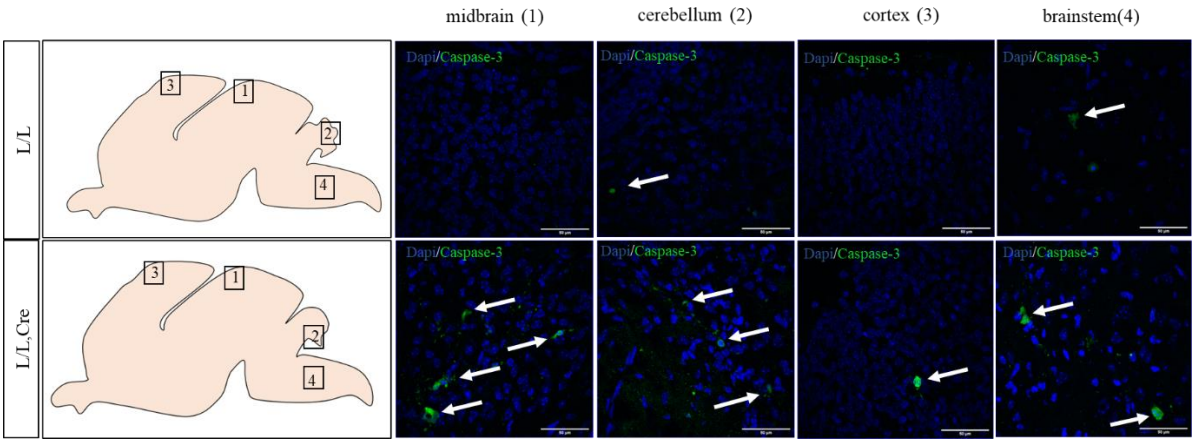


Figure 24. Loss of Lrpprc increased cell death in midbrain and cerebellum of newly born MCKO pups. Immunofluorescence analysis of sagittal sections across different regions of the brain from newly born control and MCKO mice, hybridized with antibody against caspase-3 that stains cells undergoing apoptosis in green. Dapi counterstains nuclei in blue. White arrows indicate cells undergoing apoptosis. Representative images from 3 independent experiments are shown.Scale bar, 50µm.

II. Loss of Lrpprc during mouse embryonic development

Previous results comparing newly born controls and MCKO mice revealed a clear defect of specific cells in the midbrain and the cerebellum of MCKO pups; DNs arise from the midbrain ventral zone around E11.5 by the induction of Shh at ventral midbrain, and FGF8 at the midbrain-hindbrain boundary (Albéri, Sgadò and Simon, 2004; Gale and Li, 2008); Purkinje cells, arising also from the ventricular zone of the cerebellum around E10.5, migrate their somas along the radial glia fibres to reach the forming PCL around E17.5 (Bellamy, 2006; Fleming and Chiang, 2015). Pcs control GCPs proliferation and migration through the secretion of Shh around E17.5. En1-Cre recombination occurring as early as embryonic day E9.5 in MCKO mice, therefore it became important to know if the cellular defects observed at newly born stage, were already visible since different embryonic stages.

1. Cerebellar developmental delay during embryogenesis of MCKO mice

Arising from the ventral zone of the cerebellum, Pcs in normal embryos migrate through the cerebellar cortex to reach their final location at the PCL. At E15.5, haematoxylin-eosin staining showed an underdeveloped cerebellum in MCKO embryos (Fig.25 A). Immunofluorescence staining of brain sections from control and MCKO embryos using antisera against Calbindin showed an obvious reduction and a defect of migration of Purkinje cells in MCKO cerebella, suggesting that Lrpprc plays an important role in Purkinje cells development during embryogenesis (Fig.25 B). Moreover, using antisera against and Pax6 in E15.5-old embryos, the external granular layer of cerebellum, appeared thinner with less GCPs (Fig.25 B).

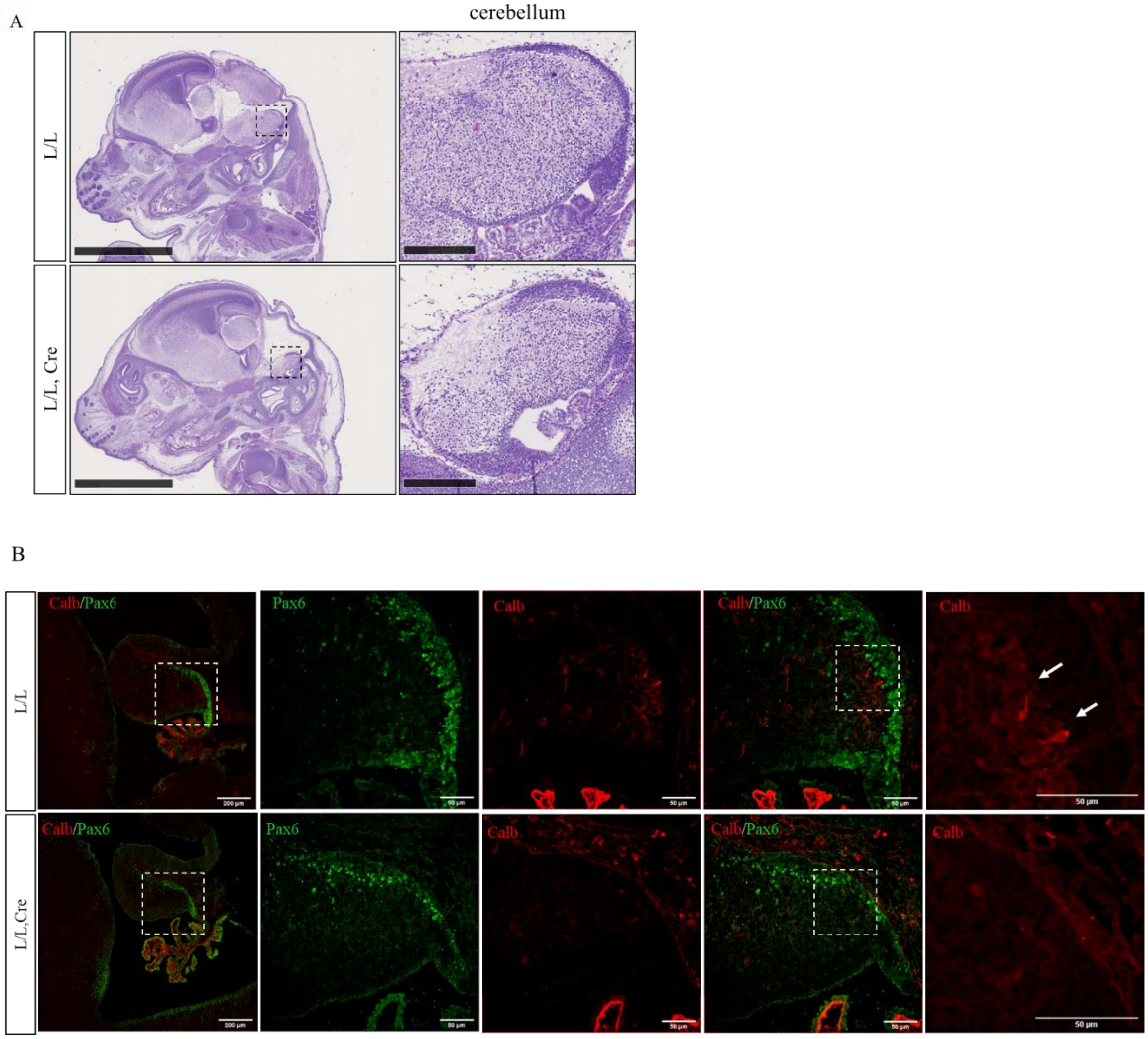


Figure 25. Cerebellar developmental delay in MCKO embryos. (A) Haematoxylin-Eosin staining of sagittal sections from L/L and L/L, Cre embryos at E15.5 showing underdeveloped cerebellum in MCKO embryo. Representative images from a single independent experiment are shown. On the first left-hand panel, scale bar was 2.5 mm; second panel, scale bar was 100 µm. (B) Fluorescence images of sagittal cerebellar sections from E15.5 embryos hybridized with Calbindin- and Pax6-specific antibodies (red and green, respectively). Magnified areas are indicated by dashed rectangles. Right-most panels show magnified area containing Pcs (white arrows) in control embryos. Representative images from 3 independent experiments are shown. Scale bars: first left-hand IF panel, 200µm; magnification panel, 50µm, remaining panels, 50µm.

2. Abundance of dopaminergic neurons in substantia nigra from MCKO embryos is mildly affected at E15.5

DNs development was assessed by immunofluorescence of sections from embryos at E15.5 using a TH-specific antibody This analysis revealed that abundance of DNs in MCKO embryos was not as profoundly affected as in newly born mice (Fig. 26 A, B).

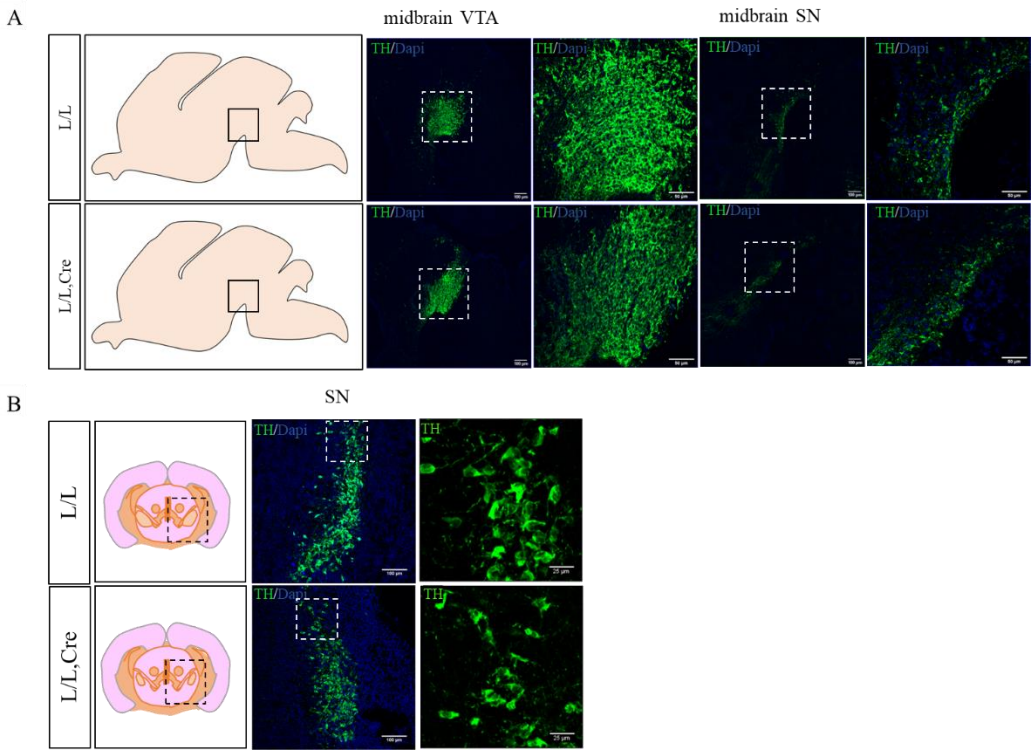


Figure 26. Abundance of dopaminergic neurons in the substantia nigra of E15.5 MCKO embryos is not substantially changed when compared to controls. (A) Fluorescence images of sagittal (midbrain VTA) and mid-sagittal (midbrain SN) sections across midbrain regions from E15.5 L/L and L/L, Cre embryos, hybridized with antibody against TH (green). Dapi counterstains nuclei (blue). Representative images from 3 independent experiments are shown. Scale bars: magnification panels, 50µm; remaining panels, 100µm. (B) Fluorescence images of coronal sections across substantia nigra region in the midbrain from E15.5 L/L and L/L, Cre embryos, hybridized with anti-Tyrosine Hydroxylase (TH) that stains DNs in green. Dapi counterstains all nuclei in blue. Representative images from 2 independent experiments are shown. Scale bars: first left-hand panel, 100µm; magnification panel, 25µm.

3. Activated caspase 3 in midbrain of MCKO embryos suggests an increase in apoptosis

Apoptosis was assessed by the detection of activated caspase 3. Immunofluorescence staining of different brain regions from control and MCKO embryos was carried out using caspase 3-specific antisera. Cells undergoing apoptosis were detected in midbrain of MCKO embryos suggesting an increase in apoptosis as observed in newly born mice (Fig.27 A, B).

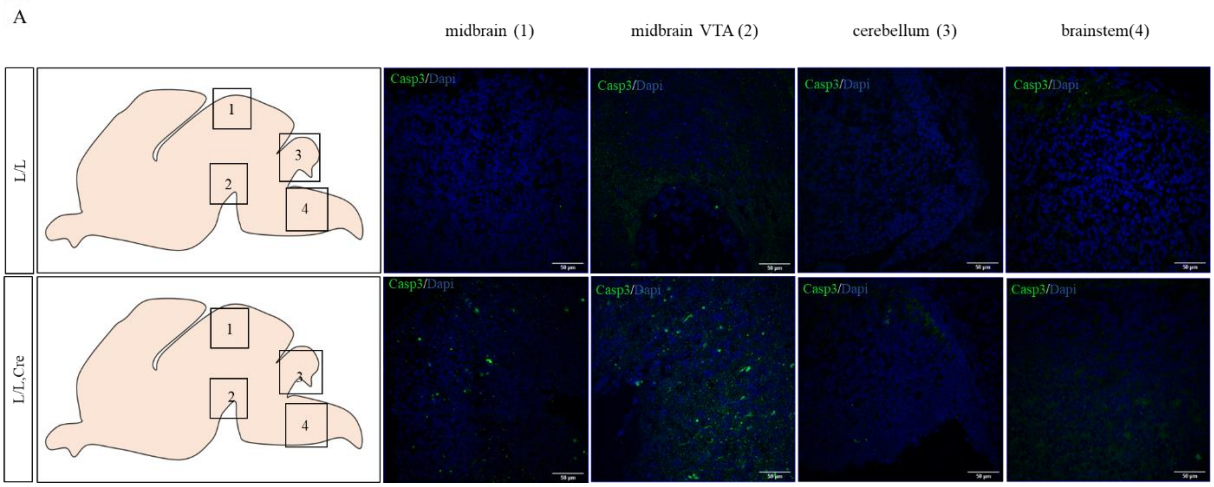


Figure 27. Increased the number of apoptotic cells in midbrain (and cerebellum) of E15.5. (A) Fluorescence images of different regions of the brain from L/L and L/L, Cre embryos et E15.5, hybridized with anti-caspase-3 that stains the dead cells in green. Dapi counterstains all nucleus in blue. Representative images of 3 independent experiments are shown. Scale bar, 50µm

4. Impaired dendrite and axonal growth, in vitro, of dopaminergic neurons isolated from MCKO mice

To gain further insight on how loss of Lrpprc affects neurogenesis and to focus on the maturation of specific cell types in a two-dimensional growth system, primary cell cultures from ventral mesencephalon from embryos at E13.5-14.5 were established.

Immunofluorescence using TH antisera and morphometric analysis revealed a reduction in the number of projections originating from DNs isolated from MCKO embryos and a decrease in the DN cell body area (Fig.28 A-C). This suggests that loss of Lrpprc is detrimental to the maturation of DNs.

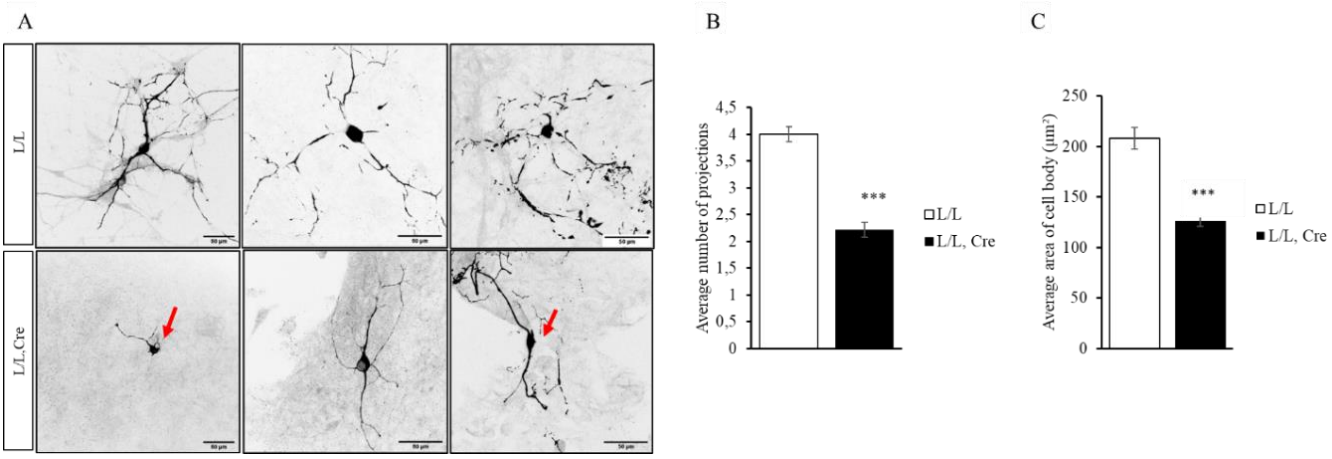


Figure 28. Primary cells culture suggests defects in dendrite and axonal growth of MCKO dopaminergic neurons. (A) Immunofluorescence analysis using anti-TH antibodies towards dopaminergic neurons (DNs) from primary cell culture from embryos mesencephalon at E14.5. Arrows indicates underdeveloped dendrites. Scale bar, 50µm. (B) Morphometric analysis of DNs from primary cell culture of E14.5 ventral mesencephalon from L/L (n=71) neurons and L/L,Cre (n=98) neurons. Quantification of dendrites and axons from DNs primary cell cultures. Data are plotted as the mean ± standard error of the mean and were analysed using Student's t-test; ***, $p<0.001$. (C) Morphometric analysis of DNs from primary cell culture of E14.5 ventral mesencephalon from L/L (n=71) neurons and L/L,Cre (n=98) neurons. Quantification of neuronal cell body from DNs primary cell cultures. Data are plotted as the mean ± standard error of the mean and were analysed using Student's t-test; ***, $p<0.001$.

III. ELAC2 and mitochondrial disease

1. Identification of novel homozygous and compound heterozygous pathogenic variants in the *ELAC2* gene.

The 16.6 kb mtDNA is transcribed into a long polycistronic precursor, which is processed following the so-called tRNA punctuation model (Ojala, Montoya and Attardi, 1981). Specific endonucleases at 5', RNAse P (Holzmann *et al.*, 2008), and RNAse Z at 3' (Brzezniak *et al.*, 2011), cleave these precursors allowing the release of individual mRNAs, rRNAs and tRNAs. RNAse Z, also referred as ELAC2, is encoded by the nuclear gene *ELAC2* (MIM 605367) (Dubrovsky *et al.*, 2004; Rossmanith, 2011).

To date, 19 pathogenic variants have been reported in *ELAC2* (MIM 605367, NM_018127.6) linked to mitochondrial diseases, commonly leading to hypertrophic cardiomyopathy, but also to neurodevelopmental delay, lactic acidosis, and OXPHOS defects (Haack *et al.*, 2013; Akawi *et al.*, 2016; Kim *et al.*, 2017; Shinwari *et al.*, 2017; Paucar *et al.*, 2018; Saoura *et al.*, 2019).

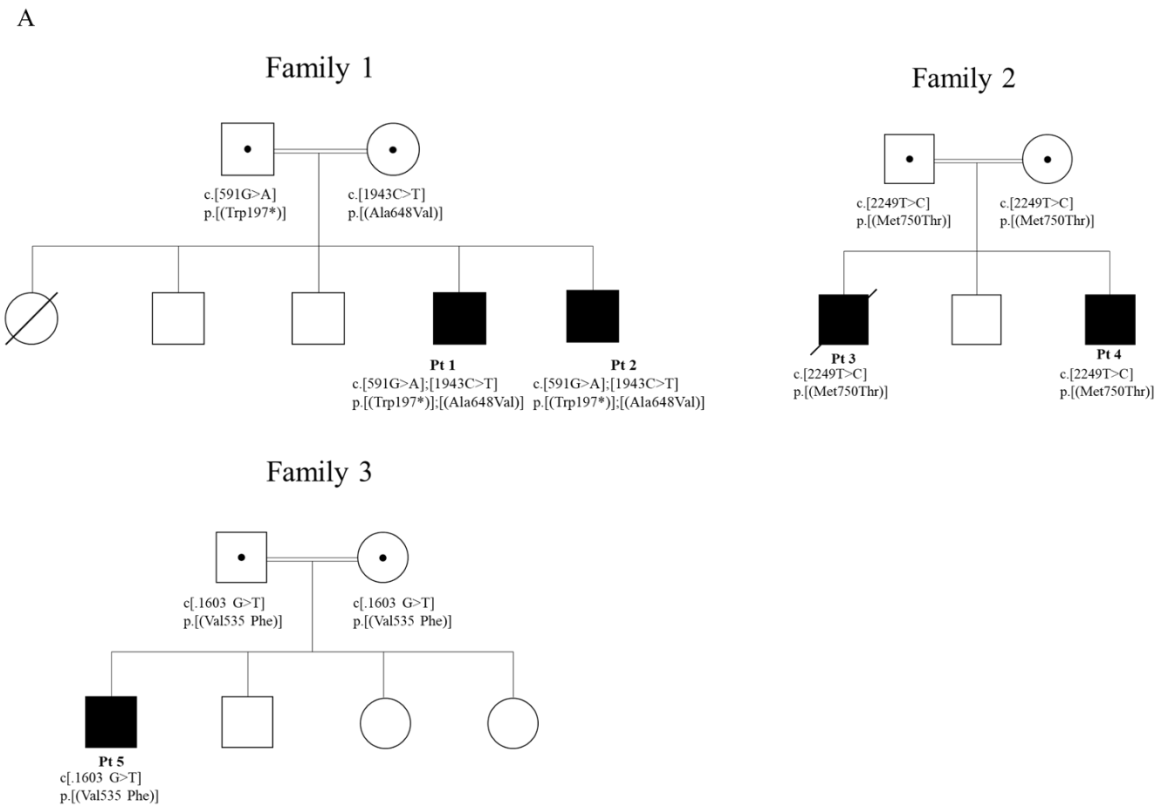
We identified novel pathogenic variants in the *ELAC2* gene in five patients from three unrelated families (Table 7). The five patients, all males, were born to consanguineous parents, and all presented with neurodevelopmental delay within the first months of life. One of them (Pt3) presented with similar clinical and biochemical features as those previously described (Haack T.B. et al., 2013; Shinwari Z.M.A. et al., 2017; Saoura M. et al., 2019). Patients from families 1 and 3, had no cardiac involvement but had neurological disease including myoclonic epilepsy and deafness associated with lactic acidosis and OXPHOS defects (Pt1), or microcephaly and psychomotor delays in concordance with gyri abnormalities and white matter hyperintensities in brain MRI (Pt5).

Next generation sequencing was used to determine the pathogenic variants in the three families. Patient 1 and 2 from family 1 carried two compound heterozygous variants: a variant affecting the exon 7, c.[591G>A] p.[(Trp197*)], and the missense variant c.[1943C>T] p.[(Ala648Val)], affecting a conserved amino acid residue in the C-terminal domain of ELAC 2. Each of the parents carry one variant: c.591G>A being on the paternal allele and c.1943C>T, on the maternal allele (Fig.29 A, B). Patient 3 and 4 from family 2 carried the homozygous missense variant c.[2249T>C] p.[(Met750Thr)] (Fig.29 A), affecting a conserved amino acid residue in

the ribonuclease Z -like domain (Fig.29 B). Patient 5 from family 3 carried the homozygous missense variant c.[1603G>T] p.[(Val535Phe)] (Fig.29 A) affecting a conserved amino acid residue in the C-terminal domain of ELAC2 (Fig.29 B). None of these variants were ever reported in the literature. Presence of the different variants in the parents was also confirmed.

Patient	ELAC2 variants	Clinical features	Brain MRI	Biochemistry
Pt1 Male	Compound heterozygous c.[591G>A];[1943C>T] p.[(Trp197*)];[(Ala648Val)]	Myoclonic epilepsy, cognitive delay, deafness	N.A	Lactic acidosis
Pt3 Male	Homozygous c.[2249T>C] p.[(Met750Thr)]	Cardiomyopathy, normal development until 10 months of age when Pt3 died	N.A	N.A
Pt5 Male	Homozygous c[.1603 G>T] p.[(Val535 Phe)]	Psychomotor delay, severe microcephaly, dystonia, oculomotor apraxia, Normal electromyogram normal heart and kidney ultrasounds.	Severe simplified gyral pattern, hyperintensities in globi pallidi, abnormalities and hyperintensities in white matter	No lactic acidosis in CSF

Table 7: Clinical features, brain MRI and biochemical analyses of the reported patients carrying *ELAC2* variants. N.A, not performed; CSF, Cerebrospinal Fluid



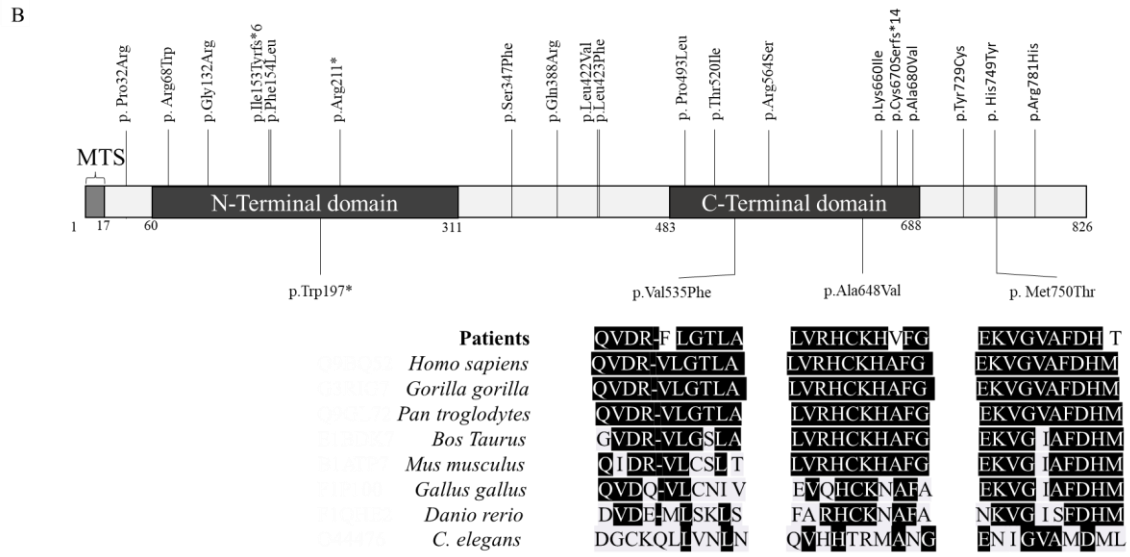


Figure 29. Pedigree of three affected families and evolutionary conservation of the affected amino acids. (A) Pedigree of the patients newly reported. (B) Linear map of the ELAC2 protein showing previously reported pathogenic variants (top) and the variants newly reported (bottom). Multiple alignments of the regions containing the affected amino acids are presented for different species.

2. Decreased abundance of ELAC2 in patient fibroblasts

To understand the effect of the identified variants on ELAC2, we carried out immunoblot analyses of protein extracts from primary skin fibroblasts from two controls (C1, C2) and three patients—one from each family. Immunoprobing with ELAC2 specific antibodies revealed a significant decrease in ELAC2 in fibroblasts from all three patients (Fig.30 A, D). In contrast, LRPPRC and MRPPR2 (a subunit of RNAse P) were unchanged or slightly upregulated in patient fibroblasts revealing the specific effect of the identified variants on the abundance of the ELAC2 protein (Fig.30 B, C, E, F).

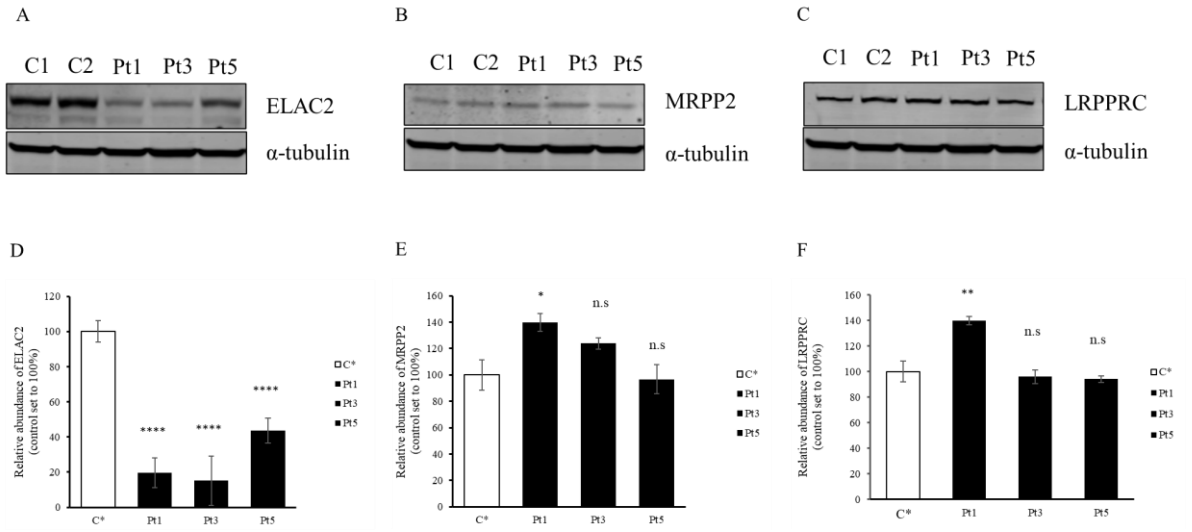


Figure 30. Decreased abundance of ELAC2 in patient fibroblasts do not lead to decrease of other proteins involved in mtRNA metabolism in fibroblasts of patients (Pt1, Pt3, Pt5) compared to controls (C1, C2). Immunoblot analysis of fibroblasts lysates from controls (each control n=3) and patients (each patient n=3), using antibodies against ELAC2 (A), MRPP2 (B) and LRPPRC (C); antibody against α-tubulin was used as a loading control. (D, E, F) Quantification of the different immunoblots in panel A, B, C; Abundance of ELAC2, MRPPR2 and LRPPRC in the two controls (C*) was average and set to 100%. C* n=6, each patient n=3. Data are plotted as the mean ± standard error of the mean and were analysed using Student's t-test; *, $p<0.05$; **, $p<0.01$; ****, $p<0.0001$; n.s means non-significant.

3. Accumulation of unprocessed tRNA^{VAL} precursor in patient fibroblasts

ELAC2 is responsible for the 3'-end processing at tRNA locations and a reduction in its activity has been shown to lead to the accumulation of tRNA precursors in patient fibroblasts (Haack *et al.*, 2013; Paucar *et al.*, 2018; Saoura *et al.*, 2019). To determine if, likewise, fibroblasts from the patients identified here accumulated tRNA precursors, we carried out Northern blot analyses using a radiolabeled oligonucleotide complimentary to tRNA^{VAL}. Consistent with the previous reports mentioned above, this analysis revealed an accumulation of the mt-tRNA^{VAL}-16S rRNA precursor in patient 1 and patient 3 fibroblasts and to a much lesser extent in patient 5 (Figure 31).

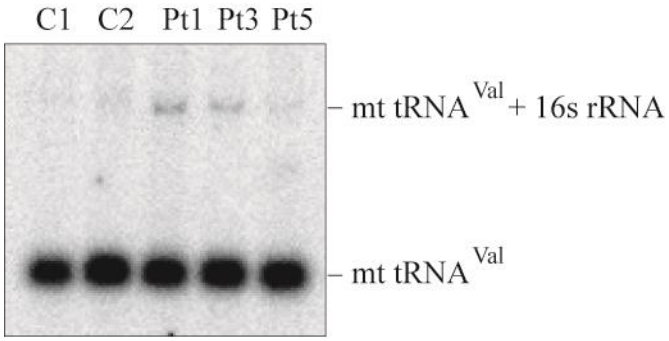


Figure 31. Northern blot analysis of RNA extracts from three patients carrying pathogenic ELAC2 variants. The accumulation of the precursor molecules containg mt-tRNA^{VAL} and 16S rRNA is detectable by the accumulation of a slow migrating band using radiolabeled oligo complementary to mt-tRNA^{VAL}. Fully processed mt-tRNA^{VAL} is the faster migrating band at the bottom of the figure.

4. ELAC2 defects in fibroblasts of patients did not lead to defects in OXPHOS proteins

Impaired precursor processing caused by decreased ELAC2 activity can be expected to negatively affect the availability of mature tRNAs and mRNAs, reduced rate of mitochondrial translation and a decreased abundance of mtDNA- and some nuclear-encoded OXPHOS proteins (Haack *et al.*, 2013; Deutschmann *et al.*, 2014; Siira *et al.*, 2017; Saoura *et al.*, 2019). To test this, I carried out an immunoblot analysis of patient fibroblast extracts using antibodies against individual proteins from the five OXPHOS complexes. This analysis revealed no significant decrease in the abundance of neither mtDNA-encoded nor nuclear-encoded OXPHOS proteins (Fig.32 A).

Cumulatively, these results revealed a significant defect in ELAC2 but did not exhibit neither significant defects in mtRNA metabolism factors (Figure 30. B, C, E, F), nor OXPHOS deficiency in fibroblasts of patients (Figure 32 A-G).

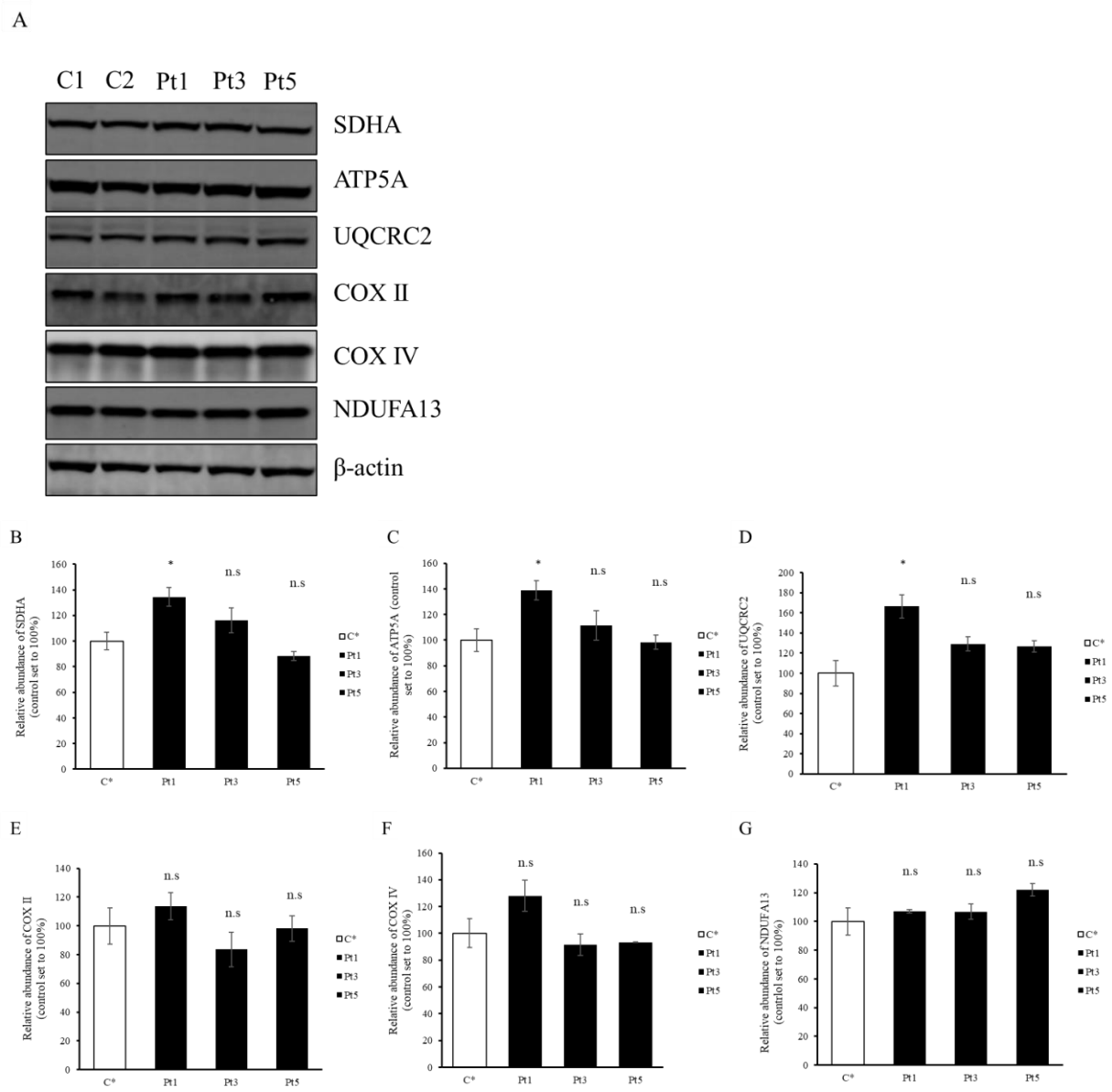


Figure 32. Decreased abundance of ELAC2 in patient fibroblasts do not lead to decrease in abundance of different OXPHOS proteins in fibroblasts of patients (Pt1, Pt3, Pt5), compared to controls (C1, C2).(A) Immunoblot analysis of fibroblasts lysates from controls (each control n=3) and patients (each patient n=3) using antibodies targeting different OXPHOS proteins. Antibody against β-actin was used as a loading control. (B-G) Quantification of the immunoblots in panels A. Abundance of the different OXPHOS proteins in the two controls (C*) was average and set to 100%. C* n=6, each patient n=3. Data are plotted as the mean ± standard error of the mean and were analysed using Student's t-test; *, $p<0.05$, n.s means non-significant.

Chapter IV: Discussion

Mitochondrial diseases are characterized by a huge clinical heterogeneity and tissue-specific involvement while they are due to mutations in ubiquitously expressed genes. These diseases are often associated with a poor prognosis and are incurable, in part, because of our poor understanding of their pathomechanisms and the lack of appropriate models recapitulating the complexity of these diseases. Therefore, it becomes important to understand MD diseases first, so that specific and effective treatments can be developed.

This PhD thesis project focused on two genes, *LRPPRC* and *ELAC2*, encoding proteins involved in mitochondrial RNA metabolism. Mutations in the mitochondrial mRNA stability and polyadenylation factor LRPPRC invariably cause neurological disease, most often progressive necrotizing encephalopathy, Leigh syndrome, one of the most frequent mitochondrial diseases, with hepatopathy (LSFC) or cardiomyopathy. Mutations in *ELAC2*, encoding a mitochondrial tRNA ribonuclease, are known to cause mainly hypertrophic cardiomyopathy, neurodevelopmental delay, and hyperlactatemia. The aim of my PhD thesis was to better understand the clinical, biochemical, and molecular consequences of mitochondrial RNA metabolism defects associated with LRPPRC and ELAC2 mutations.

Part 1: Characterisation of a midbrain-and-cerebellum-specific *Lrpprc* knock-out mouse model

Mutations in *LRPPRC* lead to specific structural abnormalities in the basal ganglia, cerebellum, and brainstem, with hepatopathy (French-Canadian variants, LSFC) or cardiomyopathy (Oláhová *et al.*, 2015), often characterized by premature death linked to severe metabolic crises. On molecular and biochemical level, LRPPRC mutations result in OXPHOS complex IV (LSFC) or combined complex I+IV deficiency detectable in patient fibroblasts and biopsies (Oláhová *et al.*, 2015; Sasarman *et al.*, 2015). The role of LRPPRC and its deficiency in the pathophysiology of LS has not been thoroughly investigated and its unveiling may help develop treatments for this, currently incurable, condition.

The first aim of my thesis project was to characterise a mouse model that could recapitulate the pathophysiological features of midbrain and cerebellar dysfunction in LS and to understand how loss of Lrpprc affects the development and function of these brain structures.

To this purpose, I generated a cerebellum-and-midbrain-specific *Lrpprc* KO mouse model by crossing conditionally targeted *Lrpprc* mice ($Lrpprc^{LoxP/LoxP}$) with mice expressing Cre recombinase under the control of *En1* promoter.

The midbrain-and-cerebellum-KO (MCKO) mouse model broadly recapitulates the LS phenotype observed in patients with LRPPRC mutations.

We first showed that MCKO mice were born with a Mendelian distribution but died within 24 hours of birth (P0). These initial results correlate with data on the lifespan of LSFC patients, who showed early lethality with a median age of 2.6 years (Debray *et al.*, 2011). Although the LS and LSFC phenotypes result from multisystem involvement, these initial observations suggest that neurological involvement accounts for a large proportion of the clinical phenotype and is consistent with the fact that mitochondrial diseases occur in the most energy consuming organs.

In addition, MCKO mice had poor feeding, as evidenced by their decreased body weight and smaller milk spot compared to controls. Failure to thrive associated to dysphagia is often observed in patient with LRPPRC mutations (Debray *et al.*, 2011; Oláhová *et al.*, 2015; Han *et al.*, 2017).

Dysphagia is a recurrent clinical feature in LS patients. It impairs the three main actions of suckling, swallowing, and breathing since the food can deviate from the oesophagus and stuck the airway, resulting in coughing or chocking, and if untreated lead to aspiration pneumonia (Fuh *et al.*, 1997; Pflug *et al.*, 2020). These vital sensorimotor processes require cross-wiring of neural centres in brainstem (*medulla oblongata*), basal ganglia, and cerebellum (Shandley *et al.*, 2021). For instance, KO mouse model of LS targeting the OXPHOS CI subunit Ndufs4 in the vestibular nucleus at the dorsal part of the *medulla oblongata*, also showed swallowing defects, failure to thrive and a fatal breathing dysfunction around 50 days (Quintana *et al.*, 2012). Vestibular nuclei, although they are part of the *medulla oblongata* receive afferent information from organs, multiple brain nuclei and regions including the cerebellum. They also convey information to multiple centres including the cerebellum. The MCKO mouse model does not target lower brainstem, but regarding the severity of its phenotype in the affected regions, it appears that cerebellum and midbrain both play a role in suckling, swallowing, or breathing. For instance, a study showed that optogenetic stimulation of the GABAergic neurons from the Substantia Nigra pars reticula projecting to the superior colliculus in the tectum midbrain, and controlling orofacial behaviour, led to licking difficulty in mice (Rossi *et al.*, 2016), highlighting the importance of midbrain for suckling and swallowing. Otherwise, in the cerebellum of a mouse model for sudden infant death syndrome, defects in Purkinje cells

projecting to the deep cerebellar fastigial nuclei, led to deficient compensatory response to an increased level CO2 in the environment, pointing the importance of cerebellum for compensatory mechanism to breathing difficulties (Calton *et al.*, 2016).

Morphometric comparison of freshly explanted brains revealed an underdeveloped midbrain in MCKO pups compared to control pups at P0. Moreover, histological staining of sagittal brain sections with haematoxylin-eosin revealed smaller midbrain and severe cerebellar foliation defects. Additionally, Nissl staining confirmed the severe cerebellar foliation defect accompanied with a complete disorganization of cellular layers in MCKO mice. Furthermore, Nissl staining showed no significant changes in cortex and lower brainstem, since they do not contain cells expressing the Cre recombinase. These results were confirmed in En1-Cre/Rosa26 tdTomato mouse that revealed the expression pattern of the promoter En1 in midbrain and cerebellum, as evidence by the red fluorescence in these regions. These brain structures are also those involved in LRPPRC-linked diseases, midbrain, basal ganglia, and cerebellum (Merante *et al.*, 1993; Sasarman *et al.*, 2015).

On molecular level, immunoblot analysis of different brain regions revealed variable and specific decrease of individual OXPHOS proteins in midbrain and cerebellum with the latter appearing less affected because of its higher complexity and the higher percentage of non-knockout cells, consistent with the results from the En1-Cre/Rosa26 tdTomato mouse. These results are in concordance with COX/SDH histochemical staining of sagittal brain sections that showed a clear complex IV deficiency throughout the midbrain and cerebellar regions of KO mice. As expected, cortex and lower brainstem did not show complex IV deficiency. Together, these results suggest a combined complex I + IV deficiency in knockout cells present in these brain structures. Furthermore, LRPPRC level was decreased but not completely absent in midbrain and cerebellum, consistent with the results from the *En1*-driven recombination in En1-Cre/Rosa26 tdTomato mouse and the cellular diversity of these brain structures. These results are also consistent with previous studies of heart specific *Lrpprc* knockout mice and patient biopsies, in which aberrant expression of LRPPRC led to an impaired OXPHOS biogenesis (Ruzzenente *et al.*, 2012; Oláhová *et al.*, 2015; Sasarman *et al.*, 2015).

LRRPRC-linked LS and LSFC are multisystemic diseases and the cause of death is mainly metabolic crises associated to severe lactatemia (excessive lactate in blood) and hyperlactatorachia (excessive lactate in cerebrospinal fluid) higher than 2-4 mmol/L (Debray *et al.*, 2011). Surprisingly in our mouse model, defects in the midbrain and cerebellum did not lead to lactic acidosis although lactate levels in MCKO were slightly increased compared to

controls. Therefore, early lethality of our model cannot be explained be a severe elevated brain lactate. Interestingly, not all LS patients present with early lethality associated to lactic acidosis. Severe increase of lactate in the CSF correlated with early onset of LS and poor prognosis due to severity of the disease (Sofou *et al.*, 2014). Thus, lactate level should be a marker for severity of LS in patients and prognosis.

It could be interesting to look at other metabolites (ATP, creatine kinase, amino acids) to obtain a complete biochemical diagnosis of our mouse model. Moreover, it would be interesting to measure breathing patterns by whole body plethysmography to better understand the consequence of loss of Lrpprc in breathing rhythm and to determine if the poor onset of the disease is the result of fatal breathing disorder. Otherwise, Purkinje cells in cerebellum are also involved in the regulation of blood pressure in a murine model of hypertension (Figueira and Israel, 2015), that may have led to cardiac failure and arrhythmia although we assume the early lethality of our model prevent the occurrence of these late stage symptoms.

Immunofluorescence analyses using specific markers allowed to identify three cell types affected by the loss of Lrpprc: dopaminergic neurons in the *substantia nigra*, Purkinje cells and granule cell precursors in the two outermost layers of the cerebellum. In MCKO mice, like in MPTP mouse model of parkinsonism (Novikova *et al.*, 2006) and LS (Lagrue *et al.*, 2009), DNs present with severe phenotypes most likely attributable to differentially expressed proteins (Chung *et al.*, 2005), lower mitochondrial mass (Liang *et al.*, 2007), and their important dendritic connectivity, highlighting their important metabolic needs (Bolam and Pissadaki, 2012; Brichta and Greengard, 2014). Regarding the early induction of the promoter En1 at E8.5-E9.5, we conclude that it plays an important role in the fate of some midbrain and cerebellum precursor cells since their development was compromised.

To better understand which cell are directly affected by the loss of Lrpprc, Rosa26 tdTomato mice were crossed with mice expressing Cre recombinase under the promoter En1. In cerebellum, co-labelling with antibodies against Pcs and GCPs confirmed that the promoter En1 was active in these cell types. In midbrain, TH-positive DNs also expressed red fluorescence indicating that these cells would also lose Lrpprc in MCKO mice. Although *En1* is necessary for the development of the posterior midbrain and hindbrain rhombomere 1, the two structures from which are derived midbrain and cerebellum, respectively (Wurst, Auerbach and Joyner, 1994), all the cells were not on the control of this promoter. Therefore, it could be

interesting to determine with other markers, what kind of cells are not under the control of the promoter En1.

The cellular phenotype of DNs observed at P0 was corroborated by results obtained at embryonic stages. Immunofluorescence on sagittal and coronal sections, using TH antibody, revealed that DNs were reduced in the SN of MCKO mice already at E15.5 embryonic stages. Furthermore, the impact of Lrpprc loss on neurogenesis and maturation of DNs was assessed by primary cell cultures from ventral mesencephalon of E13.5-14.5 embryos. DNs in KO cultures exhibited significantly decreased somas, underdeveloped axons and dendrites, confirming the importance of Lrpprc, and thus mitochondria, for neuronal development. More importantly, coronal sections and immunofluorescence using TH antibody revealed a more severe decrease in SN compared to the VTA in MCKO, indicating a location-specific sensitivity of DNs to the loss of Lrpprc. This distinction in DNs populations has been demonstrated earlier with a clear reduction of SN neurons, more than DNs from the VTA (Ricke *et al.*, 2020).

Substantia nigra and ventral tegmentum area are two close but different sources of dopaminergic neurons, part of the basal ganglia. Involved in motor function, behaviour, as well as control of emotions and motivation, these cells are of major importance regarding the diseases related: When defects occur in these neurons, it commonly leads to addiction, schizophrenia, movement defects or Parkinson disease, but mitochondrial dysfunction has also been linked to loss of DNs (Beilina and Cookson, 2016; Grünewald, Kumar and Sue, 2019; González-Rodríguez *et al.*, 2021). For instance, mitochondrial dysfunction is one of the causes leading to Parkinson disease, as evidenced by variants of *PINK1* and *PK22* encoding for PINK1 and PARKIN respectively, involved in the regulation of mitophagy (Narendra *et al.*, 2009; Beilina and Cookson, 2016; Grünewald, Kumar and Sue, 2019). Moreover, some studies have highlighted the role of alpha-synuclein, constituent of Lewy bodies, in OXPHOS CI inhibition (Surmeier, Obeso and Halliday, 2017). Moreover, the administration of neurotoxin 1-methyl-4-phenyl-1,2,3,6-tetrahydropyridine (MPTP) have been widely used to create mouse model of Parkinson disease since it leads to basal ganglia degeneration. MPTP has also been proposed to study LS when its role in inhibition of OXPHOS CI +CIV has been unveiled and selectively led to the loss of SN DNs (Lagrue *et al.*, 2009; Da Costa *et al.*, 2016). Hence, the frontier between LS studies and PD studies regarding DNs is very thin. For instance, when disrupting OXPHOS CI in a conditional Ndufs2 KO mouse model in DNs, González-Rodríguez P. and colleagues observed an induction of progressive parkinsonism (González-Rodríguez *et al.*, 2021). Knockout mice behaved like control littermates until P30, when they started to develop

a progressive degeneration of DNs, associated with axonal and somatodendritic pathologies and neurotransmission dysfunction starting at P30, until they die of unknown cause after P150. This model could have been easily transposed to study LS since it recapitulates most of the cellular defects observed in the ventral mesencephalon primary cell cultures. Finally, the vulnerability of DNs to mitochondrial dysfunction could be attributable to their high arborisation, thus their important metabolic needs for neurotransmission (Bolam and Pissadaki, 2012).

Focusing on the cerebellar phenotype, our results have previously shown that loss of *Lrpprc* led to a cerebellar underdevelopment and a foliation defect. Our results suggest that GCPs failed to migrate along the EGL from the rhombic lip. Therefore, they are unable to differentiate and migrate to the IGL after birth. Our results also showed that loss of Lrpprc affected Purkinje cells integrity since they had reduced density, and underdeveloped dendrites. Arising from the ventricular zone around E10.5, Pcs migrate their somas along the radial glia fibres around E13.5 to finally reach the forming PCL (Bellamy, 2006; Fleming and Chiang, 2015). Along their highly arborized dendrites directed toward the EGL layer, Pcs can control GCPs proliferation and migration through the secretion of sonic hedgehog Shh around E17.5 (Spassky *et al.*, 2008; Miyata *et al.*, 2010; Fleming and Chiang, 2015). Then, after birth, GCPs initiate cerebellar foliation through accumulation at fissures sites to allow invagination between folia. BG and PCs participate concomitantly to the formation of anchoring centres that are involved in the folding of the PCL and EGL (Sillitoe and Joyner, 2007; Sudarov and Joyner, 2007). Hence, Pcs are necessary for GCPs migration and differentiation.

Defects in these excitatory glutamatergic neurons and inhibitory GABAergic neurons may lead to deeper cerebellar nuclei impairments such as Fastigial nuclei (Calton *et al.*, 2016). More importantly, because of their highly arborised dendrites that require important metabolic needs, Pcs appear more vulnerable to mitochondrial dysfunctions. Therefore, we suggest that loss of Lrpprc, leading to OXPHOS deficiency in cerebellum, impaired Pcs migration along radial glia fibres around E10.5. Furthermore, we observed underdeveloped dendrites in Pcs from newly born MCKO, suggesting that Pcs that could migrate were unable to fully project their dendrites through the EGL. Because Pcs play a key role in GCPs migration and differentiation with the secretion of Shh (Corrales *et al.*, 2004), loss of Shh stimulation due to Pcs defects failed GCPs to proliferate and migrate from the rhombic lip along the EGL. Thus, thinner EGL accounts for migration and neurogenesis defects of GCPs in addition to their intrinsic loss of Lrpprc. Finally, foliation defects account for GCPs and Pcs defects but also for the potential lack of anchoring

centres scaffolds since Pcs and BGs in the PCL and GCPs in the EGL seem required to their formations (Sillitoe and Joyner, 2007; Li *et al.*, 2014).

Hence, loss of Lrpprc considerably affected the cerebellar patterning. Therefore, it can be hypothesized that the severity of this cerebellar phenotype is the reason for the early lethality observed in MCKO mice. However, severe foliation defects observed in En1-mediated *Ptpn11* KO mice at birth, did not lead to perinatal lethality (Li *et al.*, 2014). Li et al. showed in the cerebellum of KO mice that *Ptpn11* encoding the protein tyrosine phosphatase Shp2 was required for the development of BG cells that indirectly regulated GCPs in the EGL. More remarkably, the loss of BGs resulted in cerebellar foliation defects: although Pcs could form anchoring centres without BGs, PCL folding was impaired. Furthermore, the loss of BGs did not prevent the neurogenesis of GCPs, although the EGL was thinner. This was most likely due to defects in Pcs migration, resulting in lower Shh secretion by Pcs present in the PCL. Nevertheless, the GCPs could still initiate the folding of the EGL, although the basement membrane on the surface of the cerebellum did not follow the inward bending and thus gave the KO cerebellum a smooth appearance. Thus, Li et al. suggested that the defect in BG neurogenesis in response to Shp2 loss, led to an uncoupling of folding between the PCL and the surrounding basement membrane (Li *et al.*, 2014). Despite these remarkable foliation defects, KOs did not die soon after birth, suggesting that the severity of our model may not be solely attributable to the cerebellar foliation defect.

Let us notice that in humans, the more remarkable cerebellar agenesis is not always immediately lethal (Titomanlio, Romano and Del Giudice, 2005; Yu *et al.*, 2015). These clinical features could account for compensating mechanisms in other brain regions to circumvent the total absence of cerebellum (Titomanlio, Romano and Del Giudice, 2005; Yu *et al.*, 2015).

Since previous studies reported differences in mitochondrial proteomes of different neural cells in cerebellum granule cells, Pcs and astrocytes (Fecher *et al.*, 2019), our results can be complemented by proteomic and transcriptomic analyses to allow further characterisation of cells affected by the loss of Lrpprc. Most importantly, it should allow to bring new insight on how loss of Lrpprc affects nuclear and mitochondrial transcriptomes. We will be able to reveal a detailed picture of how different cell types are affected by and react to the loss of LRPPRC. In conclusion, we have generated a MCKO mouse model that recapitulates some of the clinical and biochemical features observed in LRPPRC-linked LS and LSFC patients.

Loss of Lrpprc in the MCKO mouse model led to defects in neurogenesis

Mitochondria are crucial during neurogenesis because cells undergo a metabolic switch during embryogenesis from glycolysis to greater reliance on beta oxidation. At E15.5, our results in MCKO showed a reduction and a defect of migration of Pcs, in addition to a defect of proliferation and migration of GCPs in the EGL appearing thinner. These results suggest that Lrpprc plays an important role in Pcs and GCPs neurogenesis.

Furthermore, in MCKO mice, there was no sign of neuroinflammation with no activation of astrocytes or microglia, no oxidative stress with the induction of SOD2, no induction of UPR-mt with the increase of HSP60, and no increase of the autophagy marker LC3. Since older mouse models of LS did exhibit neuroinflammation (Sörensen *et al.*, 2001; Quintana *et al.*, 2010; Bolea *et al.*, 2019), we could hypothesize that lack of neuroinflammation is attributable to the early lethality of our model, as well as lack of these other factors of neurodegeneration. However, not all mouse models of mitochondrial disorders exhibited increases of these factors. For instance, in a TFAM KO mouse model, although TFAM was significantly decreased in KO mouse cortex, oxidative stress remained as low as in control littermates. Moreover, neuroinflammation was present only at late-stage (Sörensen *et al.*, 2001). Finally, caspase-3 suggesting an increase in apoptosis due to mitochondrial dysfunction in the brain was not active in these KO mice, suggesting that programmed cells death was rather a consequence of increased neuroinflammation in these older model, corroborated by the increase of activated-caspase-8 (Sörensen *et al.*, 2001; Quintana *et al.*, 2010; Bolea *et al.*, 2019).

The MCKO mouse model exhibits activated caspase-3 in midbrain and cerebellum at P0 and during embryogenesis. These results suggest that apoptosis occurring as early as E15.5 during maturation of neural cell precursors, is a result of mitochondrial dysfunction, thus contributing to defects of midbrain and cerebellum development. It would be also interesting to perform co-localisation immunofluorescence to determine the nature of the apoptotic cells, although we hypothesize, they are DNs in the SN, Pcs in the cerebellum ventricular zone and PCL, and GCPs in the EGL. Moreover, the activation of caspase-3 in DNs has already been corelated to the increased level of lactate in a MPTP mouse model for Parkinson disease (Li *et al.*, 2022), thus we could hypothesize that the increased lactate level in MCKO midbrain could be responsible for the induction of programmed cell death via the induction of caspase-3.

In addition, culture of primary ventral midbrain KO cells E13.5-E14.5 revealed maturation defects in DNs. The DNs show reduced axonal arborisation, which most likely prevents them

from creating a large synaptic network. It would be interesting to complement the primary cell culture of DNs with a primary cell culture of mouse cerebellar cells enriched in Pcs, GCPs and BG. Thus, loss of Lrpprc in the MCKO mouse model led to maturation defects in specific neurons, resulting in increased lactate, apoptosis events in these regions, and neonatal lethality, although not all neurons in the affected areas underwent apoptosis. Again, the early lethality of MCKO mice may explain these incomplete maturation defects.

Does this model recapitulate the tissue-specificity of LRPPRC-linked disease?

A mouse model with cerebral involvement had never been documented. Therefore, it appeared crucial to create and characterise a mouse model capable of recapitulating the involvement of specific brain structures in LRPPRC-linked disease. The MCKO mouse model cannot answer the tissue-specificity question but reveals how loss of Lrpprc affects the development and function of an important energy-demanding organ as the brain, a disease-relevant tissue. To fully answer the question of tissue-specificity, a knock-in (KI) mouse model that ubiquitously expresses a disease-causing Lrpprc mutation could be more suitable. However, generating such models is also riskier as KI mice expressing recessive missense mutations for disease-causing genes often show no discernible phenotypes (Silva-Pinheiro *et al.*, 2021).

Conclusion

Here, I carried out a preliminary characterization of a mouse model for Lrpprc deficiency in the midbrain and cerebellum, frequently affected in LS and in patients with LRPRPC mutations. These mice broadly recapitulated some pathophysiological features of LS such as the early lethality, impaired midbrain and cerebellar development. Even though, they do not present an ideal model to address the tissue-specific nature of LRPPRC-linked pathology, they can be useful in gaining a better understanding of the molecular and biochemical cascades triggered by the loss of Lrpprc. Ultimately, data obtained by characterizing these mice can contribute to the development of better treatments for LS or other mitochondrial diseases.

Part 2: Identification of novels homozygous and compound heterozygous pathogenic mutations in the *ELAC2* gene in three unrelated patients

Initially associated to higher prostate cancer risk (Rebbeck *et al.*, 2000; Tavtigian *et al.*, 2001), several recent studies have associated *ELAC2* mutations to mitochondrial RNase Z defects, mainly leading to developmental delays, and infantile hypertrophic cardiomyopathy (Haack *et al.*, 2013; Shinwari *et al.*, 2017; Saoura *et al.*, 2019). RNase Z (ELAC2) together with RNAse P cleaves the long polycistronic transcripts produced from mtDNA transcription, allowing the release of individual mRNAs, rRNAs and tRNAs (Ojala, Montoya and Attardi, 1981).

Most patients expressing *ELAC2* variants presented with fatal hypertrophic cardiomyopathy, developmental delay and lactic acidosis associated to OXPHOS deficiency (especially CI), but additional phenotypes have also been reported with abnormal movements and psychiatric disorder, or mild cardiac impairment with microcephaly (Haack *et al.*, 2013; Akawi *et al.*, 2016; Shinwari *et al.*, 2017; Paucar *et al.*, 2018; Saoura *et al.*, 2019).

Characterization of fibroblasts of patients represent a first step for understanding the consequences of *ELAC2* mutations. Thanks to our collaboration with the Necker-Enfants Malades hospital, we were able to study fibroblasts from three unrelated patients with *ELAC2* mutations.

Case study and comparison with known mutations

The Pt3 (c.[2249T>C]), developed a fatal cardiomyopathy and died at 10 months of age. This severe onset is similar with previously articles describing variants of *ELAC2* that led to fatal hypertrophic cardiomyopathy (Haack *et al.*, 2013; Shinwari *et al.*, 2017; Saoura *et al.*, 2019).

The Pt5 (c.[1603G>T]) did not have any sign of lactic acidosis in the cerebrospinal fluid, although presenting with severe simplified gyral patterns and abnormal hyperintensities in the white matter and *globi pallidi*. This patient had a microcephaly, neurodevelopmental delay, dystonia, and oculomotor apraxia but no sign of cardiac impairment since the electrocardiogram and ultrasound appeared normal. Interestingly, this patient harboured clinical features similar to those of five patients, all carrying a homozygous splice site variant c.[1423 + 2 T > A]. These patients generally presented with milder cardiomyopathy and lactic acidosis, but three also had microcephaly and severe developmental delay (Akawi *et al.*, 2016).

The Pt1 (c.[591G>A]; [1943C>T]) presented with lactic acidosis, developmental delay, deafness, myoclonic epilepsy, and minimal cardiac impairment. A similar case was reported in

Korea in a 5-month infant presenting with encephalopathy, intractable epilepsy, apnoea, and hyperlactatemia with no cardiac involvement, who died prematurely (Kim *et al.*, 2017).

Although ELAC2 abundance was significantly decreased in fibroblasts from three of the five reported patients, we did not detect any changes in the abundance of OXPHOS proteins. However, RNA isolated from fibroblasts of patients and submitted to RNA blotting revealed an accumulation of unprocessed mitochondrial tRNA-Valine. This latter result is similar to the previous studies from Haak and colleagues that reported an accumulation of unprocessed precursors of mitochondrial tRNA-Valine and tRNA-Leucine (Haack *et al.*, 2013), but also from Saoura M. et al. reporting the accumulation of unprocessed precursors of mt tRNA-Valine, tRNA-Methionine and t-RNA-Leucine in patients fibroblasts (Saoura *et al.*, 2019).

Mitochondrial dysfunction affects tissues with high energy requirements like the brain, skeletal muscle and heart causing various neurological diseases, myopathy, and cardiomyopathy. ELAC2 plays an important role of in heart function and regarding the many studies and the clinical features of the patients, and animal models (Siira *et al.*, 2018; Migunova *et al.*, 2021), *ELAC2* mutations mainly lead to mitochondrial cardiomyopathies, characterised by typical enlargement of the heart structure and altered function due to defective mitochondria, like large fusiform myocytes with larger mitochondria, cytoplasm clearing and granulation (Holmgren *et al.*, 2003; Meyers, Basha and Koenig, 2013), and with the presence of ragged-red-fibres and negative COX staining (Paucar *et al.*, 2018). Regarding severity of the heart defects, it can be mild, like for Pt1 or Pt5 to severe (heart failure) like for Pt3, leading to a poor prognosis in affected children.

Conclusion

Here we report the identification of novel pathogenic *ELAC2* variants in five patients from three unrelated families. Characterisation of fibroblasts from three of these patients led to similar observations to previous studies of patients with *ELAC2* variants. Although the severity of the manifestations differed between the variants, the patients nevertheless shared similar phenotypes. Thus, to date, without broadening the phenotypic spectrum, *ELAC2* variants mainly lead to lethal hypertrophic cardiomyopathy, or milder cardiac damage with neurological disorders.

Bibliography

Adil, S.M. *et al.* (2021) 'A high-resolution interactive atlas of the human brainstem using magnetic resonance imaging', *NeuroImage*, 237, p. 118135. Available at: https://doi.org/10.1016/j.neuroimage.2021.118135.

Akawi, N.A. *et al.* (2016) 'A homozygous splicing mutation in ELAC2 suggests phenotypic variability including intellectual disability with minimal cardiac involvement', *Orphanet Journal of Rare Diseases*, 11, p. 139. Available at: https://doi.org/10.1186/s13023-016-0526-8.

Albéri, L., Sgadò, P. and Simon, H.H. (2004) 'Engrailed genes are cell-autonomously required to prevent apoptosis in mesencephalic dopaminergic neurons', *Development*, 131(13), pp. 3229–3236. Available at: https://doi.org/10.1242/dev.01128.

Allouche, M. *et al.* (2012) 'ANT-VDAC1 interaction is direct and depends on ANT isoform conformation in vitro', *Biochemical and Biophysical Research Communications*, 429(1), pp. 12–17. Available at: https://doi.org/10.1016/j.bbrc.2012.10.108.

Alston, C.L. *et al.* (2017) 'The genetics and pathology of mitochondrial disease', *The Journal of Pathology*, 241(2), pp. 236–250. Available at: https://doi.org/10.1002/path.4809.

Amiri, M. and Hollenbeck, P.J. (2008) 'Mitochondrial biogenesis in the axons of vertebrate peripheral neurons', *Developmental Neurobiology*, 68(11), pp. 1348–1361. Available at: https://doi.org/10.1002/dneu.20668.

Ángeles Fernández-Gil, M. *et al.* (2010) 'Anatomy of the Brainstem: A Gaze Into the Stem of Life', *Seminars in Ultrasound, CT and MRI*, 31(3), pp. 196–219. Available at: https://doi.org/10.1053/j.sult.2010.03.006.

Antonicka, H. *et al.* (2003) 'Mutations in COX10 result in a defect in mitochondrial heme A biosynthesis and account for multiple, early-onset clinical phenotypes associated with isolated COX deficiency', *Human Molecular Genetics*, 12(20), pp. 2693–2702. Available at: https://doi.org/10.1093/hmg/ddg284.

Antonicka, H. *et al.* (2010) 'Mutations in C12orf65 in Patients with Encephalomyopathy and a Mitochondrial Translation Defect', *American Journal of Human Genetics*, 87(1), pp. 115–122. Available at: https://doi.org/10.1016/j.ajhg.2010.06.004.

Apps, R. and Hawkes, R. (2009) 'Cerebellar cortical organization: a one-map hypothesis', *Nature Reviews Neuroscience*, 10(9), pp. 670–681. Available at: https://doi.org/10.1038/nrn2698.

Arnold, J.J. *et al.* (2012) 'Human mitochondrial RNA polymerase: structure-function, mechanism and inhibition', *Biochimica Et Biophysica Acta*, 1819(9–10), pp. 948–960. Available at: https://doi.org/10.1016/j.bbagrm.2012.04.002.

Atwal, P.S. (2013) 'Mutations in the Complex III Assembly Factor Tetratricopeptide 19 Gene TTC19 Are a Rare Cause of Leigh Syndrome', *JIMD Reports*, 14, pp. 43–45. Available at: https://doi.org/10.1007/8904_2013_282.

Auré, K., Jardel, C. and Lombès, A. (2005) '[Mitochondrial diseases: molecular mechanisms, clinical presentations and diagnosis investigations]', *Annales De Pathologie*, 25(4), pp. 270–281. Available at: https://doi.org/10.1016/s0242-6498(05)80131-2.

Avula, S. *et al.* (2014) 'Treatment of mitochondrial disorders', *Current Treatment Options in Neurology*, 16(6), p. 292. Available at: https://doi.org/10.1007/s11940-014-0292-7.

Baertling, F. *et al.* (2014) 'A guide to diagnosis and treatment of Leigh syndrome', *Journal of Neurology, Neurosurgery & Psychiatry*, 85(3), pp. 257–265. Available at: https://doi.org/10.1136/jnnp-2012-304426.

Bandara, A.B., Drake, J.C. and Brown, D.A. (2021) 'Complex II subunit SDHD is critical for cell growth and metabolism, which can be partially restored with a synthetic ubiquinone analog', *BMC Molecular and Cell Biology*, 22(1), p. 35. Available at: https://doi.org/10.1186/s12860-021-00370-w.

Bannwarth, S. *et al.* (2013) 'Prevalence of rare mitochondrial DNA mutations in mitochondrial disorders', *Journal of Medical Genetics*, 50(10), pp. 704–714. Available at: https://doi.org/10.1136/jmedgenet-2013-101604.

Bannwarth, S., Procaccio, V. and Paquis-Flucklinger, V. (2005) 'Surveyor^{TM} Nuclease: A new strategy for a rapid identification of heteroplasmic mitochondrial DNA mutations in patients with respiratory chain defects', *Human Mutation*, 25(6), pp. 575–582. Available at: https://doi.org/10.1002/humu.20177.

Baradaran, R. *et al.* (2013) 'Crystal structure of the entire respiratory complex I', *Nature*, 494(7438), pp. 443–448. Available at: https://doi.org/10.1038/nature11871.

Barcia, G. *et al.* (2020) 'Clinical, neuroimaging and biochemical findings in patients and patient fibroblasts expressing ten novel GFM1 mutations', *Human Mutation*, 41(2), pp. 397–402. Available at: https://doi.org/10.1002/humu.23937.

Barel, O. *et al.* (2008) 'Mitochondrial complex III deficiency associated with a homozygous mutation in UQCRQ', *American Journal of Human Genetics*, 82(5), pp. 1211–1216. Available at: https://doi.org/10.1016/j.ajhg.2008.03.020.

Beilina, A. and Cookson, M.R. (2016) 'Genes associated with Parkinson's disease: regulation of autophagy and beyond', *Journal of neurochemistry*, 139(Suppl 1), pp. 91–107. Available at: https://doi.org/10.1111/jnc.13266.

Bélanger, M., Allaman, I. and Magistretti, P.J. (2011) 'Brain energy metabolism: focus on astrocyte-neuron metabolic cooperation', *Cell Metabolism*, 14(6), pp. 724–738. Available at: https://doi.org/10.1016/j.cmet.2011.08.016.

Bellamy, T.C. (2006) 'Interactions between Purkinje neurones and Bergmann glia', *The Cerebellum*, 5(2), pp. 116–126. Available at: https://doi.org/10.1080/14734220600724569.

Bénit, P. *et al.* (2001) 'Large-scale deletion and point mutations of the nuclear NDUFV1 and NDUFS1 genes in mitochondrial complex I deficiency', *American Journal of Human Genetics*, 68(6), pp. 1344–1352. Available at: https://doi.org/10.1086/320603.

Bénit, P. *et al.* (2004) 'Mutant NDUFS3 subunit of mitochondrial complex I causes Leigh syndrome', *Journal of Medical Genetics*, 41(1), pp. 14–17. Available at: https://doi.org/10.1136/jmg.2003.014316.

Bernardi, P. and Azzone, G.F. (1981) 'Cytochrome c as an electron shuttle between the outer and inner mitochondrial membranes', *The Journal of Biological Chemistry*, 256(14), pp. 7187–7192.

Bianciardi, L. *et al.* (2016) 'Exome sequencing coupled with mRNA analysis identifies NDUFAF6 as a Leigh gene', *Molecular Genetics and Metabolism*, 119(3), pp. 214–222. Available at: https://doi.org/10.1016/j.ymgme.2016.09.001.

Bione, S. *et al.* (1996) 'A novel X-linked gene, G4.5. is responsible for Barth syndrome', *Nature Genetics*, 12(4), pp. 385–389. Available at: https://doi.org/10.1038/ng0496-385.

Bolam, J.P. and Pissadaki, E.K. (2012) 'Living on the edge with too many mouths to feed: Why dopamine neurons die', *Movement Disorders*, 27(12), pp. 1478–1483. Available at: https://doi.org/10.1002/mds.25135.

Bolea, I. *et al.* (2019) 'Defined neuronal populations drive fatal phenotype in a mouse model of Leigh syndrome', *eLife*, 8, p. e47163. Available at: https://doi.org/10.7554/eLife.47163.

Bonora, M. *et al.* (2012) 'ATP synthesis and storage', *Purinergic Signalling*, 8(3), pp. 343–357. Available at: https://doi.org/10.1007/s11302-012-9305-8.

van den Bosch, B.J.C. *et al.* (2012) 'Defective NDUFA9 as a novel cause of neonatally fatal complex I disease', *Journal of Medical Genetics*, 49(1), pp. 10–15. Available at: https://doi.org/10.1136/jmedgenet-2011-100466.

Bourgeron, T. *et al.* (1995) 'Mutation of a nuclear succinate dehydrogenase gene results in mitochondrial respiratory chain deficiency', *Nature Genetics*, 11(2), pp. 144–149. Available at: https://doi.org/10.1038/ng1095-144.

Boyer, P.D. (2000) 'Catalytic site forms and controls in ATP synthase catalysis', *Biochimica Et Biophysica Acta*, 1458(2–3), pp. 252–262. Available at: https://doi.org/10.1016/s0005-2728(00)00077-3.

Braymer, J.J. and Lill, R. (2017) 'Iron–sulfur cluster biogenesis and trafficking in mitochondria', *The Journal of Biological Chemistry*, 292(31), pp. 12754–12763. Available at: https://doi.org/10.1074/jbc.R117.787101.

Brichta, L. and Greengard, P. (2014) 'Molecular determinants of selective dopaminergic vulnerability in Parkinson's disease: an update', *Frontiers in Neuroanatomy*, 8. Available at: https://doi.org/10.3389/fnana.2014.00152.

Bricout, M. *et al.* (2014) 'Brain imaging in mitochondrial respiratory chain deficiency: combination of brain MRI features as a useful tool for genotype/phenotype correlations', *Journal of Medical Genetics*, 51(7), pp. 429–435. Available at: https://doi.org/10.1136/jmedgenet-2013-102256.

Brunetti, D. *et al.* (2021) 'Mitochondria in neurogenesis: Implications for mitochondrial diseases', *STEM CELLS*, 39(10), pp. 1289–1297. Available at: https://doi.org/10.1002/stem.3425.

Brzezniak, L.K. *et al.* (2011) 'Involvement of human ELAC2 gene product in 3' end processing of mitochondrial tRNAs', *RNA biology*, 8(4), pp. 616–626. Available at: https://doi.org/10.4161/rna.8.4.15393.

Burchell, V.S. *et al.* (2010) 'Targeting mitochondrial dysfunction in neurodegenerative disease: Part I', *Expert Opinion on Therapeutic Targets*, 14(4), pp. 369–385. Available at: https://doi.org/10.1517/14728221003652489.

Burelle, Y. *et al.* (2015) 'Mitochondrial Vulnerability and Increased Susceptibility to Nutrient-Induced Cytotoxicity in Fibroblasts from Leigh Syndrome French Canadian Patients', *PLoS ONE*, 10(4), p. e0120767. Available at: https://doi.org/10.1371/journal.pone.0120767.

Calì, C., Tauffenberger, A. and Magistretti, P. (2019) 'The Strategic Location of Glycogen and Lactate: From Body Energy Reserve to Brain Plasticity', *Frontiers in Cellular Neuroscience*, 13, p. 82. Available at: https://doi.org/10.3389/fncel.2019.00082.

Calton, M.A. *et al.* (2016) 'The Cerebellum and SIDS: Disordered Breathing in a Mouse Model of Developmental Cerebellar Purkinje Cell Loss during Recovery from Hypercarbia', *Frontiers in Neurology*, 7. Available at: https://www.frontiersin.org/article/10.3389/fneur.2016.00078 (Accessed: 3 July 2022).

Calvo, S.E. *et al.* (2010) 'High-throughput, pooled sequencing identifies mutations in NUBPL and FOXRED1 in human complex I deficiency', *Nature genetics*, 42(10), pp. 851–858. Available at: https://doi.org/10.1038/ng.659.

Capaldi, R.A. (1996) 'The complexity of a respiratory complex', *Nature Structural Biology*, 3(7), pp. 570–574. Available at: https://doi.org/10.1038/nsb0796-570.

Carroll, C.J., Brilhante, V. and Suomalainen, A. (2014) 'Next-generation sequencing for mitochondrial disorders', *British Journal of Pharmacology*, 171(8), pp. 1837–1853. Available at: https://doi.org/10.1111/bph.12469.

Chaban, Y., Boekema, E.J. and Dudkina, N.V. (2014) 'Structures of mitochondrial oxidative phosphorylation supercomplexes and mechanisms for their stabilisation', *Biochimica et Biophysica Acta (BBA) - Bioenergetics*, 1837(4), pp. 418–426. Available at: https://doi.org/10.1016/j.bbabio.2013.10.004.

Chalmers, R.M. *et al.* (1997) 'A mitochondrial DNA tRNA(Val) point mutation associated with adult-onset Leigh syndrome', *Neurology*, 49(2), pp. 589–592. Available at: https://doi.org/10.1212/wnl.49.2.589.

Chandel, N.S. (2015) 'Evolution of Mitochondria as Signaling Organelles', *Cell Metabolism*, 22(2), pp. 204–206. Available at: https://doi.org/10.1016/j.cmet.2015.05.013.

Chen, H., McCaffery, J.M. and Chan, D.C. (2007) 'Mitochondrial Fusion Protects against Neurodegeneration in the Cerebellum', *Cell*, 130(3), pp. 548–562. Available at: https://doi.org/10.1016/j.cell.2007.06.026.

Chujo, T. *et al.* (2012) 'LRPPRC/SLIRP suppresses PNPase-mediated mRNA decay and promotes polyadenylation in human mitochondria', *Nucleic Acids Research*, 40(16), pp. 8033–8047. Available at: https://doi.org/10.1093/nar/gks506.

Chung, C.Y. *et al.* (2005) 'Cell type-specific gene expression of midbrain dopaminergic neurons reveals molecules involved in their vulnerability and protection', *Human molecular genetics*, 14(13), pp. 1709–1725. Available at: https://doi.org/10.1093/hmg/ddi178.

Cipolat, S. *et al.* (2004) 'OPA1 requires mitofusin 1 to promote mitochondrial fusion', *Proceedings of the National Academy of Sciences*, 101(45), pp. 15927–15932. Available at: https://doi.org/10.1073/pnas.0407043101.

Claeys, K.G. *et al.* (2016) 'Novel genetic and neuropathological insights in neurogenic muscle weakness, ataxia, and retinitis pigmentosa (NARP)', *Muscle & Nerve*, 54(2), pp. 328–333. Available at: https://doi.org/10.1002/mus.25125.

Consalez, G.G. *et al.* (2021) 'Origins, Development, and Compartmentation of the Granule Cells of the Cerebellum', *Frontiers in Neural Circuits*, 14. Available at: https://www.frontiersin.org/article/10.3389/fncir.2020.611841 (Accessed: 14 March 2022).

Cori, C.F. (1981) 'The glucose-lactic acid cycle and gluconeogenesis', *Current Topics in Cellular Regulation*, 18, pp. 377–387.

Corrales, J.D. *et al.* (2004) 'Spatial pattern of sonic hedgehog signaling through Gli genes during cerebellum development', *Development (Cambridge, England)*, 131(22), pp. 5581–5590. Available at: https://doi.org/10.1242/dev.01438.

Corrales, J.D. *et al.* (2006) 'The level of sonic hedgehog signaling regulates the complexity of cerebellar foliation', *Development*, 133(9), pp. 1811–1821. Available at: https://doi.org/10.1242/dev.02351.

Cortopassi, G.A. and Arnheim, N. (1990) 'Detection of a specific mitochondrial DNA deletion in tissues of older humans.', *Nucleic Acids Research*, 18(23), pp. 6927–6933. Available at: https://www.ncbi.nlm.nih.gov/pmc/articles/PMC332752/ (Accessed: 3 November 2022).

Coughlin, C.R. *et al.* (2015) 'Mutations in the mitochondrial cysteinyl-tRNA synthase gene, CARS2, lead to a severe epileptic encephalopathy and complex movement disorder', *Journal of Medical Genetics*, 52(8), pp. 532–540. Available at: https://doi.org/10.1136/jmedgenet-2015-103049.

Craven, L. *et al.* (2017) 'Recent Advances in Mitochondrial Disease', *Annual Review of Genomics and Human Genetics*, 18, pp. 257–275. Available at: https://doi.org/10.1146/annurev-genom-091416-035426.

Cuillerier, A. *et al.* (2017) 'Loss of hepatic LRPPRC alters mitochondrial bioenergetics, regulation of permeability transition and trans-membrane ROS diffusion', *Human Molecular Genetics*, 26(16), pp. 3186–3201. Available at: https://doi.org/10.1093/hmg/ddx202.

Da Costa, B. *et al.* (2016) 'Respiratory chain inhibition: one more feature to propose MPTP intoxication as a Leigh syndrome model', *Journal of Bioenergetics and Biomembranes*, 48(5), pp. 483–491. Available at: https://doi.org/10.1007/s10863-016-9683-7.

Damasio, A. and Carvalho, G.B. (2013) ‘The nature of feelings: evolutionary and neurobiological origins’, *Nature Reviews. Neuroscience*, 14(2), pp. 143–152. Available at: https://doi.org/10.1038/nrn3403.

Debray, F.-G. *et al.* (2011) ‘LRPPRC mutations cause a phenotypically distinct form of Leigh syndrome with cytochrome c oxidase deficiency’, *Journal of Medical Genetics*, 48(3), pp. 183–189. Available at: https://doi.org/10.1136/jmg.2010.081976.

Del Negro, C.A., Funk, G.D. and Feldman, J.L. (2018) ‘Breathing matters’, *Nature Reviews. Neuroscience*, 19(6), pp. 351–367. Available at: https://doi.org/10.1038/s41583-018-0003-6.

Desmons, A. *et al.* (2020) ‘Direct liquid chromatography tandem mass spectrometry analysis of amino acids in human plasma’, *Journal of Chromatography. A*, 1622, p. 461135. Available at: https://doi.org/10.1016/j.chroma.2020.461135.

Deutschmann, A.J. *et al.* (2014) ‘Mutation or knock-down of 17β-hydroxysteroid dehydrogenase type 10 cause loss of MRPP1 and impaired processing of mitochondrial heavy strand transcripts’, *Human Molecular Genetics*, 23(13), pp. 3618–3628. Available at: https://doi.org/10.1093/hmg/ddu072.

Devine, M.J. and Kittler, J.T. (2018) ‘Mitochondria at the neuronal presynapse in health and disease’, *Nature Reviews Neuroscience*, 19(2), pp. 63–80. Available at: https://doi.org/10.1038/nrn.2017.170.

Digre, A. and Lindskog, C. (2021) ‘The Human Protein Atlas—Spatial localization of the human proteome in health and disease’, *Protein Science : A Publication of the Protein Society*, 30(1), pp. 218–233. Available at: https://doi.org/10.1002/pro.3987.

Dorn, G.W., Vega, R.B. and Kelly, D.P. (2015) ‘Mitochondrial biogenesis and dynamics in the developing and diseased heart’, *Genes & Development*, 29(19), pp. 1981–1991. Available at: https://doi.org/10.1101/gad.269894.115.

Dröse, S. and Brandt, U. (2012) ‘Molecular mechanisms of superoxide production by the mitochondrial respiratory chain’, *Advances in Experimental Medicine and Biology*, 748, pp. 145–169. Available at: https://doi.org/10.1007/978-1-4614-3573-0_6.

Dubrovsky, E.B. *et al.* (2004) ‘Drosophila RNase Z processes mitochondrial and nuclear pre-tRNA 3’ ends in vivo’, *Nucleic Acids Research*, 32(1), pp. 255–262. Available at: https://doi.org/10.1093/nar/gkh182.

Duchen, M.R. (2000) ‘Mitochondria and calcium: from cell signalling to cell death’, *The Journal of Physiology*, 529(Pt 1), pp. 57–68. Available at: https://doi.org/10.1111/j.1469-7793.2000.00057.x.

Duchen, M.R. (2012) ‘Mitochondria, calcium-dependent neuronal death and neurodegenerative disease’, *Pflugers Archiv*, 464(1), pp. 111–121. Available at: https://doi.org/10.1007/s00424-012-1112-0.

Duno, M. *et al.* (2013) ‘A novel mitochondrial mutation m.8989G>C associated with neuropathy, ataxia, retinitis pigmentosa - the NARP syndrome’, *Gene*, 515(2), pp. 372–375. Available at: https://doi.org/10.1016/j.gene.2012.12.066.

Edwards, R., Eaglesfield, R. and Tokatlidis, K. (2021) 'The mitochondrial intermembrane space: the most constricted mitochondrial sub-compartment with the largest variety of protein import pathways', *Open Biology*, 11(3), p. 210002. Available at: https://doi.org/10.1098/rsob.210002.

Ellis, T.P. *et al.* (2004) 'Aep3p Stabilizes the Mitochondrial Bicistronic mRNA Encoding Subunits 6 and 8 of the H+-translocating ATP Synthase of Saccharomyces cerevisiae*', *Journal of Biological Chemistry*, 279(16), pp. 15728–15733. Available at: https://doi.org/10.1074/jbc.M314162200.

Elpeleg, O. *et al.* (2005) 'Deficiency of the ADP-forming succinyl-CoA synthase activity is associated with encephalomyopathy and mitochondrial DNA depletion', *American Journal of Human Genetics*, 76(6), pp. 1081–1086. Available at: https://doi.org/10.1086/430843.

English, A.R. and Voeltz, G.K. (2013) 'Endoplasmic Reticulum Structure and Interconnections with Other Organelles', *Cold Spring Harbor Perspectives in Biology*, 5(4), p. a013227. Available at: https://doi.org/10.1101/cshperspect.a013227.

van Essen, M.J. *et al.* (2020) 'Deconstructing cerebellar development cell by cell', *PLoS Genetics*, 16(4), p. e1008630. Available at: https://doi.org/10.1371/journal.pgen.1008630.

Fecher, C. *et al.* (2019) 'Cell-type-specific profiling of brain mitochondria reveals functional and molecular diversity', *Nature Neuroscience*, 22(10), pp. 1731–1742. Available at: https://doi.org/10.1038/s41593-019-0479-z.

Fernandez-Moreira, D. *et al.* (2007) 'X-linked NDUFA1 gene mutations associated with mitochondrial encephalomyopathy', *Annals of Neurology*, 61(1), pp. 73–83. Available at: https://doi.org/10.1002/ana.21036.

Figueira, L. and Israel, A. (2015) 'Role of cerebellar adrenomedullin in blood pressure regulation', *Neuropeptides*, 54, pp. 59–66. Available at: https://doi.org/10.1016/j.npep.2015.07.003.

Finsterer, J. (2008) 'Leigh and Leigh-like syndrome in children and adults', *Pediatric Neurology*, 39(4), pp. 223–235. Available at: https://doi.org/10.1016/j.pediatrneurol.2008.07.013.

Fiorese, C.J. and Haynes, C.M. (2017) 'Integrating the UPRmt into the Mitochondrial Maintenance Network', *Critical reviews in biochemistry and molecular biology*, 52(3), pp. 304–313. Available at: https://doi.org/10.1080/10409238.2017.1291577.

Fischer, A.H. *et al.* (2008) 'Hematoxylin and eosin staining of tissue and cell sections', *CSH protocols*, 2008, p. pdb.prot4986. Available at: https://doi.org/10.1101/pdb.prot4986.

Fleming, J. and Chiang, C. (2015) 'The Purkinje neuron: A central orchestrator of cerebellar neurogenesis', *Neurogenesis*, 2(1). Available at: https://doi.org/10.1080/23262133.2015.1025940.

Flynn, J.M. and Melov, S. (2013) 'SOD2 in mitochondrial dysfunction and neurodegeneration', *Free Radical Biology and Medicine*, 62, pp. 4–12. Available at: https://doi.org/10.1016/j.freeradbiomed.2013.05.027.

Frank, S. *et al.* (2001) 'The role of dynamin-related protein 1, a mediator of mitochondrial fission, in apoptosis', *Developmental Cell*, 1(4), pp. 515–525. Available at: https://doi.org/10.1016/s1534-5807(01)00055-7.

Fraser, J.L. *et al.* (2014) 'Thiamine pyrophosphokinase deficiency causes a Leigh Disease like phenotype in a sibling pair: identification through whole exome sequencing and management strategies', *Molecular Genetics and Metabolism Reports*, 1, pp. 66–70. Available at: https://doi.org/10.1016/j.ymgmr.2013.12.007.

Frazier, A.E. and Thorburn, D.R. (2012) 'Biochemical Analyses of the Electron Transport Chain Complexes by Spectrophotometry', in Ph.D. Wong Lee-Jun C. (ed.) *Mitochondrial Disorders: Biochemical and Molecular Analysis*. Totowa, NJ: Humana Press (Methods in Molecular Biology), pp. 49–62. Available at: https://doi.org/10.1007/978-1-61779-504-6_4.

Friberg, H. and Wieloch, T. (2002) 'Mitochondrial permeability transition in acute neurodegeneration', *Biochimie*, 84(2–3), pp. 241–250. Available at: https://doi.org/10.1016/s0300-9084(02)01381-0.

Fuh, J.L. *et al.* (1997) 'Swallowing difficulty in Parkinson's disease', *Clinical Neurology and Neurosurgery*, 99(2), pp. 106–112. Available at: https://doi.org/10.1016/s0303-8467(97)00606-9.

Fukumura, S. *et al.* (2015) 'Compound heterozygous GFM2 mutations with Leigh syndrome complicated by arthrogryposis multiplex congenita', *Journal of Human Genetics*, 60(9), pp. 509–513. Available at: https://doi.org/10.1038/jhg.2015.57.

Gale, E. and Li, M. (2008) 'Midbrain dopaminergic neuron fate specification: Of mice and embryonic stem cells', *Molecular Brain*, 1, p. 8. Available at: https://doi.org/10.1186/1756-6606-1-8.

Ganetzky, R. and Stojinski, C. (1993) 'Mitochondrial Short-Chain Enoyl-CoA Hydratase 1 Deficiency', in M.P. Adam et al. (eds) *GeneReviews®*. Seattle (WA): University of Washington, Seattle. Available at: http://www.ncbi.nlm.nih.gov/books/NBK542806/ (Accessed: 12 March 2022).

Garrido, N. *et al.* (2003) 'Composition and dynamics of human mitochondrial nucleoids', *Molecular Biology of the Cell*, 14(4), pp. 1583–1596. Available at: https://doi.org/10.1091/mbc.e02-07-0399.

Gaven, F., Marin, P. and Claeysen, S. (2014) 'Primary culture of mouse dopaminergic neurons', *Journal of Visualized Experiments: JoVE*, (91), p. e51751. Available at: https://doi.org/10.3791/51751.

Gerards, M. *et al.* (2010) 'Defective complex I assembly due to C20orf7 mutations as a new cause of Leigh syndrome', *Journal of Medical Genetics*, 47(8), pp. 507–512. Available at: https://doi.org/10.1136/jmg.2009.067553.

Gerards, M. *et al.* (2013) 'Exome sequencing reveals a novel Moroccan founder mutation in SLC19A3 as a new cause of early-childhood fatal Leigh syndrome', *Brain: A Journal of Neurology*, 136(Pt 3), pp. 882–890. Available at: https://doi.org/10.1093/brain/awt013.

Gerards, M., Sallevelt, S.C.E.H. and Smeets, H.J.M. (2016) 'Leigh syndrome: Resolving the clinical and genetic heterogeneity paves the way for treatment options', *Molecular Genetics and Metabolism*, 117(3), pp. 300–312. Available at: https://doi.org/10.1016/j.ymgme.2015.12.004.

Ghiso, N.S. and Lennon, G.G. (1994) 'lrp130 gene assigned to chromosome 2', *In Vitro Cellular & Developmental Biology. Animal*, 30A(11), p. 744. Available at: https://doi.org/10.1007/BF02631295.

Glickstein, M. (1993) 'Motor skills but not cognitive tasks', *Trends in Neurosciences*, 16(11), pp. 450–451; discussion 453-454. Available at: https://doi.org/10.1016/0166-2236(93)90074-v.

Glickstein, M., Sultan, F. and Voogd, J. (2011) 'Functional localization in the cerebellum', *Cortex; a Journal Devoted to the Study of the Nervous System and Behavior*, 47(1), pp. 59–80. Available at: https://doi.org/10.1016/j.cortex.2009.09.001.

Gohil, V.M. *et al.* (2010) 'Mitochondrial and Nuclear Genomic Responses to Loss of LRPPRC Expression', *The Journal of Biological Chemistry*, 285(18), pp. 13742–13747. Available at: https://doi.org/10.1074/jbc.M109.098400.

González-Rodríguez, P. *et al.* (2021) 'Disruption of mitochondrial complex I induces progressive parkinsonism', *Nature*, 599(7886), pp. 650–656. Available at: https://doi.org/10.1038/s41586-021-04059-0.

Gorman, G.S. *et al.* (2015) 'Prevalence of nuclear and mitochondrial DNA mutations related to adult mitochondrial disease', *Annals of Neurology*, 77(5), pp. 753–759. Available at: https://doi.org/10.1002/ana.24362.

Gorman, G.S. *et al.* (2016) 'Mitochondrial diseases', *Nature Reviews Disease Primers*, 2(1), pp. 1–22. Available at: https://doi.org/10.1038/nrdp.2016.80.

Grace, A.A. (2016) 'Dysregulation of the dopamine system in the pathophysiology of schizophrenia and depression', *Nature Reviews. Neuroscience*, 17(8), pp. 524–532. Available at: https://doi.org/10.1038/nrn.2016.57.

Grafakou, O. *et al.* (2003) 'Leigh syndrome due to compound heterozygosity of dihydrolipoamide dehydrogenase gene mutations. Description of the first E3 splice site mutation', *European Journal of Pediatrics*, 162(10), pp. 714–718. Available at: https://doi.org/10.1007/s00431-003-1282-z.

Gray, M.W. (2012) 'Mitochondrial Evolution', *Cold Spring Harbor Perspectives in Biology*, 4(9), p. a011403. Available at: https://doi.org/10.1101/cshperspect.a011403.

Gray, M.W. (2017) 'Lynn Margulis and the endosymbiont hypothesis: 50 years later', *Molecular Biology of the Cell*, 28(10), pp. 1285–1287. Available at: https://doi.org/10.1091/mbc.E16-07-0509.

Grünewald, A., Kumar, K.R. and Sue, C.M. (2019) 'New insights into the complex role of mitochondria in Parkinson's disease', *Progress in Neurobiology*, 177, pp. 73–93. Available at: https://doi.org/10.1016/j.pneurobio.2018.09.003.

Guyenet, P.G. (2006) ‘The sympathetic control of blood pressure’, *Nature Reviews. Neuroscience*, 7(5), pp. 335–346. Available at: https://doi.org/10.1038/nrn1902.

Györfi, A.-H. *et al.* (2021) ‘Engrailed 1 coordinates cytoskeletal reorganization to induce myofibroblast differentiation’, *Journal of Experimental Medicine*, 218(9), p. e20201916. Available at: https://doi.org/10.1084/jem.20201916.

H, Z. *et al.* (2014) ‘Increased negative supercoiling of mtDNA in TOP1mt knockout mice and presence of topoisomerases IIα and IIβ in vertebrate mitochondria’, *Nucleic acids research*, 42(11). Available at: https://doi.org/10.1093/nar/gku384.

Haack, T.B. *et al.* (2013) ‘ELAC2 Mutations Cause a Mitochondrial RNA Processing Defect Associated with Hypertrophic Cardiomyopathy’, *American Journal of Human Genetics*, 93(2), pp. 211–223. Available at: https://doi.org/10.1016/j.ajhg.2013.06.006.

Ham, S.J. *et al.* (2020) ‘Decision between mitophagy and apoptosis by Parkin via VDAC1 ubiquitination’, *Proceedings of the National Academy of Sciences*, 117(8), pp. 4281–4291. Available at: https://doi.org/10.1073/pnas.1909814117.

Han, V.X. *et al.* (2017) ‘Novel LRPPRC Mutation in a Boy With Mild Leigh Syndrome, French-Canadian Type Outside of Québec’, *Child Neurology Open*, 4, p. 2329048X17737638. Available at: https://doi.org/10.1177/2329048X17737638.

Hayashi, G. and Cortopassi, G. (2015) ‘Oxidative stress in inherited mitochondrial diseases’, *Free Radical Biology and Medicine*, 88, pp. 10–17. Available at: https://doi.org/10.1016/j.freeradbiomed.2015.05.039.

Hayashi, J. *et al.* (1991) ‘Introduction of disease-related mitochondrial DNA deletions into HeLa cells lacking mitochondrial DNA results in mitochondrial dysfunction’, *Proceedings of the National Academy of Sciences of the United States of America*, 88(23), pp. 10614–10618. Available at: https://doi.org/10.1073/pnas.88.23.10614.

Herrero-Mendez, A. *et al.* (2009) ‘The bioenergetic and antioxidant status of neurons is controlled by continuous degradation of a key glycolytic enzyme by APC/C-Cdh1’, *Nature Cell Biology*, 11(6), pp. 747–752. Available at: https://doi.org/10.1038/ncb1881.

Hillen, H.S. *et al.* (2017) ‘Structural Basis of Mitochondrial Transcription Initiation’, *Cell*, 171(5), pp. 1072-1081.e10. Available at: https://doi.org/10.1016/j.cell.2017.10.036.

Hoefs, S.J.G. *et al.* (2008) ‘NDUFA2 complex I mutation leads to Leigh disease’, *American Journal of Human Genetics*, 82(6), pp. 1306–1315. Available at: https://doi.org/10.1016/j.ajhg.2008.05.007.

Hoefs, S.J.G. *et al.* (2011) ‘NDUFA10 mutations cause complex I deficiency in a patient with Leigh disease’, *European journal of human genetics: EJHG*, 19(3), pp. 270–274. Available at: https://doi.org/10.1038/ejhg.2010.204.

Holmgren, D. *et al.* (2003) ‘Cardiomyopathy in children with mitochondrial disease; clinical course and cardiological findings’, *European Heart Journal*, 24(3), pp. 280–288. Available at: https://doi.org/10.1016/s0195-668x(02)00387-1.

Holt, I.J. *et al.* (1990) 'A new mitochondrial disease associated with mitochondrial DNA heteroplasmy.', *American Journal of Human Genetics*, 46(3), pp. 428–433. Available at: https://www.ncbi.nlm.nih.gov/pmc/articles/PMC1683641/ (Accessed: 2 March 2022).

Holzmann, J. *et al.* (2008) 'RNase P without RNA: identification and functional reconstitution of the human mitochondrial tRNA processing enzyme', *Cell*, 135(3), pp. 462–474. Available at: https://doi.org/10.1016/j.cell.2008.09.013.

Hommes, F.A., Polman, H.A. and Reerink, J.D. (1968) 'Leigh's encephalomyelopathy: an inborn error of gluconeogenesis', *Archives of Disease in Childhood*, 43(230), pp. 423–426. Available at: https://doi.org/10.1136/adc.43.230.423.

Hou, J., Wang, F. and McKeehan, W.L. (1994) 'Molecular cloning and expression of the gene for a major leucine-rich protein from human hepatoblastoma cells (HepG2)', *In Vitro Cellular & Developmental Biology. Animal*, 30A(2), pp. 111–114. Available at: https://doi.org/10.1007/BF02631402.

Hou, Y.-M. (2010) 'CCA Addition to tRNA: Implications for tRNA Quality Control', *IUBMB life*, 62(4), pp. 251–260. Available at: https://doi.org/10.1002/iub.301.

Inak, G. *et al.* (2021) 'Defective metabolic programming impairs early neuronal morphogenesis in neural cultures and an organoid model of Leigh syndrome', *Nature Communications*, 12(1), p. 1929. Available at: https://doi.org/10.1038/s41467-021-22117-z.

Ito, S. and Feldheim, D.A. (2018) 'The Mouse Superior Colliculus: An Emerging Model for Studying Circuit Formation and Function', *Frontiers in Neural Circuits*, 12, p. 10. Available at: https://doi.org/10.3389/fncir.2018.00010.

Jahn, R. and Fasshauer, D. (2012) 'Molecular machines governing exocytosis of synaptic vesicles', *Nature*, 490(7419), pp. 201–207. Available at: https://doi.org/10.1038/nature11320.

Kádár, A. *et al.* (2009) 'Improved method for combination of immunocytochemistry and Nissl staining', *Journal of neuroscience methods*, 184(1), pp. 115–118. Available at: https://doi.org/10.1016/j.jneumeth.2009.07.010.

Kadenbach, B. (2021) 'Complex IV – The regulatory center of mitochondrial oxidative phosphorylation', *Mitochondrion*, 58, pp. 296–302. Available at: https://doi.org/10.1016/j.mito.2020.10.004.

Kalinichenko, S.G. and Okhotin, V.E. (2005) 'Unipolar brush cells--a new type of excitatory interneuron in the cerebellar cortex and cochlear nuclei of the brainstem', *Neuroscience and Behavioral Physiology*, 35(1), pp. 21–36. Available at: https://doi.org/10.1023/b:neab.0000049648.20702.ad.

Khorsandi, S.E., Taanman, J.W. and Heaton, N. (2017) 'Subunit composition of respiratory chain complex 1 and its responses to oxygen in mitochondria from human donor livers', *BMC Research Notes*, 10(1), p. 547. Available at: https://doi.org/10.1186/s13104-017-2863-7.

Kim, Y.A. *et al.* (2017) 'The First Korean case of combined oxidative phosphorylation deficiency-17 diagnosed by clinical and molecular investigation', *Korean Journal of Pediatrics*, 60(12), pp. 408–412. Available at: https://doi.org/10.3345/kjp.2017.60.12.408.

Kirby, D.M. *et al.* (2000) 'Leigh disease caused by the mitochondrial DNA G14459A mutation in unrelated families', *Annals of Neurology*, 48(1), pp. 102–104.

Komaki, H. *et al.* (2003) 'A novel mtDNA C11777A mutation in Leigh syndrome', *Mitochondrion*, 2(4), pp. 293–304. Available at: https://doi.org/10.1016/S1567-7249(03)00003-5.

Korver, W. *et al.* (2003) 'The product of the candidate prostate cancer susceptibility gene ELAC2 interacts with the gamma-tubulin complex', *International Journal of Cancer*, 104(3), pp. 283–288. Available at: https://doi.org/10.1002/ijc.10945.

Kühlbrandt, W. (2015) 'Structure and function of mitochondrial membrane protein complexes', *BMC Biology*, 13(1), p. 89. Available at: https://doi.org/10.1186/s12915-015-0201-x.

Lagrue, E. *et al.* (2009) 'MPTP intoxication in mice: a useful model of Leigh syndrome to study mitochondrial diseases in childhood', *Metabolic Brain Disease*, 24(2), pp. 321–335. Available at: https://doi.org/10.1007/s11011-009-9132-y.

Lake, N.J. *et al.* (2016a) 'Leigh syndrome: One disorder, more than 75 monogenic causes', *Annals of Neurology*, 79(2), pp. 190–203. Available at: https://doi.org/10.1002/ana.24551.

Lake, N.J. *et al.* (2017) 'Biallelic Mutations in MRPS34 Lead to Instability of the Small Mitoribosomal Subunit and Leigh Syndrome', *American Journal of Human Genetics*, 101(2), pp. 239–254. Available at: https://doi.org/10.1016/j.ajhg.2017.07.005.

Lang, A.E. and Lozano, A.M. (1998) 'Parkinson's disease. First of two parts', *The New England Journal of Medicine*, 339(15), pp. 1044–1053. Available at: https://doi.org/10.1056/NEJM199810083391506.

Lebre, A.S. *et al.* (2011) 'A common pattern of brain MRI imaging in mitochondrial diseases with complex I deficiency', *Journal of Medical Genetics*, 48(1), pp. 16–23. Available at: https://doi.org/10.1136/jmg.2010.079624.

Lee, S.-K. and Hollenbeck, P.J. (2003) 'Organization and translation of mRNA in sympathetic axons', *Journal of Cell Science*, 116(21), pp. 4467–4478. Available at: https://doi.org/10.1242/jcs.00745.

Lefèvre, A. *et al.* (1998) '[Clinical study and genetic 3q28 locus linkage in 2 Swiss families with Kjer dominant optic atrophy (OPA1)]', *Klinische Monatsblatter Fur Augenheilkunde*, 212(5), pp. 301–304.

Leigh, D. (1951) 'SUBACUTE NECROTIZING ENCEPHALOMYELOPATHY IN AN INFANT', *Journal of Neurology, Neurosurgery, and Psychiatry*, 14(3), pp. 216–221. Available at: https://www.ncbi.nlm.nih.gov/pmc/articles/PMC499520/ (Accessed: 23 October 2020).

Leiner, H.C., Leiner, A.L. and Dow, R.S. (1991) 'The human cerebro-cerebellar system: its computing, cognitive, and language skills', *Behavioural Brain Research*, 44(2), pp. 113–128. Available at: https://doi.org/10.1016/s0166-4328(05)80016-6.

Leto, K., Bartolini, A. and Rossi, F. (2008) 'Development of cerebellar GABAergic interneurons: origin and shaping of the "minibrain" local connections', *Cerebellum (London, England)*, 7(4), pp. 523–529. Available at: https://doi.org/10.1007/s12311-008-0079-z.

Leto, K. and Rossi, F. (2012) 'Specification and differentiation of cerebellar GABAergic neurons', *Cerebellum (London, England)*, 11(2), pp. 434–435. Available at: https://doi.org/10.1007/s12311-011-0324-8.

Li, J. *et al.* (2022) 'Upregulated hexokinase 2 expression induces the apoptosis of dopaminergic neurons by promoting lactate production in Parkinson's disease', *Neurobiology of Disease*, 163, p. 105605. Available at: https://doi.org/10.1016/j.nbd.2021.105605.

Li, K. *et al.* (2014) 'Shp2-Dependent ERK Signaling Is Essential for Induction of Bergmann Glia and Foliation of the Cerebellum', *The Journal of Neuroscience*, 34(3), pp. 922–931. Available at: https://doi.org/10.1523/JNEUROSCI.3476-13.2014.

Liang, C.-L. *et al.* (2007) 'Mitochondria mass is low in mouse substantia nigra dopamine neurons: implications for Parkinson's disease', *Experimental Neurology*, 203(2), pp. 370–380. Available at: https://doi.org/10.1016/j.expneurol.2006.08.015.

Lightowlers, R.N. and Chrzanowska-Lightowlers, Z.M. (2013) 'Human pentatricopeptide proteins', *RNA Biology*, 10(9), pp. 1433–1438. Available at: https://doi.org/10.4161/rna.24770.

Lightowlers, R.N. and Chrzanowska-Lightowlers, Z.M.A. (2008) 'PPR (pentatricopeptide repeat) proteins in mammals: important aids to mitochondrial gene expression', *Biochemical Journal*, 416(1), pp. e5–e6. Available at: https://doi.org/10.1042/BJ20081942.

Lim, S.C. *et al.* (2014) 'A founder mutation in PET100 causes isolated complex IV deficiency in Lebanese individuals with Leigh syndrome', *American Journal of Human Genetics*, 94(2), pp. 209–222. Available at: https://doi.org/10.1016/j.ajhg.2013.12.015.

Lin, D.D.M., Crawford, T.O. and Barker, P.B. (2003) 'Proton MR spectroscopy in the diagnostic evaluation of suspected mitochondrial disease', *AJNR. American journal of neuroradiology*, 24(1), pp. 33–41.

Lissens, W. *et al.* (2000) 'Mutations in the X-linked pyruvate dehydrogenase (E1) α subunit gene (PDHA1) in patients with a pyruvate dehydrogenase complex deficiency', *Human Mutation*, 15(3), pp. 209–219. Available at: https://doi.org/10.1002/(SICI)1098-1004(200003)15:3<209::AID-HUMU1>3.0.CO;2-K.

Liu, L. and McKeehan, W.L. (2002) 'Sequence analysis of LRPPRC and its SEC1 domain interaction partners suggests roles in cytoskeletal organization, vesicular trafficking, nucleocytosolic shuttling, and chromosome activity', *Genomics*, 79(1), pp. 124–136. Available at: https://doi.org/10.1006/geno.2001.6679.

Loeffen, J. *et al.* (1998) 'The first nuclear-encoded complex I mutation in a patient with Leigh syndrome', *American Journal of Human Genetics*, 63(6), pp. 1598–1608. Available at: https://doi.org/10.1086/302154.

de Lonlay, P. *et al.* (2001) ‘A mutant mitochondrial respiratory chain assembly protein causes complex III deficiency in patients with tubulopathy, encephalopathy and liver failure’, *Nature Genetics*, 29(1), pp. 57–60. Available at: https://doi.org/10.1038/ng706.

López, L.C. *et al.* (2006) ‘Leigh syndrome with nephropathy and CoQ10 deficiency due to decaprenyl diphosphate synthase subunit 2 (PDSS2) mutations’, *American Journal of Human Genetics*, 79(6), pp. 1125–1129. Available at: https://doi.org/10.1086/510023.

López-Otín, C. *et al.* (2013) ‘The hallmarks of aging’, *Cell*, 153(6), pp. 1194–1217. Available at: https://doi.org/10.1016/j.cell.2013.05.039.

Maceluch, J.A. and Niedziela, M. (2006) ‘The clinical diagnosis and molecular genetics of kearns-sayre syndrome: a complex mitochondrial encephalomyopathy’, *Pediatric endocrinology reviews: PER*, 4(2), pp. 117–137.

Madisen, L. *et al.* (2010) ‘A robust and high-throughput Cre reporting and characterization system for the whole mouse brain’, *Nature Neuroscience*, 13(1), pp. 133–140. Available at: https://doi.org/10.1038/nn.2467.

Martin, W.F., Garg, S. and Zimorski, V. (2015) ‘Endosymbiotic theories for eukaryote origin’, *Philosophical Transactions of the Royal Society B: Biological Sciences*, 370(1678), p. 20140330. Available at: https://doi.org/10.1098/rstb.2014.0330.

Matilainen, S. *et al.* (2017) ‘Defective mitochondrial RNA processing due to PNPT1 variants causes Leigh syndrome’, *Human Molecular Genetics*, 26(17), pp. 3352–3361. Available at: https://doi.org/10.1093/hmg/ddx221.

Matthews, P.M. *et al.* (1993) ‘Molecular genetic characterization of an X-linked form of Leigh’s syndrome’, *Annals of Neurology*, 33(6), pp. 652–655. Available at: https://doi.org/10.1002/ana.410330616.

Mattson, M.P. (2000) ‘Apoptosis in neurodegenerative disorders’, *Nature Reviews. Molecular Cell Biology*, 1(2), pp. 120–129. Available at: https://doi.org/10.1038/35040009.

Mayr, J.A. *et al.* (2011) ‘Heterozygous mutation in the X chromosomal NDUFA1 gene in a girl with complex I deficiency’, *Molecular Genetics and Metabolism*, 103(4), pp. 358–361. Available at: https://doi.org/10.1016/j.ymgme.2011.04.010.

McFarland, R., Taylor, R.W. and Turnbull, D.M. (2010) ‘A neurological perspective on mitochondrial disease’, *The Lancet. Neurology*, 9(8), pp. 829–840. Available at: https://doi.org/10.1016/S1474-4422(10)70116-2.

McKelvie, P. *et al.* (2012) ‘Late-adult onset Leigh syndrome’, *Journal of Clinical Neuroscience: Official Journal of the Neurosurgical Society of Australasia*, 19(2), pp. 195–202. Available at: https://doi.org/10.1016/j.jocn.2011.09.009.

Merante, F. *et al.* (1993) ‘A biochemically distinct form of cytochrome oxidase (COX) deficiency in the Saguenay-Lac-Saint-Jean region of Quebec.’, *American Journal of Human Genetics*, 53(2), pp. 481–487. Available at: https://www.ncbi.nlm.nih.gov/pmc/articles/PMC1682348/ (Accessed: 15 March 2022).

Metodiev, M.D. *et al.* (2009) 'Methylation of 12S rRNA Is Necessary for In Vivo Stability of the Small Subunit of the Mammalian Mitochondrial Ribosome', *Cell Metabolism*, 9(4), pp. 386–397. Available at: https://doi.org/10.1016/j.cmet.2009.03.001.

Metodiev, M.D. *et al.* (2014) 'NSUN4 Is a Dual Function Mitochondrial Protein Required for Both Methylation of 12S rRNA and Coordination of Mitoribosomal Assembly', *PLOS Genetics*, 10(2), p. e1004110. Available at: https://doi.org/10.1371/journal.pgen.1004110.

Meyers, D.E., Basha, H.I. and Koenig, M.K. (2013) 'Mitochondrial Cardiomyopathy', *Texas Heart Institute Journal*, 40(4), pp. 385–394. Available at: https://www.ncbi.nlm.nih.gov/pmc/articles/PMC3783139/ (Accessed: 24 June 2022).

Migunova, E. *et al.* (2021) 'ELAC2/RNaseZ-linked cardiac hypertrophy in Drosophila melanogaster', *Disease Models & Mechanisms*, 14(8), p. dmm048931. Available at: https://doi.org/10.1242/dmm.048931.

Mili, S. *et al.* (2001) 'Distinct RNP complexes of shuttling hnRNP proteins with pre-mRNA and mRNA: candidate intermediates in formation and export of mRNA', *Molecular and Cellular Biology*, 21(21), pp. 7307–7319. Available at: https://doi.org/10.1128/MCB.21.21.7307-7319.2001.

Mili, S. and Piñol-Roma, S. (2003) 'LRP130, a Pentatricopeptide Motif Protein with a Noncanonical RNA-Binding Domain, Is Bound In Vivo to Mitochondrial and Nuclear RNAs', *Molecular and Cellular Biology*, 23(14), pp. 4972–4982. Available at: https://doi.org/10.1128/MCB.23.14.4972-4982.2003.

Miyata, T. *et al.* (2010) 'Migration, early axonogenesis, and Reelin-dependent layer-forming behavior of early/posterior-born Purkinje cells in the developing mouse lateral cerebellum', *Neural Development*, 5(1), p. 23. Available at: https://doi.org/10.1186/1749-8104-5-23.

Mootha, V.K. *et al.* (2003) 'Identification of a gene causing human cytochrome c oxidase deficiency by integrative genomics', *Proceedings of the National Academy of Sciences of the United States of America*, 100(2), pp. 605–610. Available at: https://doi.org/10.1073/pnas.242716699.

Morin, C. *et al.* (1993) 'Clinical, metabolic, and genetic aspects of cytochrome C oxidase deficiency in Saguenay-Lac-Saint-Jean.', *American Journal of Human Genetics*, 53(2), pp. 488–496. Available at: https://www.ncbi.nlm.nih.gov/pmc/articles/PMC1682365/ (Accessed: 23 October 2020).

Moslemi, A.-R. *et al.* (2008) 'Progressive encephalopathy and complex I deficiency associated with mutations in MTND1', *Neuropediatrics*, 39(1), pp. 24–28. Available at: https://doi.org/10.1055/s-2008-1076739.

Mottis, A., Jovaisaite, V. and Auwerx, J. (2014) 'The mitochondrial unfolded protein response in mammalian physiology', *Mammalian Genome: Official Journal of the International Mammalian Genome Society*, 25(9–10), pp. 424–433. Available at: https://doi.org/10.1007/s00335-014-9525-z.

Munnich, A. *et al.* (1996) 'Clinical presentation of mitochondrial disorders in childhood', *Journal of Inherited Metabolic Disease*, 19(4), pp. 521–527. Available at: https://doi.org/10.1007/BF01799112.

Munnich, A. and Rustin, P. (2001) ‘Clinical spectrum and diagnosis of mitochondrial disorders’, *American Journal of Medical Genetics*, 106(1), pp. 4–17. Available at: https://doi.org/10.1002/ajmg.1391.

Nagaike, T. *et al.* (2005) ‘Human mitochondrial mRNAs are stabilized with polyadenylation regulated by mitochondria-specific poly(A) polymerase and polynucleotide phosphorylase’, *The Journal of Biological Chemistry*, 280(20), pp. 19721–19727. Available at: https://doi.org/10.1074/jbc.M500804200.

Narendra, D. *et al.* (2009) ‘Parkin-induced mitophagy in the pathogenesis of Parkinson disease’, *Autophagy*, 5(5), pp. 706–708. Available at: https://doi.org/10.4161/auto.5.5.8505.

Nashimoto, M. *et al.* (1998) ‘RNA heptamers that direct RNA cleavage by mammalian tRNA 3’ processing endoribonuclease.’, *Nucleic Acids Research*, 26(11), pp. 2565–2572. Available at: https://www.ncbi.nlm.nih.gov/pmc/articles/PMC147582/ (Accessed: 27 July 2022).

Nestler, E.J. (2005) ‘Is there a common molecular pathway for addiction?’, *Nature Neuroscience*, 8(11), pp. 1445–1449. Available at: https://doi.org/10.1038/nn1578.

Neupert, W. and Herrmann, J.M. (2007) ‘Translocation of proteins into mitochondria’, *Annual Review of Biochemistry*, 76, pp. 723–749. Available at: https://doi.org/10.1146/annurev.biochem.76.052705.163409.

Nevue, A.A. *et al.* (2016) ‘Dopaminergic Input to the Inferior Colliculus in Mice’, *Frontiers in Neuroanatomy*, 9, p. 168. Available at: https://doi.org/10.3389/fnana.2015.00168.

Newmeyer, D.D. and Ferguson-Miller, S. (2003) ‘Mitochondria: releasing power for life and unleashing the machineries of death’, *Cell*, 112(4), pp. 481–490. Available at: https://doi.org/10.1016/s0092-8674(03)00116-8.

Ngo, H.B., Kaiser, J.T. and Chan, D.C. (2011) ‘Tfam, a mitochondrial transcription and packaging factor, imposes a U-turn on mitochondrial DNA’, *Nature structural & molecular biology*, 18(11), pp. 1290–1296. Available at: https://doi.org/10.1038/nsmb.2159.

Novikova, L. *et al.* (2006) ‘Early signs of neuronal apoptosis in the substantia nigra pars compacta of the progressive neurodegenerative mouse 1-methyl-4-phenyl-1,2,3,6-tetrahydropyridine/probenecid model of Parkinson’s disease’, *Neuroscience*, 140(1), pp. 67–76. Available at: https://doi.org/10.1016/j.neuroscience.2006.02.007.

Nunnari, J. and Suomalainen, A. (2012) ‘Mitochondria: In Sickness and in Health’, *Cell*, 148(6), pp. 1145–1159. Available at: https://doi.org/10.1016/j.cell.2012.02.035.

Ogawa, E. *et al.* (2017) ‘Clinical validity of biochemical and molecular analysis in diagnosing Leigh syndrome: a study of 106 Japanese patients’, *Journal of Inherited Metabolic Disease*, 40(5), pp. 685–693. Available at: https://doi.org/10.1007/s10545-017-0042-6.

Ojala, D., Montoya, J. and Attardi, G. (1981) ‘tRNA punctuation model of RNA processing in human mitochondria’, *Nature*, 290(5806), pp. 470–474. Available at: https://doi.org/10.1038/290470a0.

Oláhová, M. *et al.* (2015) 'LRPPRC mutations cause early-onset multisystem mitochondrial disease outside of the French-Canadian population', *Brain: A Journal of Neurology*, 138(Pt 12), pp. 3503–3519. Available at: https://doi.org/10.1093/brain/awv291.

Opalińska, M. and Jańska, H. (2018) 'AAA Proteases: Guardians of Mitochondrial Function and Homeostasis', *Cells*, 7(10), p. 163. Available at: https://doi.org/10.3390/cells7100163.

Oquendo, C.E. *et al.* (2004) 'Functional and genetic studies demonstrate that mutation in the COX15 gene can cause Leigh syndrome', *Journal of Medical Genetics*, 41(7), pp. 540–544. Available at: https://doi.org/10.1136/jmg.2003.017426.

Ostergaard, E. *et al.* (2007) 'Mitochondrial encephalomyopathy with elevated methylmalonic acid is caused by SUCLA2 mutations', *Brain*, 130(3), pp. 853–861. Available at: https://doi.org/10.1093/brain/awl383.

Ostergaard, E. *et al.* (2011) 'Respiratory chain complex I deficiency due to NDUFA12 mutations as a new cause of Leigh syndrome', *Journal of Medical Genetics*, 48(11), pp. 737–740. Available at: https://doi.org/10.1136/jmg.2011.088856.

Otera, H., Ishihara, N. and Mihara, K. (2013) 'New insights into the function and regulation of mitochondrial fission', *Biochimica Et Biophysica Acta*, 1833(5), pp. 1256–1268. Available at: https://doi.org/10.1016/j.bbamcr.2013.02.002.

Papadopoulou, L.C. *et al.* (1999) 'Fatal infantile cardioencephalomyopathy with COX deficiency and mutations in SCO2, a COX assembly gene', *Nature Genetics*, 23(3), pp. 333–337. Available at: https://doi.org/10.1038/15513.

Patterson, A.J. and Zhang, L. (2010) 'Hypoxia and Fetal Heart Development', *Current molecular medicine*, 10(7), pp. 653–666. Available at: https://www.ncbi.nlm.nih.gov/pmc/articles/PMC3075953/ (Accessed: 26 June 2022).

Paucar, M. *et al.* (2018) 'Chorea, psychosis, acanthocytosis, and prolonged survival associated with ELAC2 mutations', *Neurology*, 91(15), pp. 710–712. Available at: https://doi.org/10.1212/WNL.0000000000006320.

Pavlakis, S.G. *et al.* (1984) 'Mitochondrial myopathy, encephalopathy, lactic acidosis, and strokelike episodes: A distinctive clinical syndrome', *Annals of Neurology*, 16(4), pp. 481–488. Available at: https://doi.org/10.1002/ana.410160409.

Pebay-Peyroula, E. *et al.* (2003) 'Structure of mitochondrial ADP/ATP carrier in complex with carboxyatractyloside', *Nature*, 426(6962), pp. 39–44. Available at: https://doi.org/10.1038/nature02056.

Pflug, C. *et al.* (2020) 'Impact of simultaneous subthalamic and nigral stimulation on dysphagia in Parkinson's disease', *Annals of Clinical and Translational Neurology*, 7(5), pp. 628–638. Available at: https://doi.org/10.1002/acn3.51027.

Piro, E. *et al.* (2020) 'Novel LRPPRC compound heterozygous mutation in a child with early-onset Leigh syndrome French-Canadian type: case report of an Italian patient', *Italian Journal of Pediatrics*, 46(1), p. 140. Available at: https://doi.org/10.1186/s13052-020-00903-7.

Pitceathly, R.D.S. *et al.* (2013) 'NDUFA4 mutations underlie dysfunction of a cytochrome c oxidase subunit linked to human neurological disease', *Cell Reports*, 3(6), pp. 1795–1805. Available at: https://doi.org/10.1016/j.celrep.2013.05.005.

Poulin, J.-F. *et al.* (2014) 'Defining midbrain dopaminergic neuron diversity by single-cell gene profiling', *Cell reports*, 9(3), pp. 930–943. Available at: https://doi.org/10.1016/j.celrep.2014.10.008.

Poulin, J.-F. *et al.* (2020) 'Classification of Midbrain Dopamine Neurons Using Single-Cell Gene Expression Profiling Approaches', *Trends in Neurosciences*, 43(3), pp. 155–169. Available at: https://doi.org/10.1016/j.tins.2020.01.004.

Quintana, A. *et al.* (2010) 'Complex I deficiency due to loss of Ndufs4 in the brain results in progressive encephalopathy resembling Leigh syndrome', *Proceedings of the National Academy of Sciences of the United States of America*, 107(24), pp. 10996–11001. Available at: https://doi.org/10.1073/pnas.1006214107.

Quintana, A. *et al.* (2012) 'Fatal breathing dysfunction in a mouse model of Leigh syndrome', *The Journal of Clinical Investigation*, 122(7), pp. 2359–2368. Available at: https://doi.org/10.1172/JCI62923.

Quintana, E. *et al.* (2009) 'PDH E1β deficiency with novel mutations in two patients with Leigh syndrome', *Journal of Inherited Metabolic Disease*, 32 Suppl 1, pp. S339-343. Available at: https://doi.org/10.1007/s10545-009-1343-1.

Quirós, P.M., Langer, T. and López-Otín, C. (2015) 'New roles for mitochondrial proteases in health, ageing and disease', *Nature Reviews Molecular Cell Biology*, 16(6), pp. 345–359. Available at: https://doi.org/10.1038/nrm3984.

Rambold, A.S. *et al.* (2011) 'Tubular network formation protects mitochondria from autophagosomal degradation during nutrient starvation', *Proceedings of the National Academy of Sciences*, 108(25), pp. 10190–10195. Available at: https://doi.org/10.1073/pnas.1107402108.

Randow, F. and Youle, R.J. (2014) 'Self and nonself: how autophagy targets mitochondria and bacteria', *Cell Host & Microbe*, 15(4), pp. 403–411. Available at: https://doi.org/10.1016/j.chom.2014.03.012.

Rantamäki, M.T. *et al.* (2005) 'Adult-onset ataxia and polyneuropathy caused by mitochondrial 8993T→C mutation', *Annals of Neurology*, 58(2), pp. 337–340. Available at: https://doi.org/10.1002/ana.20555.

Rath, S. *et al.* (2020) 'MitoCarta3.0: an updated mitochondrial proteome now with sub-organelle localization and pathway annotations', *Nucleic Acids Research*, 49(D1), pp. D1541–D1547. Available at: https://doi.org/10.1093/nar/gkaa1011.

Rebbeck, T.R. *et al.* (2000) 'Association of HPC2/ELAC2 Genotypes and Prostate Cancer', *The American Journal of Human Genetics*, 67(4), pp. 1014–1019. Available at: https://doi.org/10.1086/303096.

Ricke, K.M. *et al.* (2020) 'Mitochondrial Dysfunction Combined with High Calcium Load Leads to Impaired Antioxidant Defense Underlying the Selective Loss of Nigral

Dopaminergic Neurons', *The Journal of Neuroscience*, 40(9), pp. 1975–1986. Available at: https://doi.org/10.1523/JNEUROSCI.1345-19.2019.

Ritterhoff, J. and Tian, R. (2017) 'Metabolism in cardiomyopathy: every substrate matters', *Cardiovascular Research*, 113(4), pp. 411–421. Available at: https://doi.org/10.1093/cvr/cvx017.

Rizzuto, R., Duchen, M.R. and Pozzan, T. (2004) 'Flirting in little space: the ER/mitochondria Ca2+ liaison', *Science's STKE: signal transduction knowledge environment*, 2004(215), p. re1. Available at: https://doi.org/10.1126/stke.2152004re1.

Rodenburg, R.J.T. (2011) 'Biochemical diagnosis of mitochondrial disorders', *Journal of Inherited Metabolic Disease*, 34(2), pp. 283–292. Available at: https://doi.org/10.1007/s10545-010-9081-y.

Ross, J.M. (2011) 'Visualization of Mitochondrial Respiratory Function using Cytochrome C Oxidase / Succinate Dehydrogenase (COX/SDH) Double-labeling Histochemistry', *Journal of Visualized Experiments : JoVE*, (57), p. 3266. Available at: https://doi.org/10.3791/3266.

Rossi, M.A. *et al.* (2016) 'A GABAergic nigrotectal pathway for coordination of drinking behavior', *Nature Neuroscience*, 19(5), pp. 742–748. Available at: https://doi.org/10.1038/nn.4285.

Rossmanith, W. (2011) 'Localization of Human RNase Z Isoforms: Dual Nuclear/Mitochondrial Targeting of the ELAC2 Gene Product by Alternative Translation Initiation', *PLOS ONE*, 6(4), p. e19152. Available at: https://doi.org/10.1371/journal.pone.0019152.

Rötig, A. *et al.* (1990) 'Pearson's marrow-pancreas syndrome. A multisystem mitochondrial disorder in infancy', *The Journal of Clinical Investigation*, 86(5), pp. 1601–1608. Available at: https://doi.org/10.1172/JCI114881.

Rouzier, C. *et al.* (2019) 'NDUFS6 related Leigh syndrome: a case report and review of the literature', *Journal of Human Genetics*, 64(7), pp. 637–645. Available at: https://doi.org/10.1038/s10038-019-0594-4.

Ruhoy, I.S. and Saneto, R.P. (2014) 'The genetics of Leigh syndrome and its implications for clinical practice and risk management', *The Application of Clinical Genetics*, 7, pp. 221–234. Available at: https://doi.org/10.2147/TACG.S46176.

Ruigrok, T.J. (1997) 'Cerebellar nuclei: the olivary connection', *Progress in Brain Research*, 114, pp. 167–192. Available at: https://doi.org/10.1016/s0079-6123(08)63364-6.

Rustin, P. *et al.* (1994) 'Biochemical and molecular investigations in respiratory chain deficiencies', *Clinica Chimica Acta; International Journal of Clinical Chemistry*, 228(1), pp. 35–51. Available at: https://doi.org/10.1016/0009-8981(94)90055-8.

Ruzzenente, B. *et al.* (2012) 'LRPPRC is necessary for polyadenylation and coordination of translation of mitochondrial mRNAs', *The EMBO Journal*, 31(2), pp. 443–456. Available at: https://doi.org/10.1038/emboj.2011.392.

Ruzzenente, B. *et al.* (2018) 'Inhibition of mitochondrial translation in fibroblasts from a patient expressing the KARS p.(Pro228Leu) variant and presenting with sensorineural deafness, developmental delay, and lactic acidosis', *Human Mutation*, 39(12), pp. 2047–2059. Available at: https://doi.org/10.1002/humu.23657.

Sagan, L. (1967) 'On the origin of mitosing cells', *Journal of Theoretical Biology*, 14(3), pp. 255–274. Available at: https://doi.org/10.1016/0022-5193(67)90079-3.

Sala-Coromina, J. *et al.* (2021) 'Leigh syndrome associated with TRMU gene mutations', *Molecular Genetics and Metabolism Reports*, 26, p. 100690. Available at: https://doi.org/10.1016/j.ymgmr.2020.100690.

Santorelli, F.M. *et al.* (1997) 'Maternally inherited encephalopathy associated with a single-base insertion in the mitochondrial tRNATrp gene', *Annals of Neurology*, 42(2), pp. 256–260. Available at: https://doi.org/10.1002/ana.410420220.

Saoura, M. *et al.* (2019) 'Mutations in ELAC2 associated with hypertrophic cardiomyopathy impair mitochondrial tRNA 3′-end processing', *Human Mutation*, 40(10), pp. 1731–1748. Available at: https://doi.org/10.1002/humu.23777.

Sasarman, F. *et al.* (2010) 'LRPPRC and SLIRP Interact in a Ribonucleoprotein Complex That Regulates Posttranscriptional Gene Expression in Mitochondria', *Molecular Biology of the Cell*, 21(8), pp. 1315–1323. Available at: https://doi.org/10.1091/mbc.E10-01-0047.

Sasarman, F. *et al.* (2015) 'Tissue-specific responses to the LRPPRC founder mutation in French Canadian Leigh Syndrome', *Human Molecular Genetics*, 24(2), pp. 480–491. Available at: https://doi.org/10.1093/hmg/ddu468.

Scala, M. *et al.* (2019) 'Novel homozygous TSFM pathogenic variant associated with encephalocardiomyopathy with sensorineural hearing loss and peculiar neuroradiologic findings', *Neurogenetics*, 20(3), pp. 165–172. Available at: https://doi.org/10.1007/s10048-019-00582-5.

Scalais, E. *et al.* (2012) 'Polymerase gamma deficiency (POLG): clinical course in a child with a two stage evolution from infantile myocerebrohepatopathy spectrum to an Alpers syndrome and neuropathological findings of Leigh's encephalopathy', *European journal of paediatric neurology: EJPN: official journal of the European Paediatric Neurology Society*, 16(5), pp. 542–548. Available at: https://doi.org/10.1016/j.ejpn.2012.01.013.

Schieber, M. and Chandel, N.S. (2014) 'ROS function in redox signaling and oxidative stress', *Current biology: CB*, 24(10), pp. R453-462. Available at: https://doi.org/10.1016/j.cub.2014.03.034.

Schiff, M. *et al.* (2006) 'Leigh's disease due to a new mutation in the PDHX gene', *Annals of Neurology*, 59(4), pp. 709–714. Available at: https://doi.org/10.1002/ana.20818.

Schmahmann, J.D. and Caplan, D. (2006) 'Cognition, emotion and the cerebellum', *Brain: A Journal of Neurology*, 129(Pt 2), pp. 290–292. Available at: https://doi.org/10.1093/brain/awh729.

Schmidt, O., Pfanner, N. and Meisinger, C. (2010) 'Mitochondrial protein import: from proteomics to functional mechanisms', *Nature Reviews. Molecular Cell Biology*, 11(9), pp. 655–667. Available at: https://doi.org/10.1038/nrm2959.

Schwartzentruber, J. *et al.* (2014) 'Mutation in the nuclear-encoded mitochondrial isoleucyl-tRNA synthetase IARS2 in patients with cataracts, growth hormone deficiency with short stature, partial sensorineural deafness, and peripheral neuropathy or with Leigh syndrome', *Human Mutation*, 35(11), pp. 1285–1289. Available at: https://doi.org/10.1002/humu.22629.

Schwinghammer, K. *et al.* (2013) 'Structure of human mitochondrial RNA polymerase elongation complex', *Nature structural & molecular biology*, 20(11), pp. 1298–1303. Available at: https://doi.org/10.1038/nsmb.2683.

Semeraro, M. *et al.* (2018) 'The urinary organic acids profile in single large-scale mitochondrial DNA deletion disorders', *Clinica Chimica Acta; International Journal of Clinical Chemistry*, 481, pp. 156–160. Available at: https://doi.org/10.1016/j.cca.2018.03.002.

Shandley, S. *et al.* (2021) 'Abnormal Nutritive Sucking as an Indicator of Neonatal Brain Injury', *Frontiers in Pediatrics*, 8. Available at: https://www.frontiersin.org/article/10.3389/fped.2020.599633 (Accessed: 2 July 2022).

Sharma, M.R. *et al.* (2003) 'Structure of the mammalian mitochondrial ribosome reveals an expanded functional role for its component proteins', *Cell*, 115(1), pp. 97–108. Available at: https://doi.org/10.1016/s0092-8674(03)00762-1.

Shi, Y. *et al.* (2003) 'Identification of the protein-protein contact site and interaction mode of human VDAC1 with Bcl-2 family proteins', *Biochemical and Biophysical Research Communications*, 305(4), pp. 989–996. Available at: https://doi.org/10.1016/s0006-291x(03)00871-4.

Shimizu, S., Narita, M. and Tsujimoto, Y. (1999) 'Bcl-2 family proteins regulate the release of apoptogenic cytochrome c by the mitochondrial channel VDAC', *Nature*, 399(6735), pp. 483–487. Available at: https://doi.org/10.1038/20959.

Shinwari, Z.M.A. *et al.* (2017) 'The Phenotype and Outcome of Infantile Cardiomyopathy Caused by a Homozygous ELAC2 Mutation', *Cardiology*, 137(3), pp. 188–192. Available at: https://doi.org/10.1159/000465516.

Shoubridge, E.A. (2001) 'Cytochrome c oxidase deficiency', *American Journal of Medical Genetics*, 106(1), pp. 46–52. Available at: https://doi.org/10.1002/ajmg.1378.

Shtilbans, A. *et al.* (2000) 'G8363A mutation in the mitochondrial DNA transfer ribonucleic acidLys gene: another cause of Leigh syndrome', *Journal of Child Neurology*, 15(11), pp. 759–761. Available at: https://doi.org/10.1177/088307380001501109.

de la Sierra-Gallay, I.L., Pellegrini, O. and Condon, C. (2005) 'Structural basis for substrate binding, cleavage and allostery in the tRNA maturase RNase Z', *Nature*, 433(7026), pp. 657–661. Available at: https://doi.org/10.1038/nature03284.

Siira, S.J. *et al.* (2018) 'Concerted regulation of mitochondrial and nuclear non-coding RNAs by a dual-targeted RNase Z', *EMBO Reports*, 19(10), p. e46198. Available at: https://doi.org/10.15252/embr.201846198.

Sillitoe, R.V. and Joyner, A.L. (2007) 'Morphology, molecular codes, and circuitry produce the three-dimensional complexity of the cerebellum', *Annual Review of Cell and Developmental Biology*, 23, pp. 549–577. Available at: https://doi.org/10.1146/annurev.cellbio.23.090506.123237.

Silva-Pinheiro, P. *et al.* (2021) 'DNA polymerase gamma mutations that impair holoenzyme stability cause catalytic subunit depletion', *Nucleic Acids Research*, 49(9), pp. 5230–5248. Available at: https://doi.org/10.1093/nar/gkab282.

Simon, M. *et al.* (2015) 'Mutations of human NARS2, encoding the mitochondrial asparaginyl-tRNA synthetase, cause nonsyndromic deafness and Leigh syndrome', *PLoS genetics*, 11(3), p. e1005097. Available at: https://doi.org/10.1371/journal.pgen.1005097.

Sjöstedt, E. *et al.* (2020) 'An atlas of the protein-coding genes in the human, pig, and mouse brain', *Science*, 367(6482), p. eaay5947. Available at: https://doi.org/10.1126/science.aay5947.

Smith, P.M., Fox, J.L. and Winge, D.R. (2012) 'Biogenesis of the cytochrome bc1 complex and role of assembly factors', *Biochimica et Biophysica Acta*, 1817(2), pp. 276–286. Available at: https://doi.org/10.1016/j.bbabio.2011.11.009.

Soeters, P.B. *et al.* (2021) 'The anabolic role of the Warburg, Cori-cycle and Crabtree effects in health and disease', *Clinical Nutrition*, 40(5), pp. 2988–2998. Available at: https://doi.org/10.1016/j.clnu.2021.02.012.

Sofou, K. *et al.* (2014) 'A multicenter study on Leigh syndrome: disease course and predictors of survival', *Orphanet Journal of Rare Diseases*, 9(1), p. 52. Available at: https://doi.org/10.1186/1750-1172-9-52.

Sologub, M. *et al.* (2009) 'TFB2 is a transient component of the catalytic site of the human mitochondrial RNA polymerase', *Cell*, 139(5), pp. 934–944. Available at: https://doi.org/10.1016/j.cell.2009.10.031.

Son, J.H. *et al.* (2012) 'Neuronal autophagy and neurodegenerative diseases', *Experimental & Molecular Medicine*, 44(2), pp. 89–98. Available at: https://doi.org/10.3858/emm.2012.44.2.031.

Sörensen, L. *et al.* (2001) 'Late-Onset Corticohippocampal Neurodepletion Attributable to Catastrophic Failure of Oxidative Phosphorylation in MILON Mice', *The Journal of Neuroscience*, 21(20), pp. 8082–8090. Available at: https://doi.org/10.1523/JNEUROSCI.21-20-08082.2001.

Soreze, Y. *et al.* (2013) 'Mutations in human lipoyltransferase gene LIPT1 cause a Leigh disease with secondary deficiency for pyruvate and alpha-ketoglutarate dehydrogenase', *Orphanet Journal of Rare Diseases*, 8, p. 192. Available at: https://doi.org/10.1186/1750-1172-8-192.

Sorice, M. *et al.* (2009) 'Cardiolipin-enriched raft-like microdomains are essential activating platforms for apoptotic signals on mitochondria', *FEBS Letters*, 583(15), pp. 2447–2450. Available at: https://doi.org/10.1016/j.febslet.2009.07.018.

Spassky, N. *et al.* (2008) 'Primary cilia are required for cerebellar development and Shh-dependent expansion of progenitor pool', *Developmental Biology*, 317(1), pp. 246–259. Available at: https://doi.org/10.1016/j.ydbio.2008.02.026.

Sproule, D.M. and Kaufmann, P. (2008) 'Mitochondrial encephalopathy, lactic acidosis, and strokelike episodes: basic concepts, clinical phenotype, and therapeutic management of MELAS syndrome', *Annals of the New York Academy of Sciences*, 1142, pp. 133–158. Available at: https://doi.org/10.1196/annals.1444.011.

Srivastava, S. (2017) 'The Mitochondrial Basis of Aging and Age-Related Disorders', *Genes*, 8(12), p. 398. Available at: https://doi.org/10.3390/genes8120398.

Stellingwerff, M.D. *et al.* (2021) 'LBSL: Case Series and DARS2 Variant Analysis in Early Severe Forms With Unexpected Presentations', *Neurology. Genetics*, 7(2), p. e559. Available at: https://doi.org/10.1212/NXG.0000000000000559.

Stenton, S.L. and Prokisch, H. (2020) 'Genetics of mitochondrial diseases: Identifying mutations to help diagnosis', *EBioMedicine*, 56. Available at: https://doi.org/10.1016/j.ebiom.2020.102784.

Stewart, J.B. and Chinnery, P.F. (2021) 'Extreme heterogeneity of human mitochondrial DNA from organelles to populations', *Nature Reviews. Genetics*, 22(2), pp. 106–118. Available at: https://doi.org/10.1038/s41576-020-00284-x.

Stuart, R. (2002) 'Insertion of proteins into the inner membrane of mitochondria: the role of the Oxa1 complex', *Biochimica Et Biophysica Acta*, 1592(1), pp. 79–87. Available at: https://doi.org/10.1016/s0167-4889(02)00266-5.

Sudarov, A. and Joyner, A.L. (2007) 'Cerebellum morphogenesis: the foliation pattern is orchestrated by multi-cellular anchoring centers', *Neural Development*, 2, p. 26. Available at: https://doi.org/10.1186/1749-8104-2-26.

Sun, F. *et al.* (2005) 'Crystal Structure of Mitochondrial Respiratory Membrane Protein Complex II', *Cell*, 121(7), pp. 1043–1057. Available at: https://doi.org/10.1016/j.cell.2005.05.025.

Sun, Y. *et al.* (2012) 'Voltage-dependent anion channels (VDACs) recruit Parkin to defective mitochondria to promote mitochondrial autophagy', *The Journal of Biological Chemistry*, 287(48), pp. 40652–40660. Available at: https://doi.org/10.1074/jbc.M112.419721.

Surmeier, D.J., Obeso, J.A. and Halliday, G.M. (2017) 'Selective neuronal vulnerability in Parkinson disease', *Nature reviews. Neuroscience*, 18(2), pp. 101–113. Available at: https://doi.org/10.1038/nrn.2016.178.

Suzuki, Takeo and Suzuki, Tsutomu (2014) 'A complete landscape of post-transcriptional modifications in mammalian mitochondrial tRNAs', *Nucleic Acids Research*, 42(11), pp. 7346–7357. Available at: https://doi.org/10.1093/nar/gku390.

Szabadkai, G. *et al.* (2006) 'Mitochondrial dynamics and Ca2+ signaling', *Biochimica Et Biophysica Acta*, 1763(5–6), pp. 442–449. Available at: https://doi.org/10.1016/j.bbamcr.2006.04.002.

Takaku, H. *et al.* (2003) 'A candidate prostate cancer susceptibility gene encodes tRNA 3' processing endoribonuclease', *Nucleic Acids Research*, 31(9), pp. 2272–2278. Available at: https://doi.org/10.1093/nar/gkg337.

Tatsuta, T., Model, K. and Langer, T. (2005) 'Formation of Membrane-bound Ring Complexes by Prohibitins in Mitochondria', *Molecular Biology of the Cell*, 16(1), pp. 248–259. Available at: https://doi.org/10.1091/mbc.E04-09-0807.

Tatuch, Y. *et al.* (1992) 'Heteroplasmic mtDNA mutation (T----G) at 8993 can cause Leigh disease when the percentage of abnormal mtDNA is high', *American Journal of Human Genetics*, 50(4), pp. 852–858.

Tavtigian, S.V. *et al.* (2001) 'A candidate prostate cancer susceptibility gene at chromosome 17p', *Nature Genetics*, 27(2), pp. 172–180. Available at: https://doi.org/10.1038/84808.

Taylor, R.W. *et al.* (2001) 'Progressive mitochondrial disease resulting from a novel missense mutation in the mitochondrial DNA ND3 gene', *Annals of Neurology*, 50(1), pp. 104–107. Available at: https://doi.org/10.1002/ana.1084.

Taylor, R.W. *et al.* (2002) 'Leigh disease associated with a novel mitochondrial DNA ND5 mutation', *European journal of human genetics: EJHG*, 10(2), pp. 141–144. Available at: https://doi.org/10.1038/sj.ejhg.5200773.

Taylor, R.W. and Turnbull, D.M. (2005) 'MITOCHONDRIAL DNA MUTATIONS IN HUMAN DISEASE', *Nature reviews. Genetics*, 6(5), pp. 389–402. Available at: https://doi.org/10.1038/nrg1606.

Temperley, R.J. *et al.* (2010) 'Human mitochondrial mRNAs—like members of all families, similar but different', *Biochimica et Biophysica Acta (BBA) - Bioenergetics*, 1797(6), pp. 1081–1085. Available at: https://doi.org/10.1016/j.bbabio.2010.02.036.

Thorburn, D.R., Rahman, J. and Rahman, S. (1993) 'Mitochondrial DNA-Associated Leigh Syndrome and NARP', in M.P. Adam et al. (eds) *GeneReviews*®. Seattle (WA): University of Washington, Seattle. Available at: http://www.ncbi.nlm.nih.gov/books/NBK1173/ (Accessed: 2 March 2022).

Tian, T. *et al.* (2012) 'Role of leucine-rich pentatricopeptide repeat motif-containing protein (LRPPRC) for anti-apoptosis and tumourigenesis in cancers', *European Journal of Cancer*, 48(15), pp. 2462–2473. Available at: https://doi.org/10.1016/j.ejca.2012.01.018.

Tilokani, L. *et al.* (2018) 'Mitochondrial dynamics: overview of molecular mechanisms', *Essays in Biochemistry*, 62(3), pp. 341–360. Available at: https://doi.org/10.1042/EBC20170104.

Tiranti, V. *et al.* (1998) 'Mutations of SURF-1 in Leigh disease associated with cytochrome c oxidase deficiency', *American Journal of Human Genetics*, 63(6), pp. 1609–1621. Available at: https://doi.org/10.1086/302150.

Tiranti, V. *et al.* (2000) 'A novel frameshift mutation of the mtDNA COIII gene leads to impaired assembly of cytochrome c oxidase in a patient affected by Leigh-like syndrome', *Human Molecular Genetics*, 9(18), pp. 2733–2742. Available at: https://doi.org/10.1093/hmg/9.18.2733.

Titomanlio, L., Romano, A. and Del Giudice, E. (2005) 'Cerebellar agenesis', *Neurology*, 64(6), p. E21. Available at: https://doi.org/10.1212/wnl.64.6.e21.

Tomecki, R. *et al.* (2004) 'Identification of a novel human nuclear-encoded mitochondrial poly(A) polymerase', *Nucleic Acids Research*, 32(20), pp. 6001–6014. Available at: https://doi.org/10.1093/nar/gkh923.

Touati, G. *et al.* (1997) 'In vivo functional investigations of lactic acid in patients with respiratory chain disorders', *Archives of Disease in Childhood*, 76(1), pp. 16–21. Available at: https://doi.org/10.1136/adc.76.1.16.

Triepels, R.H. *et al.* (1999) 'Leigh syndrome associated with a mutation in the NDUFS7 (PSST) nuclear encoded subunit of complex I', *Annals of Neurology*, 45(6), pp. 787–790. Available at: https://doi.org/10.1002/1531-8249(199906)45:6<787::AID-ANA13>3.0.CO;2-6.

Trifunovic, A. *et al.* (2004) 'Premature ageing in mice expressing defective mitochondrial DNA polymerase', *Nature*, 429(6990), pp. 417–423. Available at: https://doi.org/10.1038/nature02517.

Tsuchiya, N. *et al.* (2002) 'LRP130, a protein containing nine pentatricopeptide repeat motifs, interacts with a single-stranded cytosine-rich sequence of mouse hypervariable minisatellite Pc-1', *European Journal of Biochemistry*, 269(12), pp. 2927–2933. Available at: https://doi.org/10.1046/j.1432-1033.2002.02966.x.

Tucker, E.J. *et al.* (2011) 'Mutations in MTFMT underlie a human disorder of formylation causing impaired mitochondrial translation', *Cell Metabolism*, 14(3), pp. 428–434. Available at: https://doi.org/10.1016/j.cmet.2011.07.010.

Tuppen, H.A.L. *et al.* (2010) 'Mitochondrial DNA mutations and human disease', *Biochimica Et Biophysica Acta*, 1797(2), pp. 113–128. Available at: https://doi.org/10.1016/j.bbabio.2009.09.005.

Ugalde, C. *et al.* (2007) 'Mutated ND2 impairs mitochondrial complex I assembly and leads to Leigh syndrome', *Molecular Genetics and Metabolism*, 90(1), pp. 10–14. Available at: https://doi.org/10.1016/j.ymgme.2006.08.003.

Uusisaari, M., Obata, K. and Knöpfel, T. (2007) 'Morphological and electrophysiological properties of GABAergic and non-GABAergic cells in the deep cerebellar nuclei', *Journal of Neurophysiology*, 97(1), pp. 901–911. Available at: https://doi.org/10.1152/jn.00974.2006.

Uusisaari, M.Y. and Knöpfel, T. (2012) 'Diversity of neuronal elements and circuitry in the cerebellar nuclei', *Cerebellum (London, England)*, 11(2), pp. 420–421. Available at: https://doi.org/10.1007/s12311-011-0350-6.

Uziel, G. *et al.* (1997) 'Mitochondrial disease associated with the T8993G mutation of the mitochondrial ATPase 6 gene: a clinical, biochemical, and molecular study in six families',

Journal of Neurology, Neurosurgery, and Psychiatry, 63(1), pp. 16–22. Available at: https://www.ncbi.nlm.nih.gov/pmc/articles/PMC2169628/ (Accessed: 2 March 2022).

Valnot, I. *et al.* (2000) 'A mutation in the human heme A:farnesyltransferase gene (COX10) causes cytochrome c oxidase deficiency', *Human Molecular Genetics*, 9(8), pp. 1245–1249. Available at: https://doi.org/10.1093/hmg/9.8.1245.

Van Goethem, G. *et al.* (2001) 'Mutation of POLG is associated with progressive external ophthalmoplegia characterized by mtDNA deletions', *Nature Genetics*, 28(3), pp. 211–212. Available at: https://doi.org/10.1038/90034.

Van Hove, J.L.K. *et al.* (2010) 'Succinyl-CoA ligase deficiency: a mitochondrial hepatoencephalomyopathy', *Pediatric research*, 68(2), pp. 159–164. Available at: https://doi.org/10.1203/PDR.0b013e3181e5c3a4.

Velez-Bartolomei, F., Lee, C. and Enns, G. (1993) 'MERRF', in M.P. Adam et al. (eds) *GeneReviews*®. Seattle (WA): University of Washington, Seattle. Available at: http://www.ncbi.nlm.nih.gov/books/NBK1520/ (Accessed: 4 March 2022).

Vento, J.M. and Pappa, B. (2013) 'Genetic Counseling in Mitochondrial Disease', *Neurotherapeutics*, 10(2), pp. 243–250. Available at: https://doi.org/10.1007/s13311-012-0173-2.

Verkhratsky, A. and Nedergaard, M. (2018) 'Physiology of Astroglia', *Physiological Reviews*, 98(1), pp. 239–389. Available at: https://doi.org/10.1152/physrev.00042.2016.

Vermulst, M. *et al.* (2008) 'DNA deletions and clonal mutations drive premature aging in mitochondrial mutator mice', *NATURE GENETICS*, 40(4), p. 3.

Vilarinho, L. *et al.* (1997) 'Heterogeneous presentation in Leigh syndrome', *Journal of Inherited Metabolic Disease*, 20(5), pp. 704–705. Available at: https://doi.org/10.1023/a:1005330611147.

Viscomi, C. (2016) 'Toward a therapy for mitochondrial disease', *Biochemical Society Transactions*, 44(5), pp. 1483–1490. Available at: https://doi.org/10.1042/BST20160085.

Vogel, A. *et al.* (2002) 'ElaC Encodes a Novel Binuclear Zinc Phosphodiesterase*', *Journal of Biological Chemistry*, 277(32), pp. 29078–29085. Available at: https://doi.org/10.1074/jbc.M112047200.

Voogd, J. and Glickstein, M. (1998) 'The anatomy of the cerebellum', *Trends in Neurosciences*, 21(9), pp. 370–375. Available at: https://doi.org/10.1016/s0166-2236(98)01318-6.

Weraarpachai, W. *et al.* (2009) 'Mutation in TACO1, encoding a translational activator of COX I, results in cytochrome c oxidase deficiency and late-onset Leigh syndrome', *Nature Genetics*, 41(7), pp. 833–837. Available at: https://doi.org/10.1038/ng.390.

Willems, J.L. *et al.* (1977) 'Leigh's encephalomyelopathy in a patient with cytochrome c oxidase deficiency in muscle tissue', *Pediatrics*, 60(6), pp. 850–857.

Wimplinger, I. *et al.* (2006) 'Mutations of the mitochondrial holocytochrome c-type synthase in X-linked dominant microphthalmia with linear skin defects syndrome', *American Journal of Human Genetics*, 79(5), pp. 878–889. Available at: https://doi.org/10.1086/508474.

Wong, L.-J.C. (2007) 'Pathogenic mitochondrial DNA mutations in protein-coding genes', *Muscle & Nerve*, 36(3), pp. 279–293. Available at: https://doi.org/10.1002/mus.20807.

Wurst, W., Auerbach, A.B. and Joyner, A.L. (1994) 'Multiple developmental defects in Engrailed-1 mutant mice: an early mid-hindbrain deletion and patterning defects in forelimbs and sternum', *Development*, 120(7), pp. 2065–2075. Available at: https://doi.org/10.1242/dev.120.7.2065.

Xu, B. *et al.* (2010) 'ELAC2 polymorphisms and prostate cancer risk: a meta-analysis based on 18 case–control studies', *Prostate Cancer and Prostatic Diseases*, 13(3), pp. 270–277. Available at: https://doi.org/10.1038/pcan.2010.6.

Xu, F. *et al.* (2004) 'The role of the LRPPRC (leucine-rich pentatricopeptide repeat cassette) gene in cytochrome oxidase assembly: mutation causes lowered levels of COX (cytochrome c oxidase) I and COX III mRNA', *The Biochemical Journal*, 382(Pt 1), pp. 331–336. Available at: https://doi.org/10.1042/BJ20040469.

Xu, F. *et al.* (2008) 'Disruption of a mitochondrial RNA-binding protein gene results in decreased cytochrome b expression and a marked reduction in ubiquinol–cytochrome c reductase activity in mouse heart mitochondria', *Biochemical Journal*, 416(1), pp. 15–26. Available at: https://doi.org/10.1042/BJ20080847.

Xu, F. *et al.* (2012) 'LRPPRC mutation suppresses cytochrome oxidase activity by altering mitochondrial RNA transcript stability in a mouse model', *Biochemical Journal*, 441(1), pp. 275–283. Available at: https://doi.org/10.1042/BJ20110985.

Yakubovskaya, E. *et al.* (2014) 'Organization of the human mitochondrial transcription initiation complex', *Nucleic Acids Research*, 42(6), pp. 4100–4112. Available at: https://doi.org/10.1093/nar/gkt1360.

Ylikallio, E. and Suomalainen, A. (2012) 'Mechanisms of mitochondrial diseases', *Annals of Medicine*, 44(1), pp. 41–59. Available at: https://doi.org/10.3109/07853890.2011.598547.

Young, R.A. and Davis, R.W. (1983) 'Efficient isolation of genes by using antibody probes.', *Proceedings of the National Academy of Sciences of the United States of America*, 80(5), pp. 1194–1198. Available at: https://www.ncbi.nlm.nih.gov/pmc/articles/PMC393560/ (Accessed: 26 July 2022).

Yu, F. *et al.* (2015) 'A new case of complete primary cerebellar agenesis: clinical and imaging findings in a living patient', *Brain*, 138(6), p. e353. Available at: https://doi.org/10.1093/brain/awu239.

Yu-Wai-Man, P. and Chinnery, P.F. (1993) 'Leber Hereditary Optic Neuropathy', in M.P. Adam et al. (eds) *GeneReviews*®. Seattle (WA): University of Washington, Seattle. Available at: http://www.ncbi.nlm.nih.gov/books/NBK1174/ (Accessed: 27 February 2022).

Zhang, H. *et al.* (2001) 'Human mitochondrial topoisomerase I', *Proceedings of the National Academy of Sciences of the United States of America*, 98(19), pp. 10608–10613. Available at: https://doi.org/10.1073/pnas.191321998.

Zhao, Q. *et al.* (2002) 'A mitochondrial specific stress response in mammalian cells', *The EMBO journal*, 21(17), pp. 4411–4419. Available at: https://doi.org/10.1093/emboj/cdf445.

Zhu, Z. *et al.* (1998) 'SURF1, encoding a factor involved in the biogenesis of cytochrome c oxidase, is mutated in Leigh syndrome', *Nature Genetics*, 20(4), pp. 337–343. Available at: https://doi.org/10.1038/3804.

Zou, J. *et al.* (2014) 'Autophagy Inhibitor LRPPRC Suppresses Mitophagy through Interaction with Mitophagy Initiator Parkin', *PLoS ONE*. Edited by C. Yan, 9(4), p. e94903. Available at: https://doi.org/10.1371/journal.pone.0094903.

Résumé en français

Défauts du métabolisme des ARN mitochondriaux dans le développement des maladies mitochondriales

Les maladies mitochondriales sont des maladies cliniquement et génétiquement hétérogènes présentant des défauts dans la phosphorylation oxydative (OXPHOS) et la production d'ATP. Les maladies mitochondriales touchent 1 naissance sur 5000 et sont souvent associées à un pronostic défavorable chez les enfants. Elles peuvent survenir dans l'enfance ou à l'âge adulte et des mutations dans de nombreux gènes peuvent provoquer des maladies mitochondriales avec une implication similaire ou très différente selon les tissus. Généralement, le dysfonctionnement mitochondrial affecte les tissus à forte demande énergétique tels que le cerveau, les muscles squelettiques et le cœur, provoquant diverses maladies neurologiques, des myopathies et des cardiomyopathies; des cas d'insuffisance hépatique, de néphropathies et même d'affections cutanées ont également été signalés. À ce jour, des mutations dans 338 gènes nucléaires et mitochondriaux ont été associées à des maladies mitochondriales, qui sont malheureusement incurables.

L'une des présentations cliniques les plus courantes des maladies mitochondriales chez les patients pédiatriques est le syndrome de Leigh. Le syndrome de Leigh est une maladie neurologique progressive dont l'incidence est de 1 sur 40 000. La neuro-imagerie révèle des lésions caractéristiques dans les noyaux gris centraux et le tronc cérébral, mais aussi dans le cervelet, le thalamus, la substance blanche et la moelle épinière. Elle se caractérise par une perte progressive des capacités mentales et motrices et conduit à la mort dans la petite enfance, en raison d'une insuffisance respiratoire. Des mutations dans plus de 75 gènes, nucléaires ou mitochondriaux, entraînant notamment des défauts dans le système OXPHOS et la production d'ATP, ont été associées au syndrome de Leigh.

La neurodégénérescence désigne une atteinte sévère dans laquelle les neurones de régions spécifiques sont affectés et meurent, altérant progressivement les fonctions cognitives et motrices du cerveau. Les mitochondries sont impliquées dans la mort des neurones au cours de la mort cellulaire programmée. Les neurones dépendant de l'OXPHOS, en cas de déficience de celle-ci, ces dernières n'ont pas la capacité de réguler leur approvisionnement énergétique et deviennent donc très vulnérables.

Une autre affection fréquente liée aux maladies mitochondriales concerne les cardiomyopathies mitochondriales qui se caractérisent par des défauts typiques de la structure et de la fonction cardiaques, tels que la cardiomyopathie hypertrophique, les arythmies et l'insuffisance cardiaque. La présentation de la maladie peut être légère à sévère (insuffisance cardiaque et arythmies), entraînant un pronostic défavorable chez les enfants affectés, de façon concomitante à une crise métabolique. Le phénotype cellulaire de la cardiomyopathie mitochondriale décrit notamment de grands myocytes fusiformes présentant des mitochondries plus volumineuses.

L'absence de remède(s) contre les maladies mitochondriales est, en partie, le résultat de notre mauvaise compréhension de ses mécanismes pathologiques, et de l'absence de modèles animaux appropriés récapitulant la complexité de la maladie. Ce projet de thèse s'est concentré sur deux gènes responsables de maladies mitochondriales, *LRPPRC* et *ELAC2*, qui codent pour des protéines impliquées dans le métabolisme de l'ARN mitochondrial.

Le gène *LRPRPC*, Leucine Rich Pentatricopeptide Repeats Containing code pour une protéine de 130 kDa située dans la matrice mitochondriale. Avec un motif répété de 35 acides aminés,

LRPRPC appartient à la famille des protéines à répétitions pentatricopeptidiques (PPR), qui portent toutes un nombre variable de motifs PPR, et qui confèrent aux membres de cette famille la capacité d'interagir avec les acides nucléiques.

Des études *in vivo* ont également rapporté que LRPPRC agit comme un chaperon d'ARN, permettant le repliement correct des transcrits mitochondriaux. LRPPRC joue un rôle essentiel dans la stabilisation, la polyadénylation et la traduction des ARN messagers mitochondriaux. Elle est donc nécessaire à la régulation de l'expression des gènes mitochondriaux, qui est cruciale pour maintenir l'OXPHOS et l'homéostasie énergétique.

La protéine LRPPRC a suscité l'intérêt lorsqu'elle a été liée au syndrome de Leigh, variant canadien (LSFC). Les mutations du facteur de stabilité et de polyadénylation de l'ARNm mitochondrial LRPPRC provoquent invariablement une maladie neurologique, le syndrome de Leigh, accompagnée d'une hépatopathie (LSFC) ou d'une cardiomyopathie. Les patients atteints de LSFC développent des symptômes graves et sont confrontés à une létalité précoce à un âge médian de 2,6 ans après une crise métabolique fatale causée par une acidose lactique.

Le gène nucléaire *ELAC2* code pour la protéine mitochondriale ELAC2. Cette protéine de 826 acides aminés est une endoribonucléase des ARNt mitochondriaux, essentielle à leur maturation. Présente chez de nombreux eucaryotes, ELAC2 possède un domaine métallo-bêta-lactamase avec un bras catalytique de liaison métallique capable d'hydrolyser les liaisons phosphodiesters indispensables au clivage et la maturation des ARN mitochondriaux.

En effet, l'ADN mitochondrial de 16 kb est transcrit en un long précurseur polycistronique qui est clivé pour permettre la libération des ARNm , des ARNr et des ARNt : Une endonucléase spécifique, la RNase P, un complexe de trois protéines codées par le noyau, MRPP1, MRPP2 et MRPP3, clive les ARNt immatures en amont en 5', précédé par un clivage des ARNt en aval en 3' par l'activité tRNase d'ELAC2, permettant la libération des ARNm, ARNr et ARNt individuels. Une fois coupés, les ARN subissent des modifications pour obtenir leurs formes matures. Les mutations d'*ELAC2*, sont connues pour provoquer principalement une cardiomyopathie hypertrophique, un retard de développement neurologique et une acidose lactique.

L'objectif global de ma thèse était de mieux comprendre les conséquences cliniques, biochimiques et moléculaires des défauts du métabolisme de l'ARN mitochondrial associés aux mutations de *LRPPRC* et *ELAC2*.

La fonction moléculaire de LRPPRC a été précédemment étudiée à l'aide de modèles animaux et cellulaires. Cependant, les mécanismes par lesquels sa perte entraîne des présentations cliniques tissu-spécifiques n'affectant que quelques organes restent inconnus. Le premier objectif de mon projet de thèse était de caractériser un modèle de souris knockout Lrpprc spécifique du mésencéphale et du cervelet (MCKO) qui pourrait mettre en lumière la façon dont la perte de Lrpprc dans ces structures cérébrales affecte leur fonction et leur développement. Ceci était important car le mésencéphale et le cervelet sont des régions cérébrales typiquement affectées dans le développement du syndrome de Leigh et du LSFC.

Les souris MCKO ont été générées en croisant des souris Lrpprc conditionnellement ciblées (Lrpprc$^{LoxP/LoxP}$) avec des souris exprimant la recombinase Cre sous le contrôle du promoteur En1. Ce dernier restreint l'expression de la Cre au mésencéphale et au cervelet, ce qui a pour effet de supprimer Lrpprc uniquement dans ces structures.

La caractérisation de ce modèle de souris qui pourrait récapituler les principaux phénotypes du LSFC apparaît cruciale pour une meilleure compréhension du syndrome de Leigh et plus spécifiquement des conséquences des mutations de *LRPPRC* dans différents types cellulaires du système nerveux.

Les souris MCKO naissent avec une distribution mendélienne mais meurent dans les 24 heures qui suivent leur naissance. Elles sont morphologiquement indiscernables des souris contrôles, à l'exception d'un poids corporel légèrement diminué. La comparaison morphométrique de cerveaux fraîchement explantés de souris contrôles et MCKO à la naissance a révélé un sous-développement du mésencéphale chez les souris MCKO. La coloration de Nissl de coupes sagittales du cerveau a révélé, en outre, un sous-développement du mésencéphale et un grave défaut de foliation cérébelleuse chez les souris MCKO. La coloration à l'hématoxyline-éosine a également révélé un sous-développement du mésencéphale et un grave défaut de foliation du cervelet accompagnés d'une désorganisation complète des trois feuillets cellulaires. L'immunofluorescence utilisant des marqueurs cellulaires spécifiques des cellules de Purkinje (Pcs) et des précurseurs des cellules granulaires (GCPs) a confirmé leur réduction, de même

qu’un défaut de foliation cérébelleuse, associé à une désorganisation complète des différents feuillets cellulaires chez les souris MCKO.

L'analyse par immunoblot des extraits protéiques du mésencéphale, du cervelet a révélé une diminution spécifique et statistiquement significative de l'abondance de Lrpprc et de plusieurs protéines des complexes I et IV dans le cervelet et le mésencéphale des souris KO ; l'histochimie COX/SDH de coupes sagittales de cerveau a révélé une déficience manifeste du complexe IV dans l'ensemble du mésencéphale et du cervelet des souris knockout. Ces résultats sont cohérents avec des études antérieures de souris Lrpprc KO cœur-spécifiques et de biopsies de patients dans lesquelles une expression aberrante de Lrpprc entraînait une altération de la biogenèse de l’OXPHOS.

La coloration des coupes sagittales et coronales avec la tyrosine hydroxylase (TH) - un marqueur des neurones dopaminergiques (DNs) qui font partie de la substantia nigra (SN) et de l'aire tegmentale ventrale (VTA) du mésencéphale a montré que cette population neuronale était gravement diminuée chez les souris KO. En particulier, les coupes coronales ont révélé une diminution plus sévère dans la région SN que dans la région VTA, ce qui indique une sensibilité spécifique des neurones dopaminergiques à la perte de Lrpprc.

Pour mieux comprendre comment la perte de Lrpprc affecte la neurogenèse et pour se concentrer sur la maturation de types de cellules spécifiques dans un système de croissance bidimensionnel, des cultures de cellules primaires provenant du mésencéphale ventral d'embryons a E13.5 et E14.5 (4-5 jours après le début de l'expression de Cre) ont été établies. Les données *in vitro* suggèrent une réduction du nombre de projections provenant des DNs isolés des embryons MCKO et une diminution de la surface du corps cellulaire des DNs. Ceci suggère que la perte de Lrpprc est préjudiciable à la maturation des DNs.

Ainsi l'analyse de différentes populations cellulaires dans ces structures cérébrales a révélé que LRPPRC joue un rôle important dans le développement des Pcs, des GCPs et des DNs. De plus, le modèle de souris MCKO présente également une activation de la caspase-3 dans le mésencéphale et le cervelet à P0 et aussi pendant l'embryogenèse. Enfin, un niveau relativement élevé de lactate dans le mésencéphale et le cervelet a été observé à P0 par analyse par chromatographie liquide et spectrométrie de masse en tandem. Ainsi, la perte de Lrpprc dans le modèle de souris MCKO a conduit à des défauts de maturation dans des neurones spécifiques, entraînant une augmentation du lactate, des événements d'apoptose et une létalité néonatale.

Les variants du gène *ELAC2* entraînent un autre phénotype clinique principalement caractérisé par une cardiomyopathie hypertrophique et une acidose lactique. Des phénotypes cliniques hétérogènes, avec des mouvements anormaux et des troubles psychiatriques, ou une légère déficience cardiaque avec microcéphalie ont également été rapportés.

La caractérisation des fibroblastes des patients représente une première étape pour comprendre les conséquences des variantes d'*ELAC2*. Grâce à l'activité de diagnostic de l'hôpital Necker-Enfants Malades, j'ai pu accéder aux fibroblastes de trois patients non apparentés porteurs de variants *ELAC2*. Le second objectif de ma thèse était de caractériser les fibroblastes de ces patients non apparentés et de déterminer si leur étude permet d'élargir le spectre du phénotype clinique, biochimique et moléculaire associé aux variants d'*ELAC2*.

La caractérisation de ces fibroblastes mutants peut être une étape importante pour mieux comprendre la fonction de la protéine, et pour proposer de nouveaux modèles expérimentaux in vivo, étape clé pour développer de nouveaux traitements pour la cardiomyopathie hypertrophique, les caractéristiques pathologiques les plus sévères.

Des analyses par immunoblot ont révélé que les mutations entraînaient une diminution de l'abondance de la protéine ELAC2, mais n'affectaient pas de façon significative MRPP2, sous-unité de l'endoribonucléase RNase P et de LRPPRC, protéines impliquées dans le métabolisme des ARN mitochondriaux, ni l'abondance des protéines OXPHOS. Cependant, une accumulation du précurseur de l'ARNt-Val mitochondrial non-clivé a été détectée.

En somme, une caractérisation préliminaire d'un modèle de souris a donc été réalisée pour un déficit en Lrpprc dans le mésencéphale et le cervelet, fréquemment affectés dans le syndrome de Leigh et chez les patients avec des mutations de *LRPRPC*. Ces souris récapitulent largement certaines caractéristiques physiopathologiques telles que la létalité précoce, l'altération du développement du mésencéphale et du cervelet. Même si elles ne constituent pas un modèle idéal pour étudier la spécificité tissulaire des pathologies liées aux mutations de *LRPPRC*, elles peuvent être utiles pour mieux comprendre les cascades moléculaires et biochimiques déclenchées par la perte de Lrpprc.

Concernant les variants d'*ELAC2*, nous rapportons l'identification de nouveaux variants pathogènes chez cinq patients issus de trois familles non apparentées. La caractérisation des fibroblastes de trois de ces patients a conduit à des observations similaires à celles des études

précédentes sur les patients porteurs de variants d'*ELAC2*. Bien que la gravité des manifestations diffère selon les variants, les patients partagent néanmoins des phénotypes similaires. Ainsi, à ce jour, sans élargir le spectre phénotypique, les nouveaux variants identifiés d'*ELAC2* conduisent principalement à une cardiomyopathie hypertrophique létale, ou à des atteintes cardiaques plus légères accompagnées de désordres neurologiques.

En définitive, les données obtenues par la caractérisation des souris MCKO et des fibroblastes de patients porteurs de variants d'*ELAC2* nouvellement identifiés peuvent contribuer au développement de meilleurs traitements pour le syndrome de Leigh et d'autres maladies mitochondriales.

Mots clés : métabolisme des ARNm mitochondriaux, *LRPPRC*, syndrome de Leigh, *ELAC2*, cardiomyopathie hypertrophique.